

Synthesis and characterization of stimuli responsive block copolymers, self-assembly behavior and applications

by

Michael Duane Determan

A dissertation submitted to the graduate faculty
in partial fulfillment of requirements for the degree of
DOCTOR OF PHILOSOPHY

Major: Chemical Engineering

Program of Study Committee:
Surya K. Mallapragada, Major Professor
Monica H. Lamm
Balaji Narasimhan
Joerg Schmalian
Victor Shang-Yi Lin

Iowa State University

Ames, Iowa

2006

Graduate College
Iowa State University

This is to certify that the doctoral dissertation of

Michael Duane Determan

has met the dissertation requirements of Iowa State University

M. Snyders

Major Professor

For the Major Program

TABLE OF CONTENTS

CHAPTER 1	INTRODUCTION	1
1.1.	Introduction	1
1.2.	Research Objectives	2
1.3.	Dissertation Organization	4
1.3.	References	5
CHAPTER 2	BACKGROUND AND LITERATURE REVIEW	7
2.1	Amphiphilic Block Copolymers	7
2.2	Stimuli Responsive Materials	11
	2.2.1 Stimuli Responsive Nano-scale materials	16
	2.2.1.1 Biomedical Applications	22
	2.2.2 Stimuli Responsive Hydrogels	24
	2.2.2.1 Crosslinked Hydrgels	25
	2.2.2.2 Physical Hydrogels	26
	2.2.2.3 Biomedical Applications of Hydrogels	31
2.3	Synthetic Methods	32
	2.3.1 Living Radical Polymerization	35
2.4	Characterization Methods	37
	2.4.1 Spectroscopic Techniques	37
	2.4.2 Energetics of Self Assembly	38
	2.4.3 Cyogenic Transmission Electron Microscopy	39
	2.4.4 Small angel X-ray and Neutron scattering	40
	2.4.5 Light Scattering	42
	2.4.6 Mechanical Properties	43
2.5.	References	45
CHAPTER 3	SYNTHESIS AND CHARACTERIZATION OF TEMPERATURE AND PH-RESPONSIVE PENTABLOCK COPOLYMERS	59
3.1.	Abstract	59
3.2.	Introduction	60
3.3.	Experimental Section	62
3.4.	Results and Discussion	69
3.5.	Conclusions	84
3.6.	Acknowledgements	84
3.7.	References	85
CHAPTER 4	CHARACTERIZATION OF PH- AND TEMPERATURE RESPONSIVE PENTABLOCK COPOLYMER MICELLES BY SMALL ANGLE NEUTRON SCATTERING	88
4.1.	Abstract	88

4.2.	Introduction	89
4.3.	Experimental Section	90
4.4.	Results and Discussion	93
4.5.	Conclusions	106
4.6.	Acknowledgements	106
4.7.	References	106
CHAPTER 5	SUPRAMOLECULAR SELF-ASSEMBLY OF MULTIBLOCK COPOLYMERS IN SOLUTION	109
5.1	Abstract	109
5.2	Introduction	110
5.3	Experimental Section	112
5.4	Results and Discussion	114
5.5	Conclusions	119
5.6	Acknowledgements	121
5.7	References	122
CHAPTER 6	DRUG RELEASE FROM PH-RESPONSIVE THERMOGELLING PENTABLOCK COPOLYMERS	125
6.1.	Abstract	125
6.2	Introduction	126
6.3	Materials and Methods	128
6.4	Results and Discussion	132
6.5	Conclusions	140
6.6	Acknowledgements	141
6.7	References	141
CHAPTER 7	GENERAL CONCLUSIONS	144
7.1	General Conclusions	144
7.2	References	147
7.3	Acknowledgements	148

CHAPTER 1. INTRODUCTION

1.1. Introduction

Water-soluble stimuli responsive block copolymers are a rapidly emerging class of materials with great potential in biomedical and technological applications. Amphiphilic block copolymers are composed of two or more covalently linked hydrophilic and hydrophobic macromolecular segments. This results in surfactant-like materials with macromolecular dimensions, capable of self-assembling in solution. The enormous theoretical and technological potential of amphiphilic block copolymers has been well recognized [1]. Several synthetic polymers are known to have stimuli responsive properties. Changes in the physical, chemical or biochemical environment of these polymers results in modulation of the solubility or chain conformation of the polymer. Integration of these stimuli responsive polymers into an amphiphilic copolymer results in a material that exhibits stimuli responsive self-assembly. The hydrophobic blocks of amphiphilic copolymers will self-associate to form supramolecular aggregates consisting of hydrophobic domains surrounded by swollen hydrophilic blocks. Macromolecular self-assembly originates on the nanoscale with the formation of spherical micelles, vesicle bilayers or tubular structures. In some cases, macroscopic gel structures are formed from these nanoscale building blocks.

There are many potential approaches of engineering stimuli responsive properties into amphiphilic polymeric materials. Thermally responsive copolymers can be developed by incorporation of polymers segments exhibiting lower critical solution temperature (LCST) that are soluble in water below a specific temperature and phase separate from water above that temperature. Similarly, the solubility of polymers with ionizable moieties depends on the solution pH. Conjugation of synthetic polymers and biomolecules results in materials

responsive to biological stimuli [2]. The spatial conformations of these copolymer architectures result in unique, often tailorabile, materials properties. Recent advances in living radical polymerization (LRP) methods have allowed for the facile synthesis of block copolymers of functional monomers. Previously, the primary means of synthesizing block copolymers with controlled molecular weight and well-defined architecture was with anionic polymerization [3, 4]. Ionic polymerization requires rigorous monomer and reagent purification and protecting group chemistry is required for many classes of functional monomers. Advances in LRP methods have overcome the central challenges of ionic polymerization schemes. This evolution of the capabilities of synthetic polymer chemistry have resulted in recent investigations of hyperbranched polymers[5], dendritic copolymers[6], star copolymers[7], block copolymer brushes[8, 9], and shell crosslinked nanoparticles[10, 11]. Micelles and self-assembled supramolecular structures have several biomedical and technological applications. These nanostructures can serve as drug carriers[12], biosensors[13], viscosity modifiers[14], molecularly thin membranes[15] and templates for biomineralization[16] and growth of mesoporous inorganic materials [17, 18].

1.2. Research Objectives

The central theme of this thesis work is to develop new block copolymer materials for biomedical applications. While there are many reports of stimuli-responsive amphiphilic[19-21] and crosslinked hydrogel materials[22], the development of an *in situ* gel forming, pH responsive pentablock copolymer is a novel contribution to the field. Figure 1.1 is a sketch of an ABCBA pentablock copolymer. The A blocks are cationic tertiary amine methacrylates blocked to a central Pluronic F127 triblock copolymer.

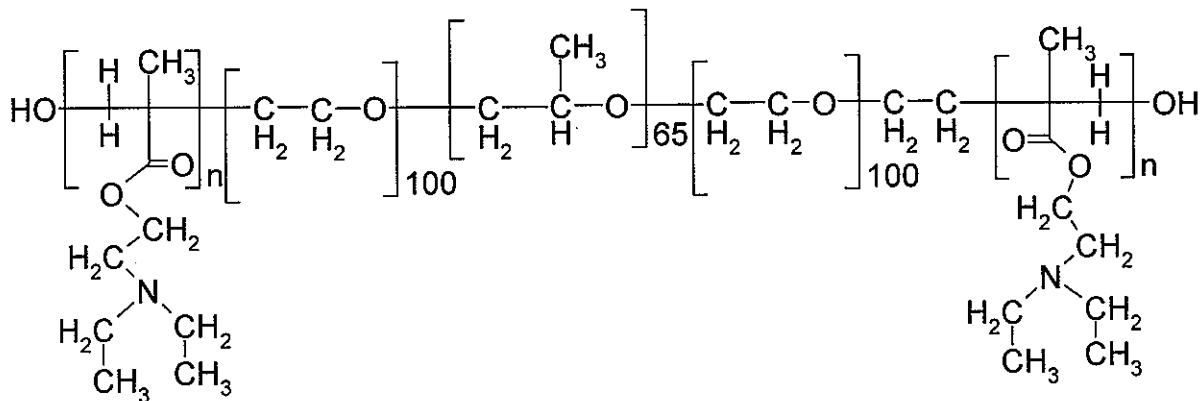


Figure 1.1: A pentablock copolymer of poly($(N,N'$ -diethyl aminoethyl methacrylate)-b-(ethylene oxide)-b-(propylene oxide)-b-(ethylene oxide)-b-(N,N' -diethyl aminoethyl methacrylate))

In addition to the prerequisite synthetic and macromolecular characterization of these new materials, the self-assembled supramolecular structures formed by the pentablock were experimentally evaluated. This synthesis and characterization process serves to elucidate the important structure property relationships of these novel materials. The pH and temperature responsive behavior of the pentablock copolymer were explored especially with consideration towards injectable drug delivery applications. Future synthesis work will focus on enhancing and tuning the cell specific targeting of DNA/pentablock copolymer polyplexes.

The specific goals of this research are:

1. Develop a synthetic route for gel forming pentablock block copolymers with pH and temperature sensitive properties. Synthesis of these novel copolymers is accomplished with ATRP, yielding low polydispersity and control of the block copolymer architecture. Well defined macromolecular characteristics are required to tailor the phase behavior of these materials.

2. Characterize relationship between the size and shape of pentablock copolymer micelles and gel structure and the pH and temperature of the copolymer solutions with SAXS, SANS and CryoTEM.
3. Evaluate the temperature and pH induced phase separation and macroscopic self-assembly phenomenon of the pentablock copolymer.
4. Utilize the knowledge gained from first three goals to design and formulate drug delivery formulations based on the multi-responsive properties of the pentablock copolymer. Demonstrate potential biomedical applications of these materials with *in vitro* drug release studies from pentablock copolymer hydrogels.

The intent of this work is to contribute to the knowledge necessary for further tailoring of these, and other functional block copolymer materials for biomedical applications.

1.3. Dissertation Organization

This dissertation is organized into seven chapters. Chapter 2 is a general background of stimuli responsive soft materials, as well as approaches to characterizing these materials. Potential applications of soft materials for gene therapy and injectable drug depot formulations are briefly reviewed. The intention of this review is to provide the context for the motivation and goals of this work and includes an outline of the specific objectives of this work. Chapter 3 is a paper published in the journal Polymer that addresses the synthesis and characterization of a novel family of amphiphilic pentablock copolymers. Detailed investigations into the temperature and pH dependent phase behavior of the pentablock copolymers are presented in Chapters 4 and 5. Chapter 6 reports on the development of a pH-responsive, injectable, depot device for controlled drug release incorporating the

pentablock copolymers. The final chapter includes general conclusions and a summary of the contributions of this work.

1.4. References

1. Hamley, I.W., *The physics of block copolymers*. 1998, New York: Oxford University Press.
2. Hoffman, A.S., *Bioconjugates of Intelligent Polymers and Recognition Proteins for Use in Diagnostics and Affinity Separations*. Clinical Chemistry, 2000. **46**(9): p. 1478-1486.
3. Bates, F.S. and G.H. Fredrickson, *Block Copolymer Thermodynamics: Theory and Experiment*. Annu. Rev. Phys. Chem, 1990. **41**: p. 525-557.
4. Szwarc, M., *Living Polymers. Their Discovery, Characterization, and Properties*. Journal of Polymer Science Part A: Polymer Chemistry, 1998. **36**(1): p. ix.
5. Jikei, M. and M.-a. Kakimoto, *Hyperbranched polymers: a promising new class of materials*. Progress in Polymer Science, 2001. **26**: p. 1233-1285.
6. Carlmark, A. and E.E. Malmstrom, *ATRP of Dendronized Aliphatic Macromonomers of Generation One, Two, and Three*. Macromolecules, 2004. **37**: p. 7491-7496.
7. Francis, R., et al., *Toward an Easy Access to Asymmetric Stars and Miktoarm Stars by Atom Transfer Radical Polymerization*. Macromolecules, 2002. **35**: p. 9001-9008.
8. Pyun, J., T. Kowalewski, and K. Matyjaszewski, *Synthesis of Polymer Brushes Using Atom Transfer Radical Polymerization*. Macromolecules Rapid Communications, 2003. **24**(18): p. 1043-1059.
9. Kizhakkedathu, J.N., et al., *Synthesis and characterization of well-defined hydrophilic block copolymer brushes by aqueous ATRP*. Polymer, 2004. **45**(2).
10. Ma, Q., et al., *Environmentally-Responsive, Entirely Hydrophilic, Shell Cross-linked (SCK)Nanoparticles*. Nano Letters, 2001. **1**(11): p. 651-655.
11. Liu, S. and S.P. Armes, *The Facile One-Pot Synthesis of Shell Cross-Linked Micelles in Aqueous Solution at High Solids*. J. Am. Chem. Soc., 2001. **123**(40): p. 9910-9911.
12. Rosler, A., G.W.M. Vandermeulen, and H.-A. Klok, *Advanced drug delivery devices via self-assembly of amphiphilic block copolymers*. Adv Drug Deliv Rev, 2001. **53**: p. 95-108.
13. Eddington, D.T. and D.J. Beebe, *Flow Control with Hydrogels*. Adv Drug Deliv Rev, 2004. **56**: p. 199-210.
14. Sperling, L.H., *Introduction to Physical Polymer Science*. 3rd ed. 2001, New York: John Wiley and Sons, Inc.
15. Discher, D.E. and A. Eisenberg, *Polymer Vesicles*. Science, 2002. **297**: p. 967.
16. Robinson, K.L., et al., *Synthesis of controlled-structure sulfate-based copolymers via atom transfer radical polymerization and their use as crystal habit modifiers for BaSO₄*. J. Mater. Chem., 2002. **12**: p. 890-896.
17. Abu-Lebdeh, Y.A.I., P.M. Budd, and V.M. Nace, *Preparation of mesoporous silica with poly(oxyethylene)/poly(oxybutylene)/poly(oxyethylene) triblock copolymers as templates*. Jounal of Materials Chemistry, 1998. **8**(8): p. 1839-1842.

18. Tattershall, C.E., N.P. Jerome, and P.M. Budd, *Oxyethylene/oxybutylene block copolymers as structure-directing agents in the preparation of mesoporous silica*. Journal of Materials Chemistry, 2001. **11**: p. 2979-2984.
19. Lecolley, F., et al., *Synthesis of functional polymers by living radical polymerisation*. J. Mater. Chem., 2003. **13**: p. 2689-2695.
20. Wei, J.S., et al., *Temperature- and pH-sensitive core-shell nanoparticles self-assembled from poly(n-isopropylacrylamide-co-acrylic acid-co-cholesteryl acrylate) for intracellular delivery of anticancer drugs*. Front Biosci, 2005. **10**: p. 3058-67.
21. Mertoglua, M., et al., *Stimuli responsive amphiphilic block copolymers for aqueous media synthesised via reversible addition fragmentation chain transfer polymerisation (RAFT)*. Polymer, 2005. **46**(2005): p. 7726-7740.
22. Peppas, N.A., et al., *Physicochemical Foundations and Structural Design of Hydrogels in Medicine and Biology*. Annu. Rev. Biomed. Eng., 2000. **02**: p. 9-29.

CHAPTER 2. BACKGROUND AND LITERATURE REVIEW¹

2.1. Amphiphilic Block Copolymers

The synthesis and development of new polymeric materials is a central issue in the advancement of numerous technological fields. Advanced synthetic polymeric materials have proven invaluable in applications where they displace natural and traditional materials. Increasingly polymeric materials with tailored properties exhibit properties unrealizable with traditional materials[1]. One method of engineering the properties of a new material is by combining two materials with desirable properties into a new material that exhibits the properties of both original materials. This approach is complicated by the general immiscibility of most polymers. The general lack of miscibility between different polymers stems from insignificant enthalpies of mixing and the negative entropies of mixing. This lack of miscibility results in phase separation into numerous morphologies that exhibit periodicity with the length scales of the polymer chain, typically a few to tens of nanometers [2].

The architecture of the covalent linkages between blocks is a critical parameter of materials design. Figure 2.1 depicts block, triblock and star copolymers. Many other block geometries, such as dendritic, hyperbranched and graft copolymers, have been developed to exhibit unique properties[3]. Rod-coil block copolymers, with alternating blocks of rigid and flexible random coil segments have many applications in optoelectronic devices, nanopatterning, and mechanical reinforcing agents[4-6].

¹ Portions of this chapter are reproduced with permission from: Determan, M. D.; Mallapragada, S. K. "Self-assembling Nanostructured Injectable Polymeric Gels for Drug Delivery" In *Handbook of Nanostructured Biomaterials and Their Applications in Nanobiotechnology*; Nalwa, H. S., Ed.; American Scientific Publishers, 2005; Vol. 2.

Amphiphilic copolymers are special class of copolymers consisting of hydrophilic and hydrophobic blocks. Whereas the repulsive interaction between separate blocks is the driving force for phase separation in polymer melts, the hydrophobic effect is the driving force for phase separation and self assembly in aqueous solution [7]. Hydrophobic blocks will form isolated domains, insulated from the bulk aqueous environment by the hydrophilic blocks. In many ways amphiphilic block copolymers are analogous to low molecular weight surfactants. Yet the macromolecular nature of these materials allows them to form more complex morphologies on the nanometer length scale. The hydrophobic domains of macromolecular amphiphiles are much more stable than low molecular weight surfactants, due to lower mobility of the aggregated hydrophobic chains [8]. In addition to providing the driving force for self-assembly, the hydrophobic domain formation of amphiphiles provides a hydrophobic environment for the incorporation of sparingly soluble molecules, such as hydrophobic drugs, into solution.

Hydrophobic interactions are a fundamental driving force in the assembly of amphiphilic systems, and have been the focus of theoretical and experimental work [9]. Lum and Chandler have proposed a unified theory of hydrophobic interactions of small and large apolar species in water [10]. If small hydrophobic groups, at low concentrations, are dispersed in water the hydrogen bond network may be capable of reorganizing to accept them in solution. When larger hydrophobes, such as macromolecules, are introduced the hydrogen bond network has no way of reorganizing to accept the large excluded volume of the apolar species. Thus hydrophobic objects experience a ‘drying out’ at their interfaces where the density of water molecules is highly rarified. These density fluctuations are highly unstable and result strong attractions between the large hydrophobic objects. These attractive forces

result in macromolecular self-association and lead to the formation of nanoscale ordered structures.

Self-assembly, as it will be referred to in this work, is the autonomous organization of matter into structures without direct human intervention[11]. The term self assembly is not synonymous with formation; self-assembly refers only to reversible processes which can be controlled by proper design and conditions of a collection of initially disordered components[8]. Self-assembly is one of the only practical means of assembling and controlling structures with nanometer dimensions[5]. Figure 2.2 schematically illustrates the bottom-up approach to design and synthesis of self assembled functional materials. Supramolecular structures are formed from amphiphilic block copolymers composed of stimuli responsive homopolymers. The development of an application specific material via this bottom-up approach requires understanding of the synthetic techniques, macromolecular materials properties, and the mechanisms of self-assembly.

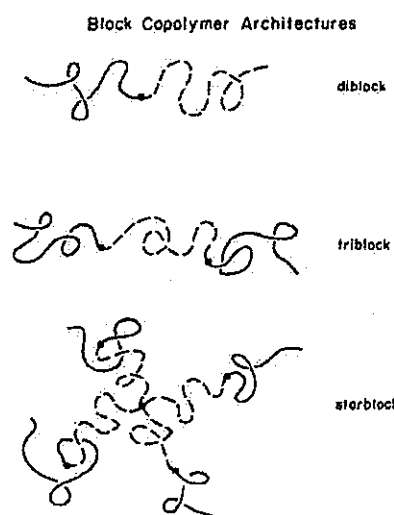


Figure 2.1. Schematic illustration of common block copolymer architectures. Solid and dashed lines represent A (hydrophilic) and B(hydrophobic) block chains. Adapted from [12]

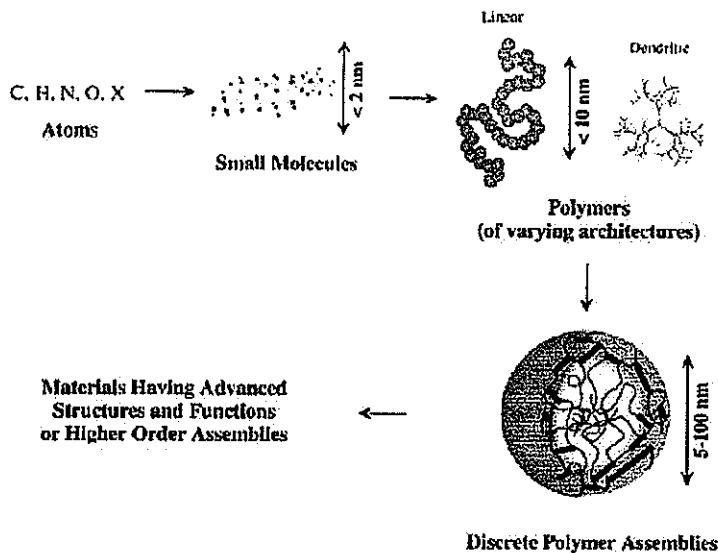


Figure 2.2. The dimensional evolution of intelligent design of self assembled functional materials. Adapted from [13]

2.2. Stimuli Responsive Materials

A great number of materials and synthetic schemes have been developed to respond to forms of environmental stimuli listed in Table 2.1[14]. Early work in responsive materials and composites relied primarily on forms of physical stimuli. For the most part however these materials have limited applicability *in vivo*. Stimuli responsive block copolymers and polymer conjugated proteins exploit changes in chemical and biochemical variables to modulate materials properties[15]. The origins of stimuli responsive properties in macromolecular materials will be discussed followed by a review of recent developments in stimuli responsive materials.

Polymers with temperature responsive behavior in aqueous solutions usually possess an upper or lower critical solution temperature (LCST). The critical solution temperature

corresponds to a discontinuous change in the composition of the polymer and solution phase. A polymer exhibiting a LCST will phase separate from solution above a critical temperature. Conversely, if the polymer only dissolves above a critical temperature the polymer has an upper critical solution temperature (UCST). Polymers exhibiting LCST are most commonly used in stimuli responsive copolymer materials for biomaterials applications. Table 2.2 lists several polymers and macromolecular surfactants with temperature sensitive properties due to a LCST. Poly(N-isopropylacrylamide) (PNIPAAm) undergoes a reversible volume phase transition caused by the coil to globule transition at the LCST[16]. The LCST of PNIPAAm can be increased by copolymerizing with a hydrophilic monomer, such as acryl amide; and decreased by copolymerization with a hydrophobic monomer, such as N-butyl-acrylamide. The LCST behavior of poly(ethylene oxide) and poly(propylene oxide) originates from temperature dependent intermolecular interactions in water. The number of hydrogen bonds a PEO or PPO monomer unit is capable of supporting decreases with increasing temperature. Above the LCST, PPO is significantly more hydrophobic than PEO due to the extra methyl group. The LCST of PPO occurs between 2-8°C and decreases with increasing molecular weight. PPO greater than 4000 g/mol does not exhibit a LCST[8]. The LCST of PEO increases with increasing molecular weight between 70 and 91°C. In addition PEO has been found to have an *in vivo* “stealth” property, it is does not react negatively with immune system. Recent reviews by Gil and Hoffman contained detailed discussions of these families of polymers with LCST in aqueous environment [16, 17].

For many applications, changes in solution pH are more practical than changes in temperature to modulate responsive behavior, particularly for biological applications. Polymers with pH responsive solubility contain ionizable backbone or pendent groups accept and donate protons in response to changes in pH. These polymers, often referred to as

polyelectrolytes, can be classified as weak polyacids and weak polybases. The degree of ionization responds to changes in environmental changes in pH. Distinct changes in the hydrodynamic volume of polyacids and polybases occur around the specific pH, or pKa corresponding to a dramatic change in chain ionization[18]. Polybases are ionized, and more hydrophilic, below the pKa; polyacids are ionized and hydrophilic above the pKa. Thus the incorporation of these monomers into an amphiphilic copolymer results in the ability to modulate the hydrophilic/hydrophobic balance of the copolymer with solution conditions[19].

Figure 2.3 shows several representative polyelectrolytes that have been utilized in pH responsive amphiphilic copolymers. The pendent tertiary amine groups of the polybasic poly(alkyl amine methacrylates) and the pyridine group of the poly(4-vinylpyridine) are ionizable and can accept and donate protons in response to environmental pH. The amine groups become ionized when they absorb protons at low pH conditions and release them under basic conditions. The choice of alkane groups attached to the amine group determines how hydrophobic the uncharged polyelectrolyte will be and affects the pKa value. Amphiphilic polymers and crosslinked hydrogels of poly(vinyl sulfadimethoxine sulfonamide) (PSD) (Figure 2.3 entry (e)) have been synthesized. Substitution of the pendants at the sulfonamide group allows tuning of the pKa value ranging from pH 3 to 11[20]. Sulfonamides (short for para-aminobenzensulfonamide) are weakly acidic due to the readily ionizable hydrogen atom in the amide bond in water. Work by Han et al. demonstrated PSD undergoes a sharp pH induced coil to globule transition around a pKa of 7.4. Amphiphilic copolymers of PEG-PSD exhibited reversible pH responsive micelle aggregation[21]. The pKa of the PSD is closer to relevant biological pH values than common carboxylic group monomers. The pKa of carboxylic acid moieties in polymers

ranges from pH 4 to 6. The carboxylic monomers in Figure 2.3 increase in hydrophobicity with substitution of the acrylic hydrogen with methyl and ethyl groups. This leads to a more discontinuous phase transition between the charged polyelectrolyte coil and the neutralized hypercoiled globule at the pK_a .

Perhaps the most promising advanced stimuli-sensitive materials are those that respond to biological cues. A number of schemes have been contrived to integrate biomimetic and biofunctional molecules into synthetic polymeric materials[15, 22, 23]. Synthetic polymer-bimolecular conjugates can be used for cell specific targeted drug delivery. Attaching protein specific ligands or antigens to stimuli responsive polymers was first utilized for protein separation and precipitation[24]. Covalently linking poly(ethylene glycol) to polypeptide drugs (PEGylation) has been shown to significantly enhance the pharmacokinetic and pharmacodynamic properties of these therapies. PEGylation of polypeptides shields antigenic epitopes of the polypeptide, reducing the reticuloendothelial clearance and recognition by the immune system and also reduces the degradation by proteolytic enzymes[25]. Figure 2.4 illustrates the common biofunctional moieties. Ongoing work has focused on the development of multi functional molecules for drug delivery and gene therapy[1, 26, 27].

Physical	Chemical	Biochemical
Temperature	pH	Enzyme substrates
Ionic Strength	Specific ions	Affinity ligands
Solvents	Chemical agents	Other biochemical agents
UV, Visible light		
Electric fields		
Mechanical Stress		
Sonic radiation		
Magnetic fields		

Table 2.1. Classification of environmental stimuli

Ether Groups	Alcohol Groups	Substituted Amide Groups	Other
Poly(ethylene oxide) PEO	Hydroxypropyl acrylate	Poly(N-substituted acrylamides)	Poly(methacrylic acid)
Poly(propylene oxide) PPO	Hydroxypropyl methylcellulose	Poly(N-acryloyl pyrrolidine)	Poly(organophosphazene)
PEO-PPO-PEO triblock copolymers	Hydroxypropyl cellulose	Poly(N-acryloyl piperidine)	
Alkyl-PEO block surfactants	Methylcellulose	Poly(acryl-L-amino acid amides)	
Poly(vinyl Methyl ether)	Poly(vinyl alcohol) derivatives		

Table 2.2. Some polymers and surfactants which show LCST behavior in aqueous solutions, adapted from [15] and [16]

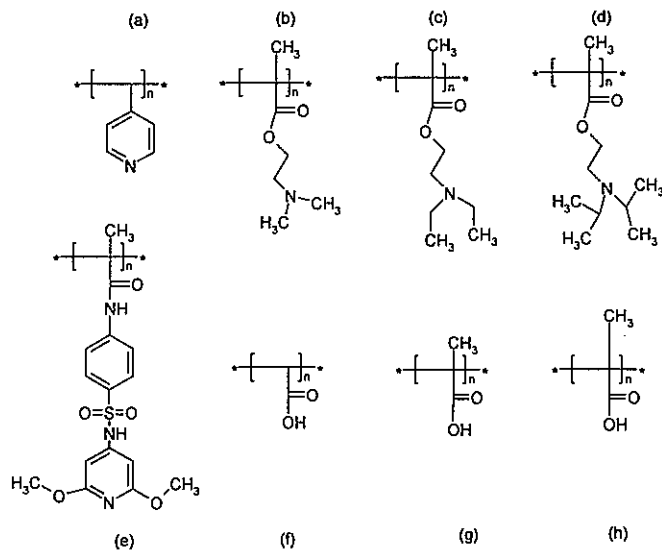


Figure 2.3. Representative polybasic polymers: (a) poly(4-vinylpyridine), $pK_a < 5$ (b) poly(N,N' -dimethyl aminoethyl methacrylate), $pK_a = 7.5$ (c) poly(N,N' -diethyl aminoethyl methacrylate), $pK_a < 7.6$ (d) poly(N,N' -di-isopropyl aminoethyl methacrylate), $pK_a < 6.4$ (e) poly(vinyl sulfadimethoxine sulfonamide) $pK_a = 6.1$ (f) poly(acrylic acid) (g) poly(methacrylic acid) (h) poly(2-ethyl acrylic acid)

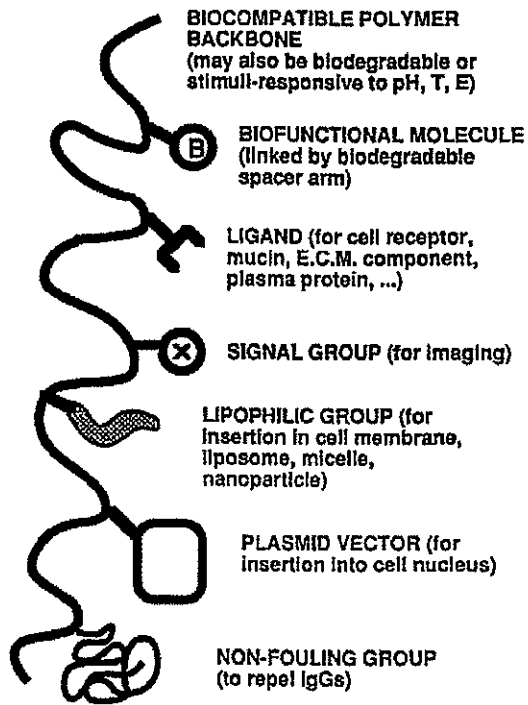


Figure 2.4. Schematic of variety of natural or synthetic biomolecules that may be conjugated to a smart polymer. From [15]

2.2.1. *Stimuli responsive nano-scale materials*

Thermally responsive amphiphilic copolymers typically consist of one or more blocks exhibiting a lower or upper critical solution temperature. At the critical temperature of a polymer segment the hydrophilic/hydrophobic balance of the copolymer is altered, resulting in aggregation of hydrophobic domains through self assembly. Similarly, for pH responsive polymers such as polyelectrolytes, the solubility of the polyelectrolyte blocks undergoes a dramatic transition near the pK_a of the particular polyelectrolyte segment. Combining pH and temperature sensitive segments into a block copolymer architecture is one strategy for creating multi-responsive block copolymers. There are many instances of multi-responsive amphiphilic materials. Copolymers with dual temperature, temperature-pH, and dual pH responsive blocks have been prepared. These materials have are capable of forming micelles

and reverse micelles in response to solution conditions. Figure 2.5 is an illustration of various schemes of stimuli responsive block copolymer design.

A temperature sensitive diblock copolymer, combining blocks exhibiting LCST and UCST was recently reported. PNIPAM and a zwitterionic monomer 3-[N-(3-methacrylamidopropyl)-N,N-dimethyl]ammoniopropane sulfonate (SSP) was synthesized by sequential RAFT polymerization[28]. PNIPAM has a well characterized LCST and P(SSP) exhibits a UCST due to strong mutual intermolecular attraction of zwitterionic groups. This results in a dual thermoresponsive hydrophilic copolymer. Below the UCST of the P(SSP) the copolymer forms micelles with P(SSP) cores surrounded by PNIPAM coronas. At intermediate temperatures both blocks are hydrophilic and the copolymer is molecularly dissolved. Above the LCST of PNIPAM, micelles form with collapsed PNIPAM cores and swollen P(SSP) coronas. Unlike the native homopolymers, the copolymer remains in solution between 0 and 100°C.

A copolymer of 2-(dimethylamino)ethyl methacrylate-b-2(N-morpholino)ethyl methacrylate (PDMA-b-PMEMA) was synthesized via group transfer polymerization[29]. The DMA block was converted to a sulfobetaine methacrylate by selectively quaternizing with 1,3-propane sulfone. The zwitterionic poly(sulfobetaine methacrylate) (PSBMA) becomes soluble above 25°C, whereas the PMEMA has a LCST between 34 and 49°C. This copolymer formed micelles with PSBMA cores at low temperature, dissolved molecularly at intermediate temperatures, between 25 and 50°C, and formed 'reverse' micelles with PMEMA cores. Static light scattering revealed that near monodisperse micelles formed were 42 and 50 nm in diameter at low and high temperatures respectively.

Zwitterionic diblock copolymers, i.e. copolymers with both polyacid and polybasic segments, have been shown to exhibit dual pH responsive self assembly and have been of

interest for many years[30-32]. Liu and Armes prepared a poly(4-vinyl benzoic acid-b-2-(diethylamino)ethyl methacrylate (VBA-DEA) copolymer by ATRP using protecting group chemistry[33]. Subsequently the ATRP synthesis of zwitterionic diblock copolymers without the use of protecting group chemistry has been reported[34]. The polybasic DEA and the polyacidic VBA have pK_a values of 7.3 and 7.1 respectively. At pH 6.8 the uncharged VBA block is hydrophobic. Because the DEA block is highly charged and hydrophilic at this pH the copolymer forms well-defined micelles with VBA cores and DEA coronas. Because both blocks are uncharged and hydrophobic in a pH range around the isoelectric point of the copolymer, between pH 6.8 and 8.3, the copolymer precipitates. This is observed by an increase in turbidity of the solution, and can be attributed to the formation of large non-micellar aggregates[35]. Above pH 8.3 the VBA groups become charged and hydrophilic, resulting in formation of DEA-core, VBA-corona micelles. The same authors recently reported a similar pH responsive system of PEO-DEA copolymer codissolved with PMMA homopolymer[36]. Four distinct, pH dependent micellar and polyionic complexes were identified; PEO/PMAA-core, PDE corona micelles at low pH, a DEA-PMAA complex stabilized in solution by the hydrophilic PEO block with increasing pH, micelles formed with neutral DEA-PMMA complex cores and PEO coronas, and at high pH PDEA-core, PEO-corona micelles formed, excluding the hydrophilic PMMA homopolymer to the solution phase[36].

Copolymers that undergo temperature and pH responsive self-assembly are formed by combining a polyelectrolyte block and a nonionic block with a LCST. A diblock copolymer of PPO and DEA was synthesized by ATRP[37]. The LCST of the PPO block ($M_n = 2000$) was 20°C . At low pH, where the DEA block is hydrophilic, the copolymer could be

dissolved as unimers below 20°C, or form PPO core micelles above 20°C. DEA core micelles could be formed at high pH and temperatures below 20°C.

The pH dependent, reversible micelle formation of polyelectrolyte block copolymer poly(N,N' -diethyleaminoethyl methacrylate)-b-poly(N,N' -dimethylaminoethyl methacrylate) (PDEAM-b-PDMA) were characterized with light and small angle neutron scattering[38]. Because both PDEAM and PDMA blocks are polybasic the copolymer is a highly charged polyelectrolyte at low pH. Increasing the pH of the copolymer solution results in deprotonation of the tertiary amine pendants of both blocks. Onset of micelles formation occurred when just over half of each block is deprotonated. The more hydrophobic PDEAM blocks aggregate to form a core domain surround by hydrophilic PDMA. The pH dependent micelle formation was designed to be capable of encapsulating drugs during the micellization process, followed by release the drug when the micelle dissolves in a low pH environment. The addition of salt was shown to screen the repulsive ionic interaction of charged amine groups leading to micellization at lower pH. Small angle neutron scattering (SANS) was utilized to investigate the ionic strength and charge dependence of micelle dimensions[39]. The overall micelle size was calculated from the scattering data using a starlike micelle model for the compact core and an electrostatic blob model for the corona[40].

Nanoscale cages or gels with dimensions less than 100 nm and stimuli responsive swelling properties have been developed for drug delivery applications. Either the coronal or core region of micellar structures formed by amphiphilic copolymers in solution can be stabilized by crosslinking. This results in self assembled structures with extensive structural stability. Cross-linked nanogels with biocompatible and functional or degradable monomers have enormous potential for targeted and controlled drug delivery applications[41]. These

materials are designed to overcome the drawbacks of macroscopic gels that require surgical implantation. Shell cross-linked micelles do not disassociate at low concentrations, allowing for longer circulation time *in vivo* than simple self assembled micelles. Initial work in the area of shell cross-linked micelles by Wooley, et al[13, 42] has spurred considerable interest in these novel materials. Efficient production of shell cross-linked micelles on commercially relevant scales was demonstrated, increasing the viability of this technology for biomedical applications[43].

Shell cross-linked nanoparticles containing hydrolytically degradable, crystalline core domains were prepared from poly(ϵ -caprolactone)-*b*-poly(acrylic acid) (PCL-*b*-PAA) amphiphilic copolymers. The hydrophobic polyester (PCL) core is degraded via acid hydrolysis, yielding hollow nanoscale cages. The rate of hydrolysis of the core was pH dependent, occurring more rapidly at lower pHs[44]. Thermally-responsive, entirely hydrophilic nanogels were synthesized through a similar technique. poly(acrylic acid)-*b*-poly(methyl acrylate) (PAA₉₀-*b*-PMA₂₄₀) micelles were prepared followed by selective crosslinking of the PAA corona to form a hydrogel shell. Subsequently the methyl esters of the core domain were cleaved to result in a nanogel composed of a temperature sensitive crosslinked PAA shell and linear PAA core[41]. In addition to scattering techniques usually employed to study micelle structures, atomic force microscopy (AFM) is frequently utilized to characterize dimensions and structure of cross-linked micelles due to their structural stability out of solution.

Triblock copolymers of poly[(ethylene oxide)-*b*-2-(dimethylamino)ethyl methacrylate-*b*-2-(diethylamino) methacrylate] (PEO-DMA-DEAM) were used to form pH responsive nanogels. The copolymer was synthesized by ATRP and could be unimolecularly dissolved in low pH aqueous solutions and formed micelles with DEA cores above pH 7.3.

Subsequently the inner shell of DMA was selectively crosslinked with a bifunctional alkyl iodide 1,2-bis(2-iodoethoxy)ethane[45]. The crosslinking process effectively locked in the micellar structure, preventing micelle dissolution at low pH. The reversible swelling of the DEAM core with changes in pH was studied with dynamic light scattering[46]. The crosslinked micelles swelled at low pH due to the electrostatic repulsion between charged amine groups in the PDEAEM core. Figure 2.7 compares the variations in size of the crosslinked and self assembled micelles with pH. Tuning the pH responsive properties of the cross-linked micelles was achieved through changes in crosslinking density and degree of polymerization of the individual blocks. Nanogels with crosslinked DEAM cores and a PEG shell with terminal carboxyl groups were synthesized[47]. The carboxylic acid groups located on the distal end of the PEG are highly suited for conjugation with various targeting ligands.

Temperature and pH sensitive amphiphilic microspheres, consisting of PNIPAM cores and PEI shell were synthesized. NIPAM was grafted from branched PEI (750000 Da) above the LCST of the PNIPAM, in the presence of a vinyl cross-linker. The PNIPAM phase separated as it was formed, forming the core of a colloidal structure that was cross linked *in situ*. The spherical aggregates formed were observed by TEM to have a distinct core shell structure. The PNIPAM core could be reversibly dehydrated by heating a dispersion of the microgels above the LCST of PNIPAM. Due to the pH dependent solubility of the PEI core, the hydrodynamic radius of the particles could be reversible varied from 380 to 310 nm by changing the pH from 3 to 10[48].

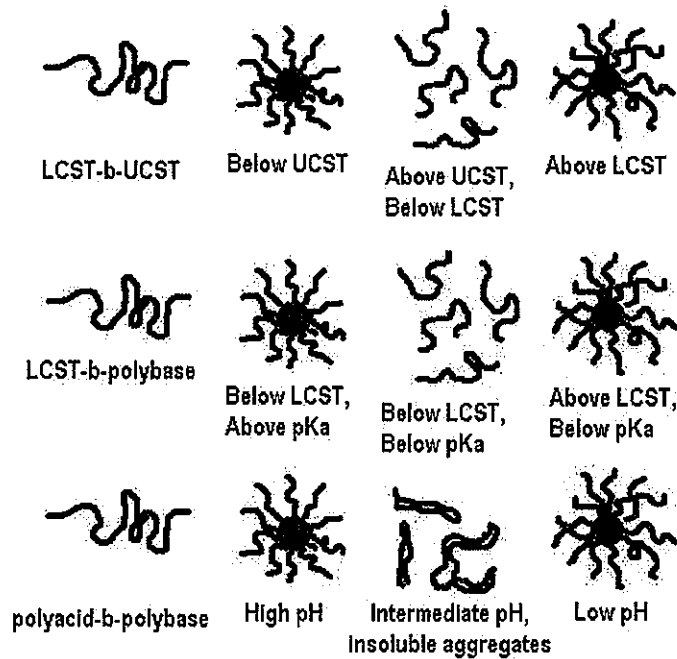


Figure 2.5. Examples of multi responsive diblock copolymers and modes of self association

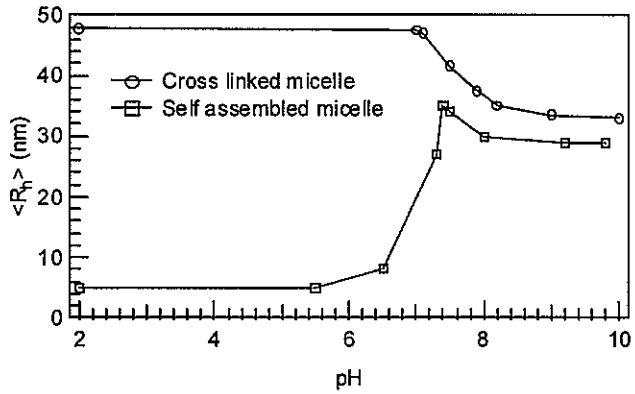


Figure 2.6. Variation of hydrodynamic radius of crosslinked and uncrosslinked, self assembled micelles of PEO-PDMAEM-PDEAEM. Adapted from [46]

2.2.1.1. Biomedical applications

Self assembled micelles have long been recognized as potential drug delivery vehicles that enhance biodistribution, circulation time and targeted delivery of drugs[49-52]. The hydrophobic core phase can act as a reservoir for therapeutic genes, enzymes and hydrophobic drugs. Block copolymer micelles with hard sphere cores and tethered gaussian coil chains are illustrated in Figure 2.7. Micelles were formed from a PEO-poly(aspartic

acid)(PASP) diblock copolymer, where the PASP block was bound to anti tumor drug adriamycin. Low biointeraction of the PEO corona with cells and proteins *in vivo* results in extended *in vivo* circulation and biodistribution[53, 54]. Several schemes for triggered dissolution of drug loaded micelles has been utilized for stimuli responsive administration from circulating micelles[55]. The attachment of targeting moieties on the surface of the corona has been shown to enhance targeting of micelle drug carriers[56].

Copolymers of methoxycapped poly(ethylene glycol)-b-poly(N,N'-dimethylaminoethyl methacrylate)-b-poly(N,N'-diethylaminoethyl methacrylate) (PDEAM-b-PDMA) MPEG-DMA-DEAM where synthesized via ATRP. This copolymer retains the pH dependent micelle forming properties of the PDEAM-PDMA copolymer. The PEO block increases the hydrophilic character of the copolymer. A hydrophobic drug was incorporated into the micelle cores by codissolving the copolymer and drug at low pH and adjusting the pH to 7.4. At pH 7.4, drug release was limited to diffusion of the hydrophobic drug out of the micelle core. At pH 3.0, the micelles break apart and the drug was rapidly released into the acidic media[57].

The development of synthetic membranes formed by self-assembly of block copolymers is excellent example of the bioinspired approach to materials development. The asymmetric property of the cellular membranes is largely responsible for the proper insertion and orientation of integral membrane proteins. Self assembled vesicle membranes formed from asymmetric ABC triblock copolymers, where the A and C blocks are different hydrophilic blocks have been shown induce a directed insertion of membrane proteins compared to a membrane formed from symmetric copolymers[58].

Non-viral delivery of genetic material into cells is a rapidly expanding field of investigation. Genetic therapy is the introduction of exogenous plasmid DNA into cells. The

inserted DNA signals the cell to produce a therapeutic or under expressed protein. The mechanism of gene therapy mimics the reproductive nature of viruses. Due to the difficulties and dangers of working with virus materials for human gene therapy many non-viral schemes have been devised. A search of the materials science and chemistry literature database revealed over 300 publications concerning non-viral gene therapy. These developments have been recently reviewed [26, 27, 59]. Many synthetic gene delivery schemes rely on formation of compact polyplex nanoparticles. Polyplexes form due to the electrostatic interactions of a cationic polymer with plasmid DNA. Polyplex formation protects the DNA from nuclease digestion and aids transport within cell. Homopolymer cationic poly(*L*-lysine), polyethyleneimin(PEI) and comb block copolymer poly(*L*-histidine)-graft-poly(*L*-lysine) have been form complex to form condensed polyplex structures with DNA upon mixing[60, 61].

Pluronic® block copolymers have been shown to enhance gene expression through mechanisms that do not involve DNA condensation. The surfactant properties of Pluronic® unimers enhance cell membrane permeability, enhancing cellular uptake of therapy. In addition, Pluronic® copolymers and Pluronic® based conjugates exhibit low toxicity, compared to PEI based gene delivery formulations, and high transfection efficiency[62]. Based on these results, amphiphilic block copolymers are expected to play an important role in development of effective gene delivery systems.

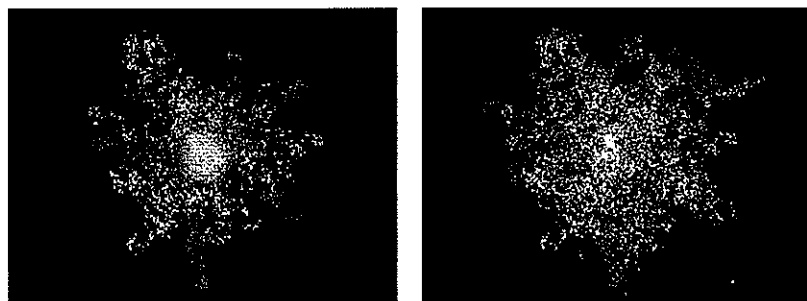


Figure 2.7. Micelles with hard sphere cores and attached Gaussian coil coronas. From [63]

2.2.2. Stimuli Responsive Hydrogels

The term hydrogel has been used to describe a wide range of aqueous soft solid materials. These systems consist of highly hydrated networks of physically or covalently bonded molecules. These gel networks contain large amounts of water that occupy the interstitial spaces formed in the network, thereby possessing favorable mechanical properties for *in vivo* biomedical applications. Physically crosslinked hydrogels are the product of a self-assembly process under controlled conditions that forms nanostructures and further forms macroscale gels. Because these gels consist of self assembled equilibrium structures, the phase of the system will respond to changes in the environment. It has been demonstrated that subtle changes in the temperature, pH, ionic strength and polymer concentration of the surrounding environment may result in dramatic changes in the structure of the hydrogel[64]. The formation of a physical hydrogel requires the self-assembly of molecules over several orders of magnitude, from isolated unimers through micelles to supramolecular aggregates. An understanding of the driving forces and mechanisms of self-assembly aids in the selection and tailoring of chemistries and block architectures that result in desirable hydrogel properties[65, 66]. The use of physically and chemically crosslinked hydrogels for drug delivery applications has been of interest for many years[67-70]. This has led to the evolution of smart materials—materials with the ability to sense physiological states and respond with appropriate therapeutic action. Recent reviews, with an emphasis on specific clinical settings, have summarized the state-of-the-art in this field[71-73]. Physically self-assembled gels have an advantage over chemically crosslinked gels in that they can be naturally removed by the body's renal system through dissolution and, in some cases, degradation. In many cases, the self-assembly process can be triggered inside the body by

physiological conditions and this *in situ* gel-forming capability can be exploited in injectable drug delivery systems.

2.2.2.1. *Crosslinked Hydrogels*

Cross-linked hydrogel materials have numerous biomedical and pharmaceutical applications[67]. Hydrogel materials are typically synthesized by free radical polymerization of a water-soluble monomer in the presence of a small percent of crosslinking agent. The covalently crosslinked polymer network is capable of swelling to absorb water or biological fluids. Hydrogels containing environmentally responsive moieties have been synthesized and their ability to respond to changes in pH, temperature and ionic strength have been characterized. The mechanisms of environmentally responsive hydrogel swelling are well understood[74, 75]. Due to the excellent biocompatibility and tunable properties hydrogels have been studied extensively as a platform for stimuli responsive drug delivery[76-80].

Polyacidic hydrogels have been developed for oral administration of insulin. At low pH values the insulin is entrapped in the collapsed hydrogel, which serves to protect the protein from the harsh environment of the upper gastro-intestinal track. Release of the insulin is triggered by the increase in the environmental pH of the small intestine[81, 82].

The diffusional transport of streptokinase from crosslinked hydrogels of poly(hydroxyethyl methacrylate)-co-poly(diethyl aminoethyl methacrylate) (PHEMA-co-PDEAEM) were investigated[83]. The transport properties were highly dependent on the pH. Near neutral pH the tertiary amine pendants are unionized and the hydrogel is collapsed inhibiting diffusion of drug out of the hydrogel network. On lowering the pH, the PDEAEM protonates, swelling the hydrogel network and increasing the effective rate of drug diffusion out of the gel. This process was shown to be fully reversible; the rate of drug release could be repeatedly modulated by changes in pH.

Glucose sensitive gels have been prepared by a number of researchers[68, 70, 84-87]. These materials function by entrapping or glucose oxides, an enzyme that reacts with glucose to form gluconic acid, within a polycationic hydrogel. When glucose concentrations increase in the presence of the hydrogel the gluconic acid produced lowers the pH in the microenvironment of the hydrogel. The lower pH causes swelling of the hydrogel network and entrapped insulin is allowed to diffuse out of the gel.

A completely synthetic glucose sensitive hydrogel, based on novel phenyl boronic acid monomers has been developed. The LCST of N-Isopropylacrylamide hydrogels, incorporating 5-20% of the novel phenyl boronic acid monomer, could be varied between 22 and 34°C by increasing the concentration of glucose in solution. This material has great potential as a self regulated, glucose-sensitive device that may aid in the treatment of diabetes[88-90].

2.2.2.2. Physical Hydrogels

Aqueous solutions of amphiphilic triblock copolymers of poly(oxyethylene)-block-poly(oxypropylene)-block-poly(oxyethylene) PEO-b-PPO-b-PEO, known by trade names of Pluronic® and Poloxamer®, exhibit thermoresponsive phase behavior due to the LCST of the PPO block. The onset of micelle formation occurs at the critical micellization temperature (CMT) which is dependent on copolymer concentration. Spherical micelles with PPO cores and PEO coronas, and dissolved unimers exist in equilibrium above the CMT. The volume fraction of the micelles continues to increase with increasing temperature due to increased aggregation number of the micelles.[91]. When the micelle volume fraction reaches a critical hard sphere packing volume the solution freezes into a cubic crystal phase[92, 93]. Figure 2.8 shows the relationship of the unimer-micelle and sol-gel transition temperatures with copolymer concentration of Pluronic® F127 PEO₁₀₀-b-PPO₆₅-b-PEO₁₀₀ in water[94]. The

micellar aggregation and gel formation of Pluronic® triblock copolymers in the presence of various salts and pharmaceutically acceptable solvents has been extensively investigated[64, 95-98]. Pluronic® F127, one of the most commonly investigated poloxamers, forms a micellar cubic gel phase within the physiological range[98-101]. The self association of reverse Pluronic®, Pluronic® R (PPO-b-PEO-b-PPO) copolymers, have also been investigated[102-104]. Reverse Pluronic® copolymers undergo various forms of association, including ‘loop’ formation, micellization and gelation. Micelle formation and gelation behavior Pluronic® and Pluronic® R copolymers is highly dependent on molecular weight and the hydrophobic/hydrophilic balance.

Pluronic® analogs with poly(oxyethylene)-block-poly(oxybutylene)-block-poly(oxyethylene) (PEO-b-PBO-b-PEO) were also synthesized by anionic polymerization; their temperature responsive micellization, gelation and drug release properties in aqueous solution were investigated[105, 106]. In addition to the body centered cubic gel phase observed in Pluronic® solutions, PEO-b-PBO-b-PEO copolymer solutions form a hexagonal phase of packed cylindrical micelles and a lamellar gel phase at higher concentrations. This is due to the increased hydrophobicity of the oxybutylene block over the oxypropylene block of the Pluronic® copolymers.

Semibranched Pluronic® and Pluronic® R analogs were synthesized via ATRP. Methoxy-capped oligo(ethylene glycol) methacrylate (OEGMA) was polymerized from a difunctional PPO macroinitiator to generate a POEGMA-b-PPO-b-POEGMA Pluronic® analog[107]. Similarly, oligo(propylene oxide) monomethacrylate (OPOMA) was polymerized from a difunctional PEO macroinitiator to form POPOMA-b-PEO-b-PEPOMA [108]. Thermoreversible micelle formation was observed in solutions of both copolymers. However, no sol-gel transition was reported. The lack of a gel phase is likely due to the

coronal branching interfering with the micelle packing efficiency necessary for gel formation.

Di- and triblock and four and eight arm star copolymers of PEO-b-PNIPAAm were found to form thermoreversible gels. Above the LCST of the PNIPAAm block(s) these copolymers formed an opaque gel phase. Rheology and calorimetry studies were used to infer the gelation mechanism of these materials. The gel formed from the diblock was attributed to closed micelle packing behavior, and the triblock and star copolymers were found to form gels due to associative network formation[109].

Solutions of poly(ethylene oxide-b-(_{D,L}-lactic acid-co-glycolic acid)-b-ethylene oxide) (PEG-PLGA-PEG) copolymers form micelles and soft solid gel phase upon warming[110]. The potential as an injectable drug delivery device has been well recognized and the copolymer is commercially known as a ReGel[®]. The biodegradable PLGA block is four times as hydrophobic as the PPO block of Pluronic[®] copolymers. Drug formulations including this material have been shown to be highly biocompatible [111]. Similar to Pluronic[®], the ReGel[®] copolymer can increase the solubility of hydrophobic drugs and enhance the pharmacokinetics of delicate drugs such as proteins. In vivo formulations of ReGel[®] have been shown to release drug through diffusion and degradation mechanisms for up to 6 weeks [112]. Although ReGel[®] copolymer solutions are liquid at low temperature and form gels upon warming, similar to Pluronic[®] copolymers, the mechanism of gelation is very different. Gel formation of a ReGel[®] solution was monitored with small angle neutron scattering. Figure 2.9 contains the scattering profiles at several temperatures and illustrations of a qualitative interpretation of the results. ReGel[®] copolymer solutions form spherical micelles that aggregate in a random, disordered manner due to macroscopic liquid-liquid phase separation at high temperature[113]. The hydrophobic interaction between core phases

leads to formation of micelle clusters. Gel formation occurs when the clustering of cores reaches a percolation threshold where all clusters are connected. Gels formed from ReGel® solutions are turbid and very soft compared to the transparent, cubic packed micelle gels formed by Pluronic® solutions.

A graft copolymer of poly(ethylene oxide-g-(_{D,L}-lactic acid-co-glycolic acid)) has also been developed that exhibits thermogelling behavior[114-116]. The graft copolymer analog to the ReGel® block copolymer was found to form gels *in vivo* after injection. Gelation of the graft copolymer solution occurred due to micelle percolation, similar to the ReGel® block copolymer[117].

pH responsive, gel forming, triblock copolymers of 2-((diisopropylamino)ethyl methacrylate) (DPA) or 2-((diethylamino)ethyl methacrylate) (DEA) and 2-methacryloyloxyethyl phosphorylcholine (MPC) were synthesized using ATRP[118]. The MPC polymer is highly hydrophilic, and is resistant to protein fouling due to a biomimetic phosphorylcholine (PC) moiety. The development of PC based materials has lead to improved biocompatibility of numerous medical devices[119]. The triblock copolymers dissolved in acidic solution but formed biocompatible free-standing gels around neutral pH in a moderately concentrated (greater than 6 wt%) aqueous solution. Diblock copolymers of MPC-DPA and MPC-DPA formed micelles above the pKa of the DPA and DEA blocks, but did not form gels[120]. The gel forming ability of the triblock copolymer is attributed to the ability of the hydrophilic MPC block to bridge the between separate micelle cores resulting in intermicellar crosslinking. Increasing the length of the hydrophilic MPC block of the copolymer led to the formation of more rigid gels. As would be expected, the gel formation of the copolymer solution had no temperature dependence. Small angle neutron scattering (SANS) was used to confirm the presence of flowerlike micelles in the free flowing solution.

SANS of the free standing gels was described with a 'mesh' model of interconnected micelles with MPC coronas and DPA cores[121].

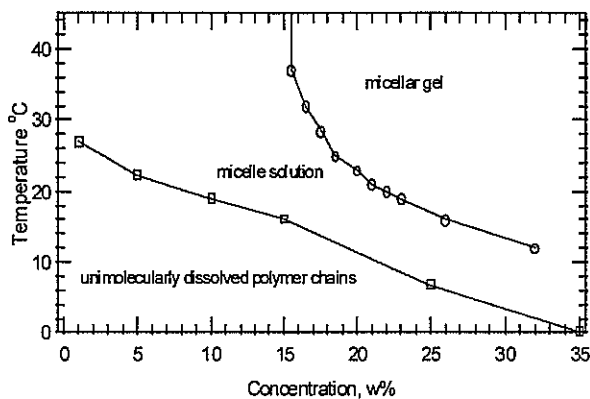


Figure 2.8. Pluronic® F127 phase behavior. Micellization transition was determined by differential scanning calorimetry (DSC) and the sol-gel transition was determined by tube inversion.

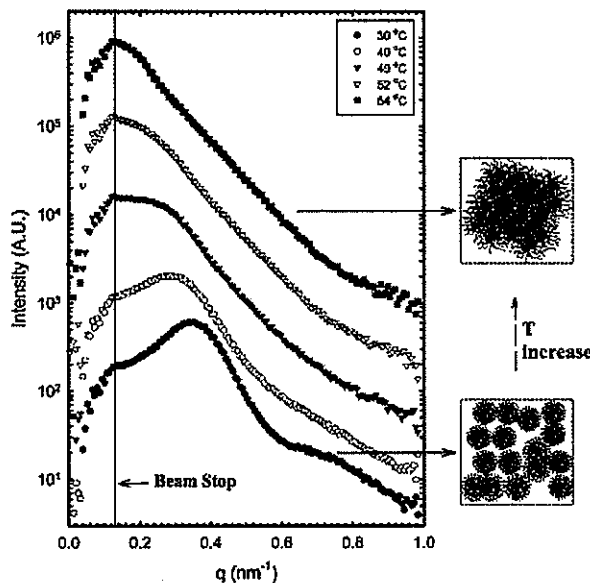


Figure 2.9. SANS profiles of a 24 wt% aqueous solution of PEO-PLGA-PEO (750-3.5K-750) [113]

2.2.2.3. Biomedical Applications of Hydrogels

Development of injectable depots for sustained administration of drugs is an extremely active area of research in academic and industrial laboratories. The efficacy of drug treatment is dependent of the availability of the drug in the body. The concentration of

a drug in the body must be maintained within a range of therapeutic concentration in the body. When the concentration falls below this range no therapeutic effect is realized, and concentrations above this range result in a toxic response. A large number of new pharmaceuticals underdevelopment today are therapeutic proteins[122]. Therapeutic proteins face the additional in vivo challenges of as short circulation times and rapid denaturation[123]. The ability to administer extended releases formulations of protein-based pharmaceuticals is being addressed by a number of schemes. Extended release delivery systems lessen the requirements for repeated administration of drugs such as vaccines.

There are numerous reports of drug release injectable, self-assembling nanostructured gels of Pluronic® F127. The mechanism of drug release from Pluronic® gels was found to be a combination of diffusion of the drug from the gel and erosion of the bulk gel phase. Both were dependent upon the diffusion of water into the gel phase[124, 125]. The safety and tolerability of Pluronic® F68 administered intravenously was tested in healthy human volunteers. Pharmacokinetic parameter values were collected and the poloxamer was determined to be eliminated primarily by renal excretion[126]. Although Pluronic® F127 was found to induce a dose-dependent hyperlipidemia in rabbits, low doses of this polymer are suitable for controlled release drug delivery applications without the untoward hyperlipidemic effect[127].

Owing to the presence of hydrophobic core microdomains within the micelle structure, the solubility of hydrophobic drugs such as naproxen and tropicamide, were significantly increased in Pluronic® formulations, enabling higher loadings[128, 129]. The most common drug delivery method involving Pluronic® copolymers has been sub-cutaneous or intramuscular injection. Pluronic® gel formulations have been extensively investigated as topical gels treatments for burn wounds [130-132] to release ketoprofen [133], piroxicam

[134-137] and silver sulfadiazine [138]. No significant differences were observed between the delivery of recombinant human growth hormone by intramuscular or sub-cutaneous injection routes[139], and an initial burst effect was observed [140]. Some of the applications of Pluronic® copolymers in drug delivery have been for the release of pilocarpine nitrate [141], inulin [142], insulin [143, 144], urease [145], interleukin [146], melanotan [147], methotrexate [148], chymotrypsin and lactose dehydrogenase[149]. Pluronic® gels were also injected in the vicinity of sciatic nerves to provide local controlled release of lidocaine[150]. Pluronic® F127 gels administered as sub-cutaneous injections for drug delivery have provided zero-order release with sustained plateau levels within 15 minutes that last for 8–9 hours[151]. The main drawback of these poloxamer vehicles for drug delivery has been their relatively short release time. Salts have been shown to reduce the drug release rate from poloxamer gels owing to an increase in microviscosity of the aqueous regions of the gel[100].

The formulation and sustained delivery of protein pharmaceuticals was shown to be possible through intra-peritoneal injections of Pluronic® F127 gels[152]. The poloxamers preserved the biological activity of select recombinant-derived protein pharmaceuticals [153, 154] but they could not prevent the thermal denaturation of the proteins at 50°C[155]. Epidural injections of poloxamer gels loaded with drugs prolonged systemic absorption [150] while causing only slight inflammatory changes[156]. Because of their thermoreversible gelation properties at physiological temperatures, Pluronic® F127 gels have also been tested for direct periodontal intrapocket administration of tetracycline[157]. Poloxamers were found to be suitable for ocular delivery [158-163] as well as for rectal administration [164-166]. Pluronic® F127 hydrogels were used for thermal and photochemical delivery of nitric oxide from S-nitrosothiols to local target areas[167].

However, the short release time from Pluronic® gels limits their application as extended release devices. Several researchers have developed extended drug delivery formulations incorporating Pluronic®. A novel reverse thermo-sensitive gel former was synthesized by polymerizing Pluronic®-F127 segments together. Gels prepared from this material were tested as drug delivery systems by releasing an anti-restenosis model drug. A 30% gel of this polymer delivered the drug over 40 days, whereas a Pluronic® F127 gel with the same concentration released the drug over 7 days[168]. An injectable formulation of poly(D,L-Lactide) (PDLA), Pluronic® 101, and lysozyme were codissolved in 1-methyl pyrrolidinone,(NMP). NMP is a biocompatible, water soluble solvent commonly used in drug formulations. The PDLA phase separates upon injection to form a biodegradable network incorporating the lysozyme. In the absence of Pluronic® 101, rapid diffusion out of the porous PDLA monolith results in a burst release of the lysozyme. Incorporation of the Pluronic® into the formulation resulted in a decrease in the initial burst of drug from the formulation and an extended release profile of the protein drugs[169].

Other stimuli responsive gel-forming materials have been applied to drug delivery applications. Gels formed from poly(acrylic acid)-graft-Pluronic® F127 copolymers form thermoreversible hydrogels at a low concentrations[170, 171]. This material has been successfully applied in ocular, nasal, dermal and vaginal drug delivery, and has the trade name Smart Hydrogel™. Gels formed from DPA-b-MPC-b-DPA copolymers demonstrated triggered drug release upon small decrease in the pH during *in vitro* experiments[172]. Thermoreversible gels formed *in situ* by aqueous solutions of enzyme-degraded xyloglucan showed release behavior similar to that of Pluronic® gels[173].

Biodegradable, injectable formulations containing PEG-b-PLGA-b-PEG copolymers have been investigated for drug delivery applications[174]. Predictions of gel degradation

and drug release behavior from PLA-b-PEG-b-PLA gels have been ascertained[175]. Kim and co-workers developed an effective injectable formulation for extended controlled delivery of insulin[176]. The PLGA-PEG-PLGA (ReGel[®]) copolymer forms a hydrogel depot upon subcutaneous injection. The hydrogel is insoluble and controlled release results through a combination of drug diffusion out of the gel network and polymer chain degradation. This formulation has been tested *in vivo* for insulin delivery. Figure 2.10 shows the basal plasma insulin level of Sprague-Dawley rats injected with insulin/ReGel[®] formulation over a 15-day period. Significant increase in the basal plasma insulin level of Sprague-Dawley rats injected with insulin/ReGel[®] formulation over a 15-day period was observed[177]. In comparison, control groups injected with only ReGel[®] were found to have undetectable amounts of plasma insulin. Solutions of Pluronic[®] [178] as well as biodegradable ReGel[®] [112] were used to successfully deliver paclitaxel to tumors through intratumoral injections.

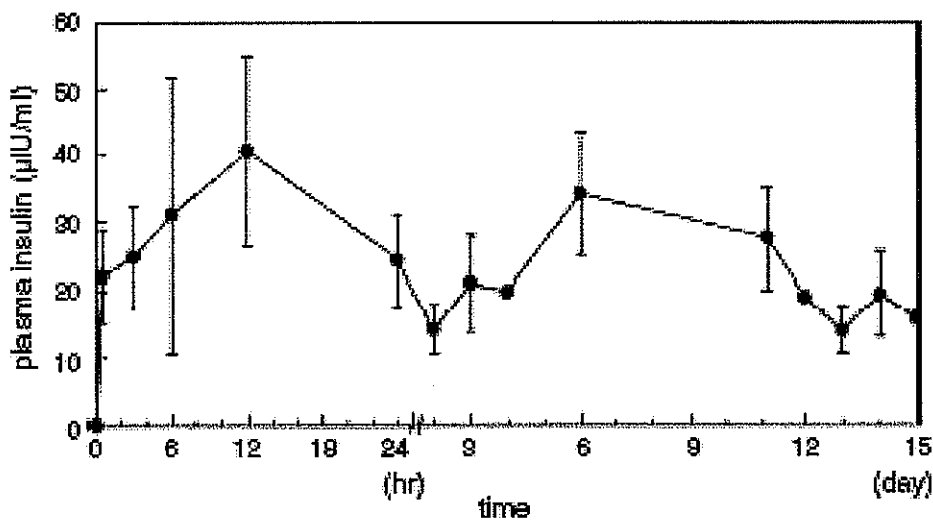


Figure 2.10. Plasma insulin level of male Sprague-Dawley rats ($n = 5$) on fasting. Polymer/insulin/zinc (0.6 ml; 23 wt.% triblock copolymer, 10 IU insulin/ml) solution was injected subcutaneously. From [177]

2.3. Living Radical Polymerization Methods

The development of living radical polymerization (LRP) synthesis has allowed the development of numerous new polymers with functional chemistries and controlled architectures. LRP techniques have many advantages over the traditional radical and anionic polymerization routes[179]. LRP techniques are a versatile means of polymerizing functional monomers, and produce characteristically narrow molecular weight distribution. Previously ionic synthesis was the only practical route towards block copolymers with controlled molecular weight and architecture[12]. Ionic synthesis techniques require rigorous exclusion of water and oxygen and cannot be applied to many functional monomers. LRP techniques have been utilized to synthesize many stimuli responsive copolymers with various controlled architectures.

Several LRP techniques have been developed, atom transfer radical polymerization (ATRP), reversible addition fragmentation transfer (RAFT) polymerization, and nitroxide mediated polymerization (NMP) are the most common. These techniques result in a dynamic equilibrium between actively propagating radicals and dormant polymer chains. Reaction conditions must be selected such that the dormant species is favored in the equilibrium. This results in persistent, low concentrations, of propagating radicals. The low instantaneous concentration of propagating radical species ensures that normal radical termination reactions are effectively suppressed. The techniques differ primarily in the chemistry of the cap on the dormant polymer chain. The ATRP, NMP and RAFT techniques utilize ω -halide, ω -alkoxamine and ω -dithioester caps respectively. ATRP appears to be the most versatile of the LRP techniques.

The first reports of successful atom transfer radical polymerization (ATRP) were independently reported by Matyjaszewski and Sawamoto in 1995[180, 181]. Figure 2.11

depicts the ATRP mechanism. The persistent low concentration of radicals was achieved through halogen transfer between alkyl halides and transition metals in the low oxidation state, to form radicals and transition metals in a high oxidation state. By careful selection of reaction conditions, where termination is effectively suppressed on the time scale of the reaction, molecular weight can be effectively controlled by changing the initiator-to-monomer ratio[182].

The first example of block copolymers produced via ATRP with the macro-initiator approach was the synthesis of polystyrene from difunctional poly(ethylene oxide) macroinitiator[183]. A macromolecule is functionalized with halide groups capable of initiating ATRP synthesis and is subsequently used to initiate reaction. The macroinitiator approach is extremely versatile; commercially available homopolymers produced via anionic techniques can easily be converted into macroinitiators. These initiating blocks generally have very low polydispersity and exhibit very uniform end or side chain functionality. Block copolymers can also be prepared by sequential addition of monomer to the living reaction system.

There are numerous examples of the versatility of LRP techniques. Near monodisperse poly(methacrylic acid) can be prepared by anionic polymerization of a tert-butyl or benzyl methacrylate followed by a step to hydrolyze the protecting group. ATRP has been shown to polymerize sodium methacrylate directly in water[184]. A homopolymer and a block copolymer, initiated by a PEO macroinitiator, of poly(sodium methacrylate) were produced. Subsequently several examples of acidic and hydroxy functional monomers have been prepared directly from ATRP[34, 185-189]. A recent review details the use of ATRP to synthesize block copolymer brushes from functional surfaces[190]. Chen and Armes recently demonstrated successful surface ATRP of a hydrophilic monomer from an

functional polyelectrolyte adsorbed to the surface of an anionic silica sol. This was the first report of a polymer-grafted, colloidally stable ultrafine silica sol prepared in a single step[191].

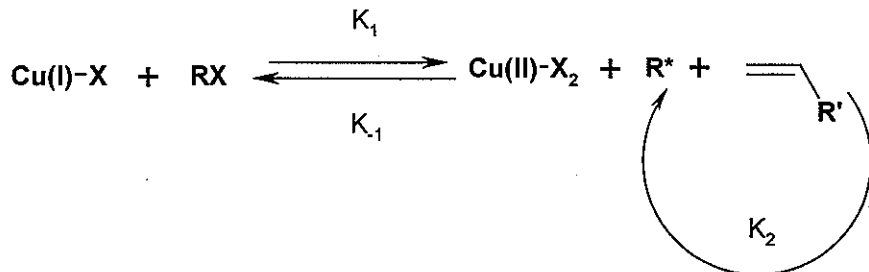


Figure 2.11. Atom transfer radical polymerization mechanism. Adapted from [179]

2.4. Characterization of supramolecular self-assembly

The length scale of self-assembly of amphiphilic block copolymers spans several orders of magnitude from unimer molecules in solution to crystalline micellar solids with centimeter dimensions[8]. Accordingly, no single characterization technique allows for the observation of the various physical transitions of the material. Self-assembly of amphiphilic copolymers is analogous to the self-assembly of low molecular weight surfactants and detergents. Unlike common low molecular-weight surfactants, polymeric amphiphiles are capable of further association on larger length scales. A wide variety of tools such as rheology, Fourier transform infrared spectroscopy (FTIR), static and dynamic light scattering, small angle X-ray scattering (SAXS), small angle neutron scattering (SANS), calorimetry, surface tension, microscopy, nuclear magnetic resonance (NMR) and probe fluorescence methods have been used to study the self-assembly process.

2.4.1 Spectroscopic Techniques

Since polymer chains located in the core of micelles are relatively dehydrated, less mobile and less polar than the corona and bulk phase, NMR can detect the relative degree of

solvation in the separate phases of separate microdomains. A number of investigators have utilized NMR as a means of observing phase separation induced by changes in either pH or temperature[114, 116, 118, 192]. FTIR can be used to track, *in situ*, the changes in hydrogen bonding and the hydration of particular bonds of a material. FTIR has been used to investigate the micellization and gelation of Pluronic® F127 by tracking the backbone ether stretch peaks and the methyl group symmetry deformation peak as a function of temperature and concentration[193, 194]. The fluorescence and UV absorbance of selected probe molecules that are selectively solvated into microdomains formed by amphiphilic block copolymers can be used to investigate self assembly[195]. The critical pH, temperature and concentration for micelle formation has been measured with probe spectroscopy techniques[196-199]. These techniques have been used to determine water content and microviscosity of the hydrophobic microdomains in solution[94, 200].

2.4.2. Energetics of self-assembly

Calorimetric techniques have been utilized to investigate the origins of micelle and gel formation of amphiphilic copolymers. The onset of micelle formation in water is usually accompanied by an endothermic first order transition, corresponding to the energy of dehydration of the hydrophobic block[95]. These results are consistent with the evidence that micellization is driven by entropic gains of segregating the hydrophobic block segments to a core domain. Early studies of the thermodynamics of Pluronic® copolymer micelle self-assembly established an empirical relationship between copolymer concentration, hydrophilic/hydrophobic composition and the critical micellization temperature (CMT)[95, 201]. The standard free energies, enthalpies and entropies of micellization for most Pluronic® copolymers have been reported by numerous authors[97, 202, 203]. The thermodynamic effects of gelation have also been studied with calorimetry. Sharp

endothermic transitions corresponding to the gel formation temperature of poly(oxyethylene)-b-poly(oxybutylene) have been noted by Booth and co-workers[204]. While the formation of Pluronic® micelles results in an easily distinguished transition, the onset of macroscopic gelation appears to have only a minor energy of transition. However, the transitions between micellar crystal mesophases of Pluronic® gels is accompanied by changes in surface area or lattice packing do exhibit first order endothermic thermal transitions[193]. The onset of gelation of the Pluronic® solutions is not due to a thermodynamic transition but because the volume fraction of micelles reaches a critical volume fraction for crystallization of hard-sphere colloidal suspensions[92].

2.4.3. Cryogenic Transmission Electron Microscopy

Cryogenic transmission electron microscopy (cryo-TEM) has been used to directly visualize the micellar structures formed by numerous block copolymers[6]. Thin films of aqueous copolymer solutions are rapidly vitrified to preserve the self assembled structures present at ambient temperature[205]. This allows for direct visual inspection of the morphologies of micelle structure. Spherical, cylindrical and bilayer or vesical micelle structures have been visualized with cryo-TEM as shown in Figure 2.12. Jain and Bates utilized cryo-TEM to observe ‘Y-junctions’ of cylindrical micelles formed from diblock copolymers. The ‘Y-junction’ structure had been predicted theoretically but had not previously been observed experimentally[9].

Zheng and co-workers used cryo-TEM image analysis to determine the corona and core dimensions of poly(ethylene oxide)-b-poly(butadiene) micelles. The relationship between the relative block lengths and micelle morphology was analyzed and a concise model for predicting core and corona dimensions of spherical and worm-like micelles explored[206]. Lam and co-workers used imaging analysis techniques to average the

dimensions from large numbers of spherical micelles formed from dilute solutions of Pluronic® F127. The mean micelle diameters were 10.8 and 6 nm at 10 and 5% concentrations, respectively. The size distribution of the micelles was attributed to the bimodal molecular weight distribution of the Pluronic® F127[207]. Won and co-workers used cryo-TEM to investigate a series of PEO-based block copolymers. The series of diblock copolymers investigated existed in a number of micellar morphologies including vesicle bilayers, cylinders and spheres. They made use of polymer scaling methods to quantitatively analyze the effect of varying the fraction of PEO on micelle dimensions. These morphologies correspond to the increase of interfacial curvature of the hydrophobic core resulting from longer PEO chains. This relationship was quantified by plotting the degree of stretching of the chains located in the hydrophobic core against the interfacial area of the hydrophobic core per chain[208].

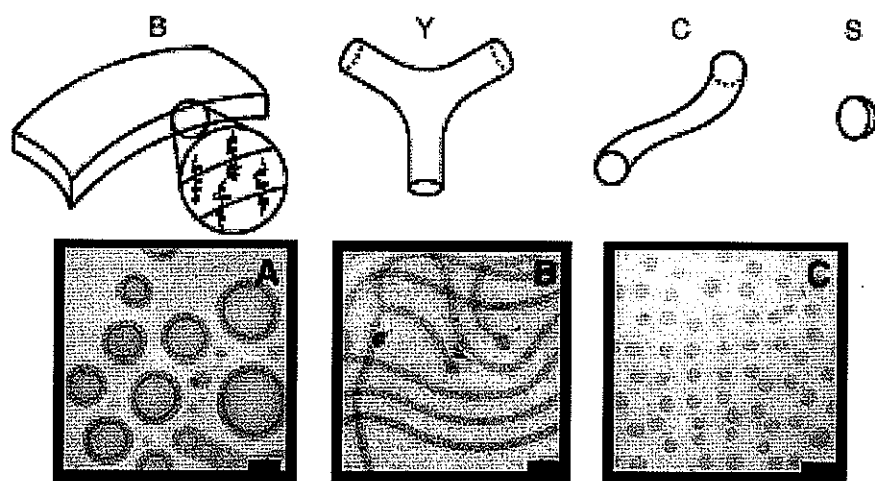


Figure 2.12. Cryo-TEM images of micelles with vesicle, cylindrical and spherical morphologies. From [9]

2.4.4. Small angle X-ray and Neutron Scattering

Small angle scattering techniques are an excellent means of characterizing structural features of with length scales in the range of tens to hundreds of angstroms. Small angle scattering is commonly used to investigate systems of particles in solution (micelles or colloids) and periodic systems (micelle networks or lamella). Small angle scattering data is the result of inhomogeneities in the scattering length density of a material. For X-rays, the scattering length density is a function of electron density and for neutrons it is dependent on the complex interactions of neutrons with atomic nuclei. Guinier and Fournet first collected the fundamental principles of small angle scattering in a classic monograph [209]. Many advances in the experimental methods, notably the development and construction of third generation synchrotron radiation and high flux spallation neutron sources, have increased the potency of the technique for structural analysis of materials [210, 211]. Several specialized methods of data analysis have been developed for block copolymer micelle systems [212, 213]. Many of these methods consist of non-linear least square fitting of analytical models to the small angle scattering data. These models are developed to describe intra-micellar scattering (the form factor) and the inter-micellar scattering (the structure factor). The implementation of these models requires careful treatment of the data and judicious usage of collaborative techniques, such as cryo-TEM, to extract physically meaningful data [214]. Recent advances in model-free analysis techniques allow for extraction of micelle dimension and shape with a minimum of *a priori* information [215]. SAXS and SANS techniques, while theoretically similar offer a number of practical differences that can be exploited experimentally. Typically there is very little contrast in electron scattering length density between organic polymers and water, while the nuclear scattering length density contrast can be varied by adjusting the D₂O/H₂O ratio in SANS experiments.

2.4.5. Laser Light Scattering

Macromolecular and colloidal particles, when immersed in a fluid are able to scatter light. The angular variation of the excess absolute scattering intensity, known as the Rayleigh ratio (R_θ), of the scattered light, depends strongly on the particle size and concentration and the wavelength of the incident radiation. Classical light scattering refers to elastic interactions between radiation and the particles in solution. That is, the light reradiated at the same frequency as the incident light is observed. The classical development of light scattering theory has been extensively described by Johnson[216]. Laser light scattering techniques are widely applied for the characterization of weight average molecular weights and radius of gyration of macromolecules[2, 217]. Light scattering can also be applied to determine size and molecular weight of micelle solutions. Micelles formed from block copolymers behave as colloidal particles, with dimensions 10-100 nm. When the particles are no longer small compared to the wavelength of light, ($d < \lambda/20$), intra-particle interference becomes important in light scattering experiments. Classical light scattering is very sensitive to intermolecular association and is commonly used to characterize the self-assembly structures of amphiphilic block copolymers. Because *a priori* knowledge of the scatterer geometry is required, and size polydispersity is often a significant factor, direct application of an intraparticle interference factor is not practical. Typically the relative scattered intensity versus scattering vector relationship, R_θ vs q , is fit via regression techniques to extrapolate dimensions of the particles. Common variations of these techniques include Zimm (R_θ^{-1} vs q^2) and Debye (R_θ vs q^2) and Berry ($R_\theta^{-1/2}$ vs q^2) analyses[217].

Lui and co-workers investigated Pluronic® L44 and P84 micelles in moderately concentrated solutions to determine molecular weight, micelle aggregation number and hydrated volume fraction as a function of temperature [218]. In order to overcome the

experimental difficulties associated with collecting useful scattering information from solutions of small particles in low concentrations, they introduced a variation on the classical Zimm formulism of calculating weight average molecular mass from light scattering data. This new analysis is analogous to the Zimm formulism and can be applied to aggregating systems over a wider range of concentrations, when the structure and nature of the particle interactions are independent of concentration. The results are in good agreement with the aggregation number determined by small angle neutron scattering.

Quasi-elastic light scattering (QELS) or photon correlation spectroscopy relies on the phenomenon that the rapid fluctuations in the re-radiated light are related to the diffusion rate of the scattering particles. The diffusion rate is used to directly calculate the effective, geometry independent, hydrodynamic radius of the particles[219]. QELS or dynamic light scattering is a particularly versatile means of characterizing of the size and size distributions of dispersed particles with dimensions in the range of 5-2500 nm.

2.4.6. Mechanical Properties

The mechanical properties of physical hydrogels formed from block copolymers have been investigated with a number a techniques. Additionally, rheology and mechanical studies offer an excellent means of investigating the sol-gel transition temperature of thermoreversible hydrogels[220]. The viscoelastic properties of hydrogels are highly dependent on temperature, concentration and chemical environment. The drug delivery applications of hydrogels are determined largely by the viscoelastic properties of the gel *in vivo*. The value of the shear modulus of a hydrogel is indicative of the structuring in the system. Investigations of the rheological properties of Pluronic® copolymers[96, 221, 222], PLLA-PEG-PLLA/PDLA-PEG-PDLA polymers [223], Pluronic®-g-PAA [224] and PEG-g-PLGA [114-116] have been conducted. The simplest of all rheological measurements, and

probably the most widely used, is the tube inversion test. Most researchers use similar criteria for the difference between solution and gel; upon inversion the contents of a gel must remain set for a few minutes to be considered a gel.

The kinetics of gelation of poloxamer gels has also been investigated using shear measurements. Pulse shearometry was used to determine the shear modulus of the semisolid gel by generating a torsional force that is transmitted through the sample at discrete time intervals. The results showed that increasing the molecular weight of the hydrophobic PPO in the poloxamers with identical PEO:PPO unit ratios decreased the concentration of the poloxamer required to achieve the same gelation temperature[221]. Wang and Johnston employed a pulse shear rheometry to measure the shear modulus of Pluronic® solutions and hydrogels. This method is especially useful for hydrogels because it is very non-invasive, thus minimizing disruptions to the gel formation process. The heat transfer through the polymer solutions dominated the kinetics of the gelation process. This result has significant implications for the parenteral injection of Pluronic®-based drug delivery devices. A slow-forming gel, once injected, could result in a ‘burst effect,’ as a low viscosity gel network does not possess the zero order release properties that make Pluronic® hydrogels an attractive delivery device[146].

Dynamic mechanical analysis provides quantitative information about the viscoelastic character of a gel. Mechanical analysis data acquired while scanning over a range of temperatures has been used to determine the gel point of a system and observe the kinetics of the gelation process. Wanka and co-workers used rheology to determine the CMT and the gelation point of Pluronic® solutions. The gelation point was marked by a 103-fold increase in the shear modulus within a small temperature range. Upon gelation the shear modulus did not significantly increase with temperature. The maximum shear in this region was a function

of the Pluronic® concentration. The onset of gelation was also accompanied by a yield stress that was not present in the low temperature solutions. This yield stress corresponded with the sudden increase in shear modulus, and suggests that moduli of the sol-gel phases are governed by different types of structures[64].

2.5. References

1. Langer, R. and N.A. Peppas, *Advances in Biomaterials, Drug Delivery, and Bionanotechnology*. AIChE J., 2003. **49**(12): p. 2990.
2. Sperling, L.H., *Introduction to Physical Polymer Science*. 3rd ed. 2001, New York: John Wiley and Sons, Inc.
3. Hamley, I.W., *The physics of block copolymers*. 1998, New York: Oxford University Press.
4. Hagberg, E.C., et al., *Development of a Versatile Methodology for the Synthesis of Poly(2,5-benzophenone) Containing Coil-Rod-Coil Triblock Copolymers*. *Macromolecules*, 2004. **37**: p. 3642-3650.
5. Kato, T., *Self-assembly of phase-segregated liquid crystal structures*. *Science*, 2002. **295**(5564): p. 2414.
6. Wang, H., et al., *Syntheses of Amphiphilic Diblock Copolymers Containing a Conjugated Block and Their Self-Assembling Properties*. *Journal of American Chemical Society*, 2000. **122**: p. 6855-6861.
7. Ball, P., *How to keep dry in water*. *Nature*, 2003. **423**: p. 25-26.
8. Alexandridis, P. and B. Lindman, *Amphiphilic Block Copolymers: Self-Assembly and Applications*. 2000, New York: Elsevier.
9. Jain, S. and F.S. Bates, *On the Origins of Morphological Complexity in Block Copolymer Surfactants*. *Science*, 2003. **300**.
10. Lum, K., D. Chandler, and J.D. Weeks, *Hydrophobicity at Small and Large Length Scales*. *J. Phys. Chem. B*, 1999. **103**: p. 4570-4577.
11. Whitesides, G.M. and B. Grzybowski, *Self-assembly at all scales*. *Science*, 2002. **295**(5564): p. 2418.
12. Bates, F.S. and G.H. Fredrickson, *Block Copolymer Thermodynamics: Theory and Experiment*. *Annu. Rev. Phys. Chem*, 1990. **41**: p. 525-557.
13. Wooley, K.L., *Shell crosslinked polymer assemblies: Nanoscale constructs inspired from biological systems*. *J. Polym. Sci., Part A: Polym. Chem.*, 2000. **38**: p. 1397.
14. Jeong, B. and A. Gutowska, *Lessons from Nature: stimuli-responsive polymers and their biomedical applications*. *Trends in Biotechnology*, 2002. **20**(7): p. 305.
15. Hoffman, A.S. *Really smart bioconjugates of smart polymers and receptor proteins*. in *Sixth World Biomaterials Congress*. 2000. Kamuela, HI.
16. Gil, E.S. and S.M. Hudson, *Stimuli-responsive polymers and their bioconjugates*. *Progress in Polymer Science*, 2004: p. 1-50.

17. Hoffman, A.S., *Thermally-induced hydrogels*. Polymer Preprints (American Chemical Society, Division of Polymer Chemistry), 2000. **41**(1): p. 707.
18. Mortimer, D.A., *Synthetic polyelectrolytes - a review*. Polym. Int., 1991. **25**(1): p. 29-41.
19. Hashidzume, A., Y. Morishima, and K. Szczbialka, *Amphiphilic Polyelectrolytes*, in *Polyelectrolytes and their Applications*, S.K. Tripathy, J. Kumar, and H.S. Nalwa, Editors. 2002, American Scientific Publishers: Stevenson Ranch. p. 2-57.
20. Park, S.Y. and Y.H. Bae, *Novel pH-sensitive polymers containing sulfonamide groups*. Macromol. Rapid Commun., 1999. **20**: p. 269-273.
21. Han, S.K., K. Na, and Y.H. Bae, *Sulfonamide based pH-sensitive polymeric micelles: physicochemical characteristics and pH-dependent aggregation*. Colloids and Surfaces, A: Physicochemical and Engineering Aspects, 2003. **214**: p. 49-59.
22. Hoffman, A.S., *Bioconjugates of Intelligent Polymers and Recognition Proteins for Use in Diagnostics and Affinity Separations*. Clinical Chemistry, 2000. **46**(9): p. 1478-1486.
23. Hoffman, A.S., et al., *Bioinspired polymers that control intracellular drug delivery*. Biotechnol. Bioprocess Eng., 2001. **6**(4): p. 205-212.
24. Chen, B., S. Piletsky, and A.P.F. Turner, *Molecular Recognition: Design of "Keys"*. Combinatorial Chemistry & High Throughput Screening, 2002. **5**(6): p. 409-427.
25. Roberts, M.J., M.D. Bentley, and J.M. Harris, *Chemistry for peptide and protein PEGylation*. Adv Drug Deliv Rev, 2002. **54**: p. 459-476.
26. Zuber, G., et al., *Towards synthetic viruses*. Adv Drug Deliv Rev, 2001. **52**: p. 245-253.
27. Kamiya, H., et al., *Intracellular trafficking and transgene expression of viral and non-viral gene vectors*. Adv Drug Deliv Rev, 2001. **52**: p. 153-164.
28. Arotcüarena, M., et al., *Switching the Inside and the Outside of Aggregates of Water-Soluble Block Copolymers with Double Thermoresponsivity*. Journal of American Chemical Society, 2002. **124**(14): p. 3787-3793.
29. Weaver, J.V.M., S.P. Armes, and V. Butun, *Synthesis and aqueous solution properties of a well-defined thermo-responsive schizophrenic diblock copolymer*. Chem. Commun, 2002. **2002**: p. 2122-2123.
30. Patrickios, C.S., et al., *Diblock, ABC triblock, and random methacrylic polyampholytes: synthesis by group transfer polymerization and solution behavior*. Macromolecules, 1994. **27**(4): p. 930-937.
31. Patrickios, C.S., et al., *Precipitation of a Water-Soluble ABC Triblock Methacrylic Polyampholyte: Effects of Time, pH, Polymer Concentration, Salt Type and Concentration, and Presence of a Protein*. Langmuir, 1999. **15**(5): p. 1613-1620.
32. Dai, S., et al., *Novel pH-Responsive Amphiphilic Diblock Copolymers with Reversible Micellization Properties*. Langmuir, 2003. **19**(12): p. 5175.
33. Liu, S. and S. P. Armes, *Polymeric Surfactants for the New Millennium: A pH-Responsive, Zwitterionic, Schizophrenic Diblock Copolymer*. Angew. Chem. Int. Ed., 2002. **41**(8): p. 1413.
34. Bories-Azeau, X., S.P. Armes, and H.J.W.v.d. Haak, *Facile Synthesis of Zwitterionic Diblock Copolymers without Protecting Group Chemistry*. Macromolecules, 2004. **37**(7): p. 2348-2352.

35. Gohy, J.-F., et al., *Aggregates Formed by Amphoteric Diblock Copolymers in Water*. *Macromolecules*, 2000. **33**(17): p. 6378-6387.
36. Weaver, J.V.M., S.P. Armes, and S. Liu, *A "Holy Trinity" of Micellar Aggregates in Aqueous Solution at Ambient Temperature: Unprecedented Self-Assembly Behavior from a Binary Mixture of a Neutral-Cationic Diblock Copolymer and an Anionic Polyelectrolyte*. *Macromolecules*, 2003. **36**: p. 9994-9998.
37. Liu, S., N.C. Billingham, and S.P. Armes, *A Schizophrenic Water-Soluble Diblock Copolymer*. *Angew. Chem. Int. Ed.*, 2001. **40**(12): p. 2328-2331.
38. Lee, A.S., et al., *Characterizing the Structure of pH Dependent Polyelectrolyte Block Copolymers Micelles*. *Macromolecules*, 1999. **32**: p. 4302-4310.
39. Lee, A.S., et al., *Structure of pH-Dependent Block Copolymer Micelles: Charge and Ionic Strength Dependence*. *Macromolecules*, 2002. **35**(22): p. 8540-8551.
40. Zhulina, E.B. and O.V. Borisov, *Polyelectrolytes grafted to curved surfaces*. *Macromolecules*, 1996. **29**(7): p. 2618-2626.
41. Ma, Q., et al., *Environmentally-Responsive, Entirely Hydrophilic, Shell Cross-linked (SCK)Nanoparticles*. *Nano Letters*, 2001. **1**(11): p. 651-655.
42. Thurmond, K.B., T. Kowalewski, and K.L. Wooley, *Water-Soluble Knebel-like Structures: The Preparation of Shell-Cross-Linked Small Particles*. *J. Am. Chem. Soc.*, 1996. **118**: p. 7239.
43. Butun, V., et al., *Synthesis of Shell Cross-Linked Micelles at High Solids in Aqueous Media*. *Macromolecules*, 2000. **33**(1).
44. Zhang, Q., E.E. Remsen, and K.L. Wooley, *Shell Cross-Linked Nanoparticles Containing Hydrolytically Degradable, Crystalline Core Domains*. *J. Am. Chem. Soc.*, 2000. **122**: p. 3642-3651.
45. Liu, S. and S.P. Armes, *The Facile One-Pot Synthesis of Shell Cross-Linked Micelles in Aqueous Solution at High Solids*. *J. Am. Chem. Soc.*, 2001. **123**(40): p. 9910-9911.
46. Liu, S., et al., *Synthesis of Shell Cross-Linked Micelles with pH-Responsive Cores Using ABC Triblock Copolymers*. *Macromolecules*, 2002. **35**(16): p. 6121-6131.
47. Hayashi, H., et al., *pH-Sensitive Nanogel Possessing Reactive PEG Tethered Chains on the Surface*. *Macromolecules*, 2004. **37**(14): p. 5389.
48. Leung, M.F., et al., *New Route to Smart Core-Shell Polymeric Microgels: Synthesis and Properties*. *Macromol. Rapid Commun.*, 2004. **25**: p. 1819-1823.
49. Rosler, A., G.W.M. Vandermeulen, and H.-A. Klok, *Advanced drug delivery devices via self-assembly of amphiphilic block copolymers*. *Adv Drug Deliv Rev*, 2001. **53**: p. 95-108.
50. Ge, H., et al., *Preparation, Characterization, and Drug Release Behaviors of Drug Nimodipine-Loaded Poly(e-caprolactone)-Poly(ethyleneoxide)-Poly(e-caprolactone) Amphiphilic Triblock Copolymer Micelles*. *Journal of Pharmaceutical Sciences*, 2002. **91**(6): p. 1463.
51. Stepanek, M., et al., *Solubilization and release of hydrophobic compounds from block copolymer micelles. I. Partitioning of pyrene between polyelectrolyte micelles and the aqueous phase*. *Acta Polymer*, 1998. **49**: p. 96-102.
52. Teng, Y., et al., *Release Kinetics Studies of Aromatic Molecules into Water from Block Polymer Micelles*. *Macromolecules*, 1998. **31**: p. 3578-3587.

53. Kwon, G.S.N., Mayumi; Kataoka, Kazunori; Yokoyama, Masayuki; Sakurai, Yasuhisa; Okano, Teruo., *Block copolymer micelles as vehicles for hydrophobic drugs*. *Colloids Surf., B*, 1994. **24**(4): p. 429-34.
54. Ya-Ping Li, X.-J.G., *PEGylated PLGA nanoparticles as protein carriers: synthesis, preparation and biodistribution in rats*. *Journal of Controlled Release*, 2001. **2**: p. 203-211.
55. Gillies, E.R. and J.M.J. Fréchet, *Development of acid-sensitive copolymer micelles for drug delivery*. *Pure Appl. Chem.*, 2004. **76**(7-8): p. 1295-1307.
56. Kataoka, K., A. Harada, and Y. Nagasaki, *Block copolymer micelles for drug delivery: design, characterization and biological significance*. *Advanced Drug Delivery Reviews*, 2001. **47**: p. 113-131.
57. Tang, Y., et al., *Solubilization and Controlled Release of a Hydrophobic Drug Using Novel Micelle-Forming ABC Triblock Copolymers*. *Biomacromolecules*, 2003. **4**(6): p. 1636-1645.
58. Stoescu, R., A. Graff, and W. Meier, *Asymmetric ABC-Triblock Copolymer Membranes Induce a Directed Insertion of Membrane Proteins*. *Macromolecular Bioscience*, 2004. **4**(10): p. 930-935.
59. Godbey, W.T. and A.G. Mikos, *Recent progress in gene delivery using non-viral transfer complexes*. *Journal of Controlled Release*, 2001. **72**: p. 115-125.
60. Lai, E. and J.H.v. Zanten, *Monitoring DNA/Poly-L-lysine Polyplex Formation with Time-Resolved Multiangle Laser Light Scattering*. *Biophysical Journal*, 2001. **80**: p. 864-873.
61. Benns, J.M., et al., *pH-Sensitive Cationic Polymer Gene Delivery Vehicle: N-Acetyl-l-histidine)-graft-poly(L-lysine) Comb Shaped Polymer*. *Bioconjugate Chemistry*, 2000. **11**(5): p. 637.
62. Kabanov, A.V., et al., *Pluronic block copolymers: novel functional molecules for gene therapy*. *Adv Drug Deliv Rev*, 2002. **54**: p. 223-233.
63. Pedersen, J.S., et al., *A Small-Angle Neutron and X-ray Contrast Variation Scattering Study of the Structure of Block Copolymer Micelles: Corona Shape and Excluded Volume Interactions*. *Macromolecules*, 2003. **34**: p. 416-433.
64. Wanka, G.H., H.; Ulbricht, W., *The aggregation behavior of poly(oxyethylene)-poly(oxypropylene)-poly(oxyethylene) block copolymers in aqueous solution*. *Colloid Polym. Sci.*, 1990. **268**(2): p. 101-17.
65. Badiger, M.V., et al., *Molecular tailoring of thermoreversible copolymer gels: Some new mechanistic insights*. *Journal of Chemical Physics*, 1998. **109**(3): p. 1175-1184.
66. Tanaka, F., *Polymer-surfactant interaction in thermoreversible gels*. *Macromolecules*, 1998. **31**(2): p. 384-393.
67. Peppas, N.A., et al., *Physicochemical Foundations and structural design of hydrogels in Medicine and Biology*. *Annu. Rev. Biomed. Eng*, 2000. **2**: p. 9-29.
68. Ishihara, K., et al., *Glucose-induced permeation control of insulin through a complex membrane consisting of immobilized glucose oxidase and a polyamine*. *Polym. J. (Tokyo)*, 1984. **16**(8): p. 625-31.
69. Gilbert, J.C., et al., *Drug release from Pluronic F-127 gels*. *Int. J. Pharm.*, 1986. **32**(2-3): p. 223-8.

70. Kost, J., et al., *Glucose-sensitive membranes containing glucose oxidase: Activity, swelling, and permeability studies*. J. Biomed. Mater. Res., 1985. **19**(9): p. 1117-33.

71. Qiu, Y. and K. Park, *Environment-sensitive hydrogels for drug delivery*. Advanced Drug Delivery Reviews, 2001(53): p. 321-339.

72. Kost, J. and R. Langer, *Responsive Polymeric delivery systems*. Advanced Drug Delivery Reviews, 2001. **46**: p. 125-148.

73. Jeong, B., S.W. Kim, and Y.H. Bae, *Thermosensitive sol-gel reversible hydrogels*. Advanced Drug Delivery Reviews, 2002(54): p. 37-51.

74. Lele, A.K., I. Devotta, and R.A. Mashelkar, *Predictions of thermoreversible volume phase transitions in copolymer gels by lattice-fluid-hydrogen-bond theory*. Journal of Chemical Physics, 1997. **106**(11): p. 4768-4772.

75. Lee, P.I. and N.A. Peppas, *Prediction of polymer dissolution in swellable controlled-release systems*. J. Controlled Release, 1987. **6**: p. 207-15.

76. Schwarte, L.M.P., Kairali; Peppas, Nicholas A, *Cationic hydrogels for controlled release of proteins and other macromolecules*. ACS Symposium Series, 1998. **709**: p. 56-66.

77. Hariharan, D. and N.A. Peppas, *Characterization, dynamic swelling behavior and solute transport in cationic networks with applications to the development of swelling-controlled release systems*. Polymer, 1996. **37**(1): p. 149-61.

78. Peppas, N.A., *Devices based on intelligent biopolymers for oral protein delivery*. Int J Pharm, 2004. **277**(1-2): p. 11-7.

79. Peppas, N.A. and Y. Huang, *Nanoscale technology of mucoadhesive interactions*. Adv Drug Deliv Rev, 2004. **56**(11): p. 1675-87.

80. Uludag, H., et al., *Engineering Temperature-Sensitive Poly(N-Isopropylacrylamide) Polymers as Carriers of Therapeutic Proteins*. biotechnology and Bioengineering, 2000. **73**(6): p. 510.

81. Foss, A.C. and N.A. Peppas, *Acrylic-Based Copolymers for Oral Insulin Delivery Systems*. Polymer Preprints, 2001. **42**(2): p. 94.

82. Morishita, M., et al., *Elucidation of the mechanism of incorporation of insulin in controlled release systems based on complexation polymers*. Journal of Controlled Release, 2002. **81**: p. 25-32.

83. Vakkalanka, S.K., C.S. Brazel, and N.A. Peppas, *Temperature and pH sensitive terpolymers for modulated delivery of streptokinase*. J. Biomater. Sci. Poly. Ed., 1996. **8**: p. 119-129.

84. Albin, G.H., Thomas A.; Ratner, Buddy D., *Glucose sensitive membranes for controlled delivery of insulin: Insulin transport studies*. J. Controlled Release, 1985. **2**: p. 153-64.

85. Ishikawa, M.S., D W; Raskin, P; Quinn, C A, *Initial evaluation of a 290-microm diameter subcutaneous glucose sensor: glucose monitoring with a biocompatible, flexible-wire, enzyme-based amperometric microsensor in diabetic and nondiabetic humans*. JOURNAL OF DIABETES AND ITS COMPLICATIONS, 1998. **12**(6): p. 295-301.

86. Kang, S.I. and Y.H. Bae, *A sulfonamide based glucose-responsive hydrogel with covalently immobilized glucose oxidase and catalase*. Journal of Controlled Release, 2003. **86**(1): p. 115-121.

87. Podual, K., F.J. Doyle, and N.A. Peppas, *Preparation and dynamic response of cationic copolymer hydrogels containing glucose oxidase*. *Polymer*, 2000. **41**: p. 3975-3983.
88. Matsumoto, A., et al., *Glucose-Responsive Polymer Bearing a Novel Phenylborate Derivative as a Glucose-Sensing Moiety Operating at Physiological pH Conditions*. *Biomacromolecules*, 2003. **4**(5): p. 1410-1416.
89. Shiomori, K., et al., *Thermoresponsive Properties of Sugar Sensitive Copolymer of N-Isopropylacrylamide and 3-(Acrylamido)phenylboronic Acid*. *Macromolecular Chemistry and Physics*, 2004. **205**: p. 27-34.
90. Matsumoto, A., R. Yoshida, and K. Kataoka, *Glucose-Responsive Polymer Gel Bearing Phenylborate Derivative as a Glucose-Sensing Moiety Operating at the Physiological pH*. *Biomacromolecules*, 2004. **5**: p. 1038-1045.
91. Wu, G.C., Benjamin; Schneider, Dieter K., *SANS Study of the Micellar Structure of PEO/PPO/PEO Aqueous Solution*. *J. Phys. Chem.*, 1995. **99**(14): p. 5094-101.
92. Mortensen, K., *Phase behavior of poly(ethylene oxide)-poly(propylene oxide)-poly(ethylene oxide) triblock-copolymer dissolved in water*. *Europhys. Lett.*, 1992. **19**(7): p. 599-604.
93. Park, M.J. and K. Char, *Two Gel States of PEO-PPO-PEO Triblock Copolymer Formed by Different Mechanisms*. *Macromol. Rapid Commun.*, 2002. **23**(12): p. 688-692.
94. Jeon, S., et al., *Microviscosity in poly(ethylene oxide)-polypropylene oxide-poly(ethylene oxide) block copolymers probed by fluorescence depolarization kinetics*. *Journal of Polymer Science Part B-Polymer Physics*, 2002. **40**(24): p. 2883-2888.
95. Wanka, G.H., H.; Ulbricht, W, *Phase Diagrams and Aggregation Behavior of Poly(oxyethylene)-Poly(oxypropylene)-Poly(oxyethylene) Triblock Copolymers in Aqueous Solutions*. *Macromolecules*, 1994. **27**(15): p. 414594149.
96. Jorgensen, E.B., et al., *Effects of Salts on the Micellization and Gelation of a Triblock Copolymer Studied by Rheology and Light Scattering*. *Macromolecules*, 1997. **30**(8): p. 2355-2364.
97. Pandit, N., et al., *Effect of Salts on the Micellization, Clouding, and Solubilization Behavior of Pluronic F127 Solutions*. *J. Colloid Interface Sci.*, 2000. **222**(2): p. 213-220.
98. Ivanova, R., B. Lindman, and P. Alexandridis, *Evolution in Structural Polymorphism of Pluronic F127 Poly(ethylene oxide)-Poly(propylene oxide) Block Copolymer in Ternary Systems with Water and Pharmaceutically Acceptable Organic Solvents: From "Glycols" to "Oils"*. *Langmuir*, 2000. **16**(23): p. 9058-9069.
99. Hecht, E., et al., *Interaction of ABA Block-Copolymers with Ionic Surfactants - Influence on Micellization and Gelation*. *Journal of Physical Chemistry*, 1995. **99**(13): p. 4866-4874.
100. Pandit, N.K. and J. Kisaka, *Loss of gelation ability of Pluronic F127 in the presence of some salts*. *Int. J. Pharm.*, 1996. **145**(1,2): p. 129-136.
101. Anderson, B.C., et al., *The effect of salts on the micellization temperature of aqueous poly(ethylene oxide)-b-poly(propylene oxide)-b-poly(ethylene oxide) solutions and the*

dissolution rate and water diffusion coefficient in their corresponding gels. Journal of Pharmaceutical Sciences, 2002. **91**(1): p. 180-188.

102. Zhou, Z. and B. Chu, *Phase Behavior and Association Properties of Poly(oxypropylene)-Poly(oxyethylene)-Poly(oxypropylene) Triblock Copolymer in Aqueous Solution.* Macromolecules, 1994. **27**(8): p. 2025-33.
103. Mortensen, K., *Cubic Phase in a Connected Micellar Network of Poly(propylene oxide)-Poly(ethylene oxide)-Poly(propylene oxide) Triblock Copolymers in Water.* Macromolecules, 1997. **30**(3): p. 503-507.
104. Mortensen, K., W. Brown, and E. Joergensen, *Phase Behavior of Poly(propylene oxide)-Poly(ethylene oxide)-Poly(propylene oxide) Triblock Copolymer Melt and Aqueous Solutions.* Macromolecules, 1994. **27**(20): p. 5654-66.
105. Li, H., et al., *Mesophase Behavior of Aqueous Micellar Solutions of Triblock Copolymers of Ethylene Oxide and 1,2-Butylene Oxide (Type EmBnEm).* Langmuir, 2003. **19**: p. 1075-1081.
106. Luo, Y.Z., et al., *Block-Copoly(Oxyethylene Oxybutylene Oxyethylene), E40b15e40, in Aqueous-Solution - Micellization, Gelation and Drug Release.* Journal of the Chemical Society-Faraday Transactions, 1993. **89**(3): p. 539-546.
107. Robinson, K.L., et al., *Synthesis of Well-Defined, Semibranchend, Hydrophilic-Hydrophobic Block Copolymers Using Atom Transfer Radical Polymerization.* Macromolecules, 2001. **34**(17): p. 5799-5805.
108. Truelsen, J.H., et al., *Novel Polymeric Surfactants: Synthesis of Semi-Branched, Non-Ionic Triblock Copolymers Using ATRP.* Macromolecular Chemistry and Physics, 2002(2003): p. 2124-2131.
109. Lin, H.-H. and Y.-L. Cheng, *In-Situ Thermoreversible Gelation of Block and Star Copolymers of Poly(ethylene glycol) and Poly(N-isopropylacrylamide) of Varying Architectures.* Macromolecules, 2001. **34**(11): p. 3710-3715.
110. Jeong, B., et al., *Biodegradable block copolymers as injectable drug-delivery systems.* Nature, 1997. **388**(6645): p. 860-862.
111. Zange, R., Y. Li, and T. Kissel, *Biocompatibility testing of ABA triblock copolymers consisting of poly(L-lactic-co-glycolic acid) A blocks attached to a central poly(ethylene oxide) block under in vitro conditions using different L929 mouse fibroblasts cell culture models.* Journal of Controlled Release, 1998. **56**: p. 249-258.
112. Zentner, G.M., et al., *Biodegradable block copolymers for delivery of proteins and water-insoluble drugs.* Journal of Controlled Release, 2001. **72**(1-3): p. 203-215.
113. Park, M.J. and K. Char, *Gelation of PEO-PLGA-PEO Triblock Copolymers Induced by Macroscopic Phase Separation.* Langmuir, 2004. **20**(6): p. 2456-2465.
114. Jeong, B., L.-Q. Wang, and A. Gutowska, *Biodegradable thermoreversible gelling PLGA-g-PEG copolymers.* Chemcomm Communication, 2001: p. 1516-1517.
115. Jeong, B., et al., *Thermogelling Biodegradable Polymers with Hydrophilic Backbones: PEG-g-PLGA.* Macromolecules, 2000(33): p. 8317-8322.
116. Chung, Y.-M., et al., *Sol-Gel Transitiong Temperature of PLGA-g-PEG Aqueous Solutions.* Biomacromolecules, 2002(3): p. 511-516.
117. Jeong, B., et al., *Phase Transition of the PLGA-g-PEG Copolymer Aqueous Solutions.* J. Phys. Chem B, 2003. **107**: p. 10032-10039.

118. Ma, Y., et al., *Synthesis of Biocompatible, Stimuli-Responsive, Physical Gels Based on ABA Triblock Copolymers*. Biomacromolecules, 2003. **4**(4): p. 864-8.
119. Ma, I.Y., et al., *Synthesis of Biocompatible Polymers. 1. Homopolymerization of 2-Methacryloyloxyethyl Phosphorylcholine via ATRP in Protic Solvents: An Optimization Study*. Macromolecules, 2002. **35**(25): p. 9306-9314.
120. Lobb, E.J., et al., *Facial Synthesis of Well-Defined, Biocompatible Phosphorylcholine-based Methacrylate Copolymers via Atom Transfer Radical Polymerization*. J. Am. Chem. Soc., 2001. **123**(32): p. 7913-7914.
121. Castelletto, V., et al., *Microstructure and Physical Properties of a pH-Responsive Gel Based on a Novel Biocompatible ABA-Type Triblock Copolymer*. Langmuir, 2004. **20**(10): p. 4306-4309.
122. Stratton, L.P., J.F. Carpenter, and M.C. Manning, *Temperature-sensitive gel for sustained delivery of protein drugs*. 1998: USA. p. 24.
123. DiBiase, M.D. and C.T. Rhodes, *Formulation and evaluation of epidermal growth factor in Pluronic F-127 gel*. Drug Dev. Ind. Pharm., 1996. **22**(8): p. 823-831.
124. Moore, T., et al., *Experimental investigation and mathematical modeling of Pluronic (R) F127 gel dissolution: drug release in stirred systems*. Journal of Controlled Release, 2000. **67**(2-3): p. 191-202.
125. Anderson, B.C., N.K. Pandit, and S.K. Mallapragada, *Understanding drug release from poly(ethylene oxide)-b-poly(propylene oxide)-b-poly(ethylene oxide) gels*. Journal of Controlled Release, 2001. **70**(1-2): p. 157-167.
126. Jewell, R.C., et al., *Pharmacokinetics of RheothRx injection in healthy male volunteers*. Journal of Pharmaceutical Sciences, 1997. **86**(7): p. 808-812.
127. Blonder, J.M., et al., *Dose-dependent hyperlipidemia in rabbits following administration of poloxamer 407 gel*. Life Sciences, 1999. **65**(21): p. P1261-P1266.
128. Suh, H. and H.W. Jun, *Physicochemical and release studies of naproxen in poloxamer gels*. International Journal of Pharmaceutics, 1996. **129**(1-2): p. 13-20.
129. Saettone, M.F., et al., *Solubilization of tropicamide by poloxamers: physicochemical data and activity data in rabbits and humans*. Int. J. Pharm., 1988. **43**(1-2): p. 67-76.
130. Safwat, S.M., *Drug release from pluronic gels*. Bull. Pharm. Sci., Assiut Univ., 1994. **17**(1): p. 41-8.
131. El-Gibaly, I., F.A. Mohamed, and M. Shehata, *Effect of some penetration enhancers on release of clotrimazole from different gel formulations and histological changes of rabbit skin*. Pharmazeutische Industrie, 1998. **60**(12): p. 1088-1095.
132. Cafaggi, S., et al., *An example of application of a mixture design with constraints to a pharmaceutical formulation*. Chemometrics and Intelligent Laboratory Systems, 2003. **65**(1): p. 139-147.
133. Chi, S.C. and H.W. Jun, *Release rates of ketoprofen from poloxamer gels in a membraneless diffusion cell*. J. Pharm. Sci., 1991. **80**(3): p. 280-3.
134. Shin, S.C., C.W. Cho, and H.K. Choi, *Permeation of piroxicam from the poloxamer gels*. Drug Development and Industrial Pharmacy, 1999. **25**(3): p. 273-278.
135. Shin, S.C., C.W. Cho, and I.J. Oh, *Enhanced efficacy by percutaneous absorption of piroxicam from the poloxamer gel in rats*. International Journal of Pharmaceutics, 2000. **193**(2): p. 213-218.

136. Shin, S.C., C.W. Cho, and I.J. Oh, *Effects of non-ionic surfactants as permeation enhancers towards piroxicam from the poloxamer gel through rat skins*. International Journal of Pharmaceutics, 2001. **222**(2): p. 199-203.
137. Shin, S.C., F.Y. Shin, and C.W. Cho, *Enhancing effects of fatty acids on piroxicam permeation through rat skins*. Drug Development and Industrial Pharmacy, 2000. **26**(5): p. 563-566.
138. Gear, A.J.L., et al., *A new silver sulfadiazine water soluble gel*. Burns, 1997. **23**(5): p. 387-391.
139. Katakam, M., W.R. Ravis, and A.K. Banga, *Controlled release of human growth hormone in rats following parenteral administration of poloxamer gels*. Journal of Controlled Release, 1997. **49**(1): p. 21-26.
140. Katakam, M., et al., *Controlled release of human growth hormone following subcutaneous administration in dogs*. International Journal of Pharmaceutics, 1997. **152**(1): p. 53-58.
141. Miller, S.C. and M.D. Donovan, *Effect of Poloxamer 407 Gel on the Miotic Activity of Pilocarpine Nitrate in Rabbits*. International Journal of Pharmaceutics, 1982. **12**(2-3): p. 147-152.
142. Johnston, T.P. and S.C. Miller, *Inulin Disposition Following Intramuscular Administration of an Inulin Poloxamer Gel Matrix*. Journal of Parenteral Science and Technology, 1989. **43**(6): p. 279-286.
143. Barichello, J.M., et al., *Enhanced rectal absorption of insulin-loaded Pluronic (R) F-127 gels containing unsaturated fatty acids*. International Journal of Pharmaceutics, 1999. **183**(2): p. 125-132.
144. Barichello, J.M., et al., *Absorption of insulin from Pluronic F-127 gels following subcutaneous administration in rats*. International Journal of Pharmaceutics, 1999. **184**(2): p. 189-198.
145. Fults, K.A. and T.P. Johnston, *Sustained-Release of Urease from a Poloxamer Gel Matrix*. Journal of Parenteral Science and Technology, 1990. **44**(2): p. 58-65.
146. Wang, P.L. and T.P. Johnston, *Sustained-Release Interleukin-2 Following Intramuscular Injection in Rats*. International Journal of Pharmaceutics, 1995. **113**(1): p. 73-81.
147. Bhardwaj, R. and J. Blanchard, *Controlled-Release Delivery System for the .alpha.-MSH Analog Melanotan-I Using Poloxamer 407*. J. Pharm. Sci., 1996. **85**(9): p. 915-919.
148. Lu, G.W. and H.W. Jun, *Diffusion studies of methotrexate in Carbopol and Poloxamer gels*. International Journal of Pharmaceutics, 1998. **160**(1): p. 1-9.
149. Stratton, L.P., et al., *Drug Delivery Matrix Containing Native Protein Precipitates Suspended in a Poloxamer Gel*. Journal of Pharmaceutical Sciences, 1997. **86**(9): p. 1006-1010.
150. Paavola, A., et al., *Controlled release gel of ibuprofen and lidocaine in epidural use - Analgesia and systemic absorption in pigs*. Pharmaceutical Research, 1998. **15**(3): p. 482-487.
151. Guzman, M., et al., *Polyoxyethylene-Polyoxypropylene Block Copolymer Gels as Sustained-Release Vehicles for Subcutaneous Drug Administration*. International Journal of Pharmaceutics, 1992. **80**(2-3): p. 119-127.

152. Johnston, T.P., M.A. Punjabi, and C.J. Froelich, *Sustained Delivery of Interleukin-2 from a Poloxamer-407 Gel Matrix Following Intraperitoneal Injection in Mice*. *Pharmaceutical Research*, 1992. **9**(3): p. 425-434.
153. Wenzel, J.G.W., et al., *Pluronic (R) F127 gel formulations of Deslorelin and GnRH reduce drug degradation and sustain drug release and effect in cattle*. *Journal of Controlled Release*, 2002. **85**(1-3): p. 51-59.
154. Pec, E.A., Z.G. Wout, and T.P. Johnston, *Biological-Activity of Urease Formulated in Poloxamer 407 after Intraperitoneal Injection in the Rat*. *Journal of Pharmaceutical Sciences*, 1992. **81**(7): p. 626-630.
155. Wang, P.L. and T.P. Johnston, *Thermal-Induced Denaturation of 2 Model Proteins - Effect of Poloxamer-407 on Solution Stability*. *International Journal of Pharmaceutics*, 1993. **96**(1-3): p. 41-49.
156. Paavola, A., J. Yliruusi, and P. Rosenberg, *Controlled release and dura mater permeability of lidocaine and ibuprofen from injectable poloxamer-based gels*. *Journal of Controlled Release*, 1998. **52**(1-2): p. 169-178.
157. Esposito, E., et al., *Comparative analysis of tetracycline-containing dental gels: Poloxamer- and monoglyceride-based formulations*. *International Journal of Pharmaceutics*, 1996. **142**(1): p. 9-23.
158. Desai, M., et al., *Temperature and salt-induced micellization of some block copolymers in aqueous solution*. *Journal of Surfactants and Detergents*, 2000. **3**(2): p. 193-199.
159. Edsman, K., J. Carlfors, and R. Petersson, *Rheological evaluation of poloxamer as an in situ gel for ophthalmic use*. *European Journal of Pharmaceutical Sciences*, 1998. **6**(2): p. 105-112.
160. Chetoni, P., et al., *Pharmacokinetics and anti-inflammatory activity in rabbits of a novel indomethacin ophthalmic solution*. *Journal of Ocular Pharmacology and Therapeutics*, 2000. **16**(4): p. 363-372.
161. El-Kamel, A.H., *In vitro and in vivo evaluation of Pluronic F127-based ocular delivery system for timolol maleate*. *International Journal of Pharmaceutics*, 2002. **241**(1): p. 47-55.
162. Kim, E.Y., et al., *RhEGF/HP-beta-CD complex in poloxamer gel for ophthalmic delivery*. *International Journal of Pharmaceutics*, 2002. **233**(1-2): p. 159-167.
163. Wei, G., et al., *Thermosetting gels with modulated gelation temperature for ophthalmic use: the rheological and gamma scintigraphic studies*. *Journal of Controlled Release*, 2002. **83**(1): p. 65-74.
164. Charrueau, C., et al., *Poloxamer 407 as a thermogelling and adhesive polymer for rectal administration of short-chain fatty acids*. *Drug Development and Industrial Pharmacy*, 2001. **27**(4): p. 351-357.
165. Yong, C.S., et al., *Effect of sodium chloride on the gelation temperature, gel strength and bioadhesive force of poloxamer gels containing diclofenac sodium*. *International Journal of Pharmaceutics*, 2001. **226**(1-2): p. 195-205.
166. Yong, C.S., et al., *Physicochemical characterization of diclofenac sodium-loaded poloxamer gel as a rectal delivery system with fast absorption*. *Drug Development and Industrial Pharmacy*, 2003. **29**(5): p. 545-553.

167. Shishido, S.M., et al., *Thermal and photochemical nitric oxide release from S-nitrosothiols incorporated in pluronic F127 gel: potential uses for local and controlled nitric oxide release*. *Biomaterials*, 2003. **24**(20): p. 3543-3553.
168. Cohn, D., A. Sosnik, and A. Levy, *Improved reverse thermo-responsive polymeric systems*. *Biomaterials*, 2003. **24**(21): p. 3707-3714.
169. DesNoyer, J.R. and A.J. McHugh, *The effect of Pluronic on the protein release kinetics of an injectable drug delivery system*. *Journal of Controlled Release*, 2003. **86**(1): p. 15-24.
170. Bromberg, L., M. Temchenko, and T.A. Hatton, *Dually Responsive Microgels from Polyether-Modified Poly(acrylic acid): Swelling and Drug Loading*. *Langmuir*, 2002. **18**: p. 4944-4952.
171. Bromberg, L.E. and E.S. Ron, *Temperature-responsive gels and thermogelling polymer matrices for protein and peptide delivery*. *Advanced Drug Delivery Reviews*, 1998. **31**(3): p. 197-221.
172. Ma, Y., et al., *Well-Defined Biocompatible Block Copolymers via Atom Transfer Radical Polymerization of 2-Methacryloyloxyethyl Phosphorylcholine in Protic Media*. *Macromolecules*, 2003. **2003**(36): p. 10.
173. Miyazaki, S., et al., *In situ gelling xyloglucan formulations for sustained release ocular delivery of pilocarpine hydrochloride*. *International Journal of Pharmaceutics*, 2001. **229**(1-2): p. 29-36.
174. Jeong, B., Y.H. Bae, and S.W. Kim, *Drug release from biodegradable injectable thermosensitive hydrogel of PEG-PLGA-PEG triblock copolymers*. *Journal of Controlled Release*, 2000. **63**: p. 155-163.
175. Mason, M.N., et al., *Predicting Controlled-Release Behavior of Degradable PLA-*b*-PEG-*b*-PLA Hydrogels*. *Macromolecules*, 2001. **34**: p. 4630-4635.
176. Kim, Y.J. and S.W. Kim, *Controlled drug delivery from injectable biodegradable triblock copolymer*. *Polymer Gels: Fundamentals and Applications*, 2003. **833**: p. 300-311.
177. Kim, Y.J., et al., *Controlled Release of Insulin from Injectable Biodegradable Triblock Copolymer*. *Pharmaceutical Research*, 2001. **18**(4): p. 548.
178. Amiji, M.M., et al., *Intratumoral administration of paclitaxel in an in situ gelling poloxamer 407 formulation*. *Pharmaceutical Development and Technology*, 2002. **7**(2): p. 195-202.
179. Matyjaszewski, K. and J. Xia, *Atom Transfer Radical Polymerization*. *Chem. Rev.*, 2001. **101**(9): p. 2921-2990.
180. Ando, T., et al., *Living Radical Polymerization of Methyl Methacrylate with Ruthenium Complex: Formation of Polymers with Controlled Molecular Weights and Very Narrow Distributions*. *Macromolecules*, 1995. **29**(3): p. 1070-1072.
181. Wang, J.-S. and K. Matyjaszewski, *Controlled/"Living" Radical Polymerization. Atom Transfer Radical Polymerization in the Presence of Transition-Metal Complexes*. *Journal of the American Chemical Society*, 1995. **117**(20): p. 5614-5614.
182. Darling, T.R., et al., *Living polymerization: Rationale for uniform terminology*. *Journal of Polymer Science Part A-Polymer Chemistry*, 2000. **38**(10): p. 1706-1708.
183. Jankova, K., et al., *Synthesis of Amphiphilic PS-*b*-PEG-*b*-PS by Atom Transfer Radical Polymerization*. *Macromolecules*, 1998. **31**(2): p. 538-541.

184. Ashford, E.J., et al., *First example of the atom transfer radical polymerization of an acidic monomer: direct synthesis of methacrylic acid copolymers in aqueous media*. *Chem. Commun.*, 1999. **1999**: p. 1285-1286.
185. Weaver, J.V.M., et al., *Stimulus-Responsive Water-Soluble Polymers Based on 2 Hydroxyethyl Methacrylate*. *Macromolecules*, 2004. **37**(7): p. 2395-2403.
186. Wang, X.S. and S.P. Armes, *Facile Atom Transfer Radical Polymerization of Methoxy-Capped Oligo(ethylene glycol) Methacrylate in Aqueous Media at Ambient Temperature*. *Macromolecules*, 2000. **33**(18): p. 6640-6647.
187. Wang, X.S., et al., *Facile Synthesis of Well-defined water soluble polymers via atom transfer radical polymerization in aqueous media at ambient temperature*. *Chemistry Communications*, 1999: p. 1817-1818.
188. Wang, X.-S., R.A. Jackson, and S.P. Armes, *Facile Synthesis of Acidic Copolymers via Atom Transfer Radical Polymerization in Aqueous Media at Ambient Temperature*. *Macromolecules*, 2000. **33**(2): p. 255-257.
189. Save, M., J.V.M. Weaver, and S.P. Armes, *Atom Transfer Radical Polymerization of Hydroxy-Functional Methacrylates at ambient temperature with 2-Hydroxypropyl Methacrylate*. *Macromolecules*, 2002. **35**(4): p. 1152-1159.
190. Pyun, J., T. Kowalewski, and K. Matyjaszewski, *Synthesis of Polymer Brushes Using Atom Transfer Radical Polymerization*. *Macromolecules Rapid Communications*, 2003. **24**(18): p. 1043-1059.
191. Chen, X. and S.P. Armes, *Surface Polymerization of Hydrophilic Methacrylates from Ultrafine Silica Sols in Protic Media at Ambient Temperature: A Novel Approach to Surface Functionalization Using A Polyelectrolytic Macroinitiator*. *Adv. Mater.*, 2003. **15**(18): p. 1558.
192. Yusa, S.-i., et al., *pH-Responsive Micellization of Amphiphilic Diblock Copolymers Synthesized via Reversible Addition-Fragmentation Chain Transfer Polymerization*. *Macromolecules*, 2003. **36**(11): p. 4208-4215.
193. Cabana, A., A. Aitkadi, and J. Juhasz, *Study of the gelation process of polyethylene oxide(a) polypropylene oxide(b) polyethylene oxide(a) copolymer (Poloxamer 407) aqueous solutions*. *Journal of Colloid and Interface Science*, 1997. **190**(2): p. 307-312.
194. Su, Y.-l., J. Wang, and H.-z. Liu, *FTIR Spectroscopic Investigation of Effects of Temperature and Concentration on PEO-PPO-PEO Block Copolymer Properties in Aqueous Solution*. *Macromolecules*, 2002(35): p. 6426-6431.
195. Winnik, F.M., *Photophysics of Preassociated Pyrenes in Aqueous Polymer Solutions and in Other Organized Media*. *Chem. Rev.*, 1993. **93**: p. 587-614.
196. Kabanov, A.V., et al., *Micelle Formation and Solubilization of Fluorescent Probes in Poly(oxyethylene-*b*-oxypropylene-*b*-oxyethylene) Solutions*. *Macromolecules*, 1995. **28**(7): p. 2303-14.
197. Sato, Y., A. Hashidzume, and Y. Morishima, *Self-Association in Water of Copolymers of Acrylic Acid and N-Dodecylmethacrylamide As Studied by Fluorescence, Dynamic Light Scattering, and Rheological Techniques*. *Macromolecules*, 2001. **34**(17): p. 6121-6130.
198. Pinteala, M., et al., *Concentration- and pH Dependent Conformational Changes and Aggregation of Block Copolymers of Poly(methacrylic acid) and*

Poly(dimethylsiloxane) in Aqueous Media, Based on Fluorescence Spectra of Pyrene and Potentiometry. *Macromolecules*, 2004. **37**(12): p. 4623-4634.

199. Almgren, M., P. Bahadur, and J. Alsins, *Fluorescence quenching and excimer formation to probe the micellization of a poly(ethylene oxide)-poly(propylene oxide)-poly(ethylene oxide) block copolymer, as modulated by potassium fluoride in aqueous solution.* *Langmuir*, 1991. **7**(3): p. 446-50.

200. Nakashima, K. and K. Takeuchi, *Water Content in Micelles of Poly(ethylene oxide)-Poly(propylene oxide)-Poly(ethylene oxide) Triblock Copolymers in Aqueous Solutions as Studied by Fluorescence Spectroscopy.* *Applied Spectroscopy*, 2001. **55**(9): p. 1237.

201. Vadnere, M., et al., *Thermodynamic studies on the gel-sol transition of some Pluronic polyols.* *Int. J. Pharm.*, 1984. **22**(2-3): p. 207-18.

202. Alexandridis, P., J.F. Holzwarth, and T.A. Hatton, *Micellization of Poly(ethylene oxide)-Poly(propylene oxide)-Poly(ethylene oxide) Triblock Copolymers in Aqueous Solutions: Thermodynamics of Copolymer Association.* *Macromolecules*, 1994. **27**(9): p. 2414-25.

203. Alexandridis, P. and J.F. Holzwarth, *Differential scanning calorimetry investigation of the effect of salts on aqueous solution properties of an amphiphilic block copolymer (poloxamer).* *Langmuir*, 1997. **13**(23): p. 6074-6082.

204. Booth, C. and G.E. Yu, *Block copolymers of ethylene oxide and 1,2-butylene oxide*, in *Amphiphilic Block Copolymers*, P. Alexandridis and B. Lindman, Editors. 2000, Elsevier: New York. p. 57.

205. Egelhaaf, S.U., P. Schurtenberger, and M. Muller, *New controlled environment vitrification system for cryo-transmission electron microscopy: design and application to surfactant solution.* *Journal of Microscopy*, 2000. **200**(2): p. 128-139.

206. Zheng, Y., et al., *Directly Resolved Core-Corona Structure of Block Copolymers Micelles by Cryo-Transmission Electron Microscopy.* *The Journal of Physical Chemistry B*, 1999. **103**(47): p. 10331-10334.

207. Lam, Y.-M.G., Nikolaus; Goldbeck-Wood, Gerhard., *Direct visualization of micelles of Pluronic block copolymers in aqueous solution by cryo-TEM.* *Physical Chemistry Chemical Physics*, 1999. **1**(14): p. 3331-3334.

208. Won, Y.-Y., et al., *Cryogenic Transmission Electron Microscopy (Cryo- TEM) of Micelles and Vesicles Formed in Water by Poly(ethylene oxide)-Based Block Copolymers.* American Chemical Society, 2001: p. A-k.

209. Guiner, A. and G. Fouurnet, *Small-Angle Scattering of X-Rays*. 1955, New York: John Wiley & Sons, Inc.

210. Feigin, L.A. and D.I. Svergun, *Structure Analysis by Small-Angle X-Ray and Neutron Scattering*, ed. G.W. Taylor. 1987, New York: Plenum Press.

211. Roe, R.-J., *Methods of X-Ray and Neutron Scattering in Polymer Science.* Topics in Polymer Science, ed. J.E. Mark. 2000, New York: Oxford University Press.

212. Pedersen, J.S., *Analysis of small-angle scattering data from colloids and polymer solutions: modeling and least-squares fitting.* *Advances in Colloid and Interface Science*, 1997. **70**: p. 171-210.

213. Castelletto, V. and I.W. Hamley, *Small-Angle Scattering Functions of Micelles.* *Fibre Diffraction Review*, 2003. **11**: p. 36-43.

214. McConnell, G.A., et al., *Disorder Order Transitions in Soft Sphere Polymer Micelles*. Physical Review Letters, 1993. **71**(13): p. 2102-2105.
215. Weyerich, B., J. Brunner-Popela, and O. Glatter, *Small-angle scattering of interacting particles. II. Generalized indirect Fourier transformation under consideration of the effective structure factor for polydisperse systems*. J. Appl. Cryst., 1999. **32**: p. 197-209.
216. Johnson, C.S. and D.A. Gabriel, *Laser Light Scattering*. 1981, New York: Dover Publications, Inc.
217. Huglin, M.B., *Light Scattering From Polymer Solutions*, ed. M.B. Huglin. 1972, New York: Academic Press.
218. Liu, Y., S.-H. Chen, and J.S. Huang, *Light Scattering Studies of Concentrated Copolymer Micellar Solutions*. Macromolecules, 1998(31): p. 6226-6233.
219. Berne, B. and R. Pecora, *Dynamic light scattering: with applications to chemistry, biology and physics*. 2000, New York: Wiley.
220. Jones, D.S., *Dynamic mechanical analysis of polymeric systems of pharmaceutical and biomedical significance*. International Journal of Pharmaceutics, 1999. **179**: p. 167-178.
221. Wang, P. and T.P. Johnston, *Kinetics of sol-to-gel transition for Poloxamer polyols*. J. Appl. Polym. Sci., 1991. **43**(2): p. 283-92.
222. Nystrom, B. and H. Walderhaug, *Dynamic viscoelasticity of an aqueous system of a poly(ethylene oxide)-poly(propylene oxide)-poly(ethylene oxide) triblock copolymer during gelation*. Journal of Physical Chemistry, 1996. **100**(13): p. 5433-5439.
223. Fujiwara, T. and T.Y. Takashi Mukose, Hideki Yammane, Shinichi Sakurai, Yoshiharu, *Novel Thermo-responsive Formation of a Hydrogel by Stereo-Complexation between PLLA-PEG-PLLA and PDLA-PEG-PDLA Block Copolymers*. Macromolecular Bioscience, 2001(1): p. 204-208.
224. Orkisz, M.J., et al., *Rheological Properties of reverse thermogelling poly(acrylic acid)-g-(oxyethylene-b-oxypropylene-b-oxyethylene) polymers (SMART HYDROGEL)*. Book of Abstracts, 213th ACS National Meeting, San Francisco, 1997.

CHAPTER 3. SYNTHESIS AND CHARACTERIZATION OF TEMPERATURE AND PH-RESPONSIVE PENTABLOCK COPOLYMERS

A paper published in the journal Polymer¹

Michael D. Determan^{2a}, James P. Cox², Soenke Seifert³, P. Thiagarajan⁴, Surya K. Mallapragada^{†,2}

3.1. Abstract

A family of amphiphilic ABCBA pentablock copolymers based on commercially available Pluronic® F127 block copolymers and various amine containing methacrylate monomers was synthesized via Cu(I) mediated controlled radical polymerization. The block architecture and chemical composition of the pentablock copolymers were engineered to exhibit both temperature and pH responsive self-assembly by exploiting the lower critical solution temperature of the poly(ethylene oxide)/poly(propylene oxide) blocks and the polycationic property of the poly(amine methacrylate) blocks, respectively. In aqueous solutions the pentablock copolymers formed temperature and pH-responsive micelles. Concentrated aqueous solutions of the copolymer formed a pH-responsive, thermoreversible gel phase. The controlled radical synthesis route yielded well-defined copolymers with narrow

¹ Republished with permission of Elsevier Ltd., Polymer 46 (2005) 6933-6946

² Department of Chemical Engineering, Iowa State University and Ames Laboratory, 144 Spedding Hall, Ames, IA 50011, USA

³ Advanced Photon Source, Argonne National Laboratory, 9700 S. Cass Avenue, Argonne, IL 60439, USA. E-mail address: seifert@anl.gov

⁴ Intense Pulsed Neutron Source, Argonne National Laboratory, 9700 S. Cass Avenue, Argonne, IL 60439, USA. E-mail address: thiaga@anl.gov

[†] Corresponding author. Phone: +1 515 294 7407 Fax: +1 515 294 2689 E-mail address: suryakm@iastate.edu

molecular weight distributions with the benefit of mild reaction conditions. Small angle X-ray scattering, laser light scattering, cryogenic transmission electron microscopy and dynamic mechanical analysis have been used to characterize the self-assembled structures of the micellar solution and gel phases of the aqueous copolymer system. These copolymers have potential applications in controlled drug delivery and non-viral gene therapy due to their tunable phase behavior and biocompatibility.

3.2. Introduction

Amphiphilic block copolymers that self-assemble into micelles and gels in response to environmental stimuli are an important class of materials. These stimuli-responsive water-soluble copolymers have many biological applications, such as drug delivery and gene therapy. Amphiphilic block copolymers and amphiphilic polyelectrolytes often exhibit stimuli responsive behavior due to reversible self-assembly in solution [1, 2]. Recent advances in controlled radical polymerization techniques have led to the facile synthesis of well-defined block copolymers with a wide range of functional monomers. Atom transfer radical polymerization (ATRP)[3-5], reversible addition fragmentation chain transfer (RAFT) polymerization[6] and nitroxide-mediated radical polymerization[7] techniques have been utilized to develop well-defined functional polymers which exhibit stimuli responsive behavior in solution.

This paper describes the ATRP synthesis of a family of novel gel forming pentablock copolymers with different amine containing methacrylate blocks. A difunctional ATRP macroinitiator was prepared from commercially available Pluronic® F127 triblock copolymer. Pluronic® F127 is a amphiphilic triblock copolymer of poly(ethyleneoxide)-block-poly(propyleneoxide)-block-poly(ethyleneoxide) (PEO-b-PPO-b-PEO). The micelle

and gel formation of Pluronic® copolymers in solution has been extensively investigated.[8-12] Due to the block architecture and lower critical solution temperature (LCST) of PEO and PPO, aqueous solutions of Pluronics® exhibit temperature-dependent micellization. Concentrated solutions of the copolymer form a thermoreversible gel phase as a result of micellar packing [13]. The family of pentablock copolymers synthesized in this work, initiated by a Pluronic® F127 macroinitiator, contain blocks of either poly(2-diethylaminoethyl methacrylate) (PDEAEM), poly(2-dimethylaminoethyl methacrylate) (PDMAEM), poly(2-diisopropylaminoethyl methacrylate) (PDiPAEM) or poly(tert-butylaminoethyl methacrylate) (PtBAEM) as the outer blocks. These amine methacrylate end blocks are hydrophilic when the amine groups are charged at low pH, and exhibit various degrees of hydrophobic character above critical pH values where they become uncharged. The pentablock copolymers exhibit reversible temperature and pH-dependent micelle and gel formation in solution. The different hydrophobic character of the pendant amino groups of the monomers result in a range of pH responsive solution properties. Additionally, the ability to control the molecular weight of the pentablock copolymers offers further opportunities to tune the materials' responsive behavior.

Recently, we reported the synthesis of a pentablock copolymer composed of Pluronic® F127 and PDEAEM [14]. The pentablock copolymer was synthesized via oxyanionic polymerization of DEAEM initiated by a difunctional carbanion of the Pluronic® F127 copolymer. The oxyanionic synthesis scheme required rigorous purification of solvents and exclusion of oxygen and water. Additionally, due to the rapid rate of propagation in oxyanionic synthesis, uniform chain growth from macroinitiators was difficult to control and resulted in low initiation efficiency and multimodal molecular weight

distributions. ATRP synthesis of the pentablock copolymers requires relatively mild conditions, less rigorous monomer purification and is applicable to a wider range of functional monomers. Careful selection of reaction conditions resulted in a controlled polymerization, and molecular weight can be effectively controlled with the initiator-to-monomer ratio. Triblock copolymers that incorporate tertiary amine methacrylate monomers have recently been synthesized via the difunctional macroinitiator ATRP approach, in aqueous [15] and organic media [5]. These materials were found to exhibit reversible lyotropic and pH dependent properties. Herein, we describe the synthesis of well-defined pentablock copolymers based on commercially available Pluronic® block copolymers and amine methacrylate monomers via ATRP in both hydrocarbon and alcoholic media. The temperature and pH dependent-micellization of these materials were monitored with small angle X-ray scattering (SAXS) and quasi-elastic and multi-angle light scattering. Pentablock copolymer micelles were directly visualized with cryogenic transmission electron microscopy (CryoTEM). The temperature dependent sol-gel behavior was characterized by dynamic mechanical analysis (DMA) to investigate the self-assembly process of these polymers in solution.

3.3. Experimental Section

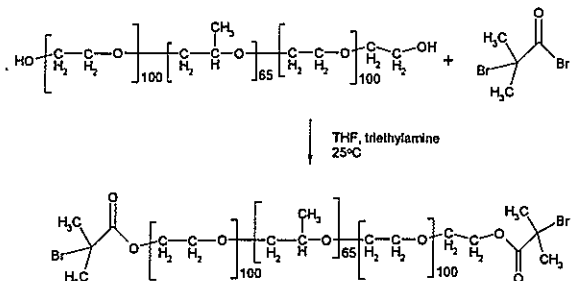
3.3.1 Reagents

2-(N,N diisopropylaminoethyl methacrylate) (DiPAEM), tert-butylaminoethyl methacrylate (tBAEM) and the inhibitor removal column were purchased from Scientific Polymer Products Inc., Ontario New York. 1-propylamine, 2-pyridinecarbaldehyde, N,N-(diethyl amino)ethyl methacrylate (DEAEM), N,N-(dimethylamino)ethyl methacrylate (DMAEM), 2-bromoisoburyryl bromide, copper(I) bromide (CuBr 99.99%), Pluronic®

F127 ($M_n = 12600$, 70% PEO) and copper powder (99%) for organic synthesis were purchased from Sigma-Aldrich, St. Louis, MO. Triethylamine, tetrahydrofuran (THF), toluene and all other chemicals were purchased from Fisher Scientific and used with no further purification. N-propyl-pyridynyl methanimine (N-PPM) was prepared by reacting 1-propylamine with 2-pyridinecarbaldehyde [16].

3.3.2 Preparation of Pluronic® ATRP Macroinitiator

The difunctional 2-bromo propionate Pluronic® F127 was synthesized as illustrated in Scheme 3.1. Pluronic® F127 (10 g, 7.94×10^{-4} mol) and triethylamine (3 molar excess) were dissolved in THF at 25°C. 2-bromoisobutyryl bromide (6 molar excess) was added and the solution was stirred overnight. The reaction mixture was filtered to remove the precipitated hydrobromide salt. The cleared solution was stirred with activated charcoal for 2 hours and then dried with $MgSO_4$. The mixture was filtered to remove the charcoal and $MgSO_4$, and the excess solvent was removed with a rotary evaporator before the product was precipitated in -72°C n-hexane and dried under vacuum. 1H NMR of the functionalized Pluronic® F127 was used to verify the quantitative modification of the end groups as shown in Figure 3.1. The integral area of the sharp singlet at $\delta = 1.97$, was assigned to the two methyl groups α to the terminal bromine atoms. The product is an off white powder (9.1 g, 91% yield); GPC (THF) $M_w = 13.64$ kDa, $M_w/M_n = 1.133$; 1H NMR (CDCl₃) δ 3.63 (s, 800H), δ 3.56–3.48 (m, 108 H), δ 3.40–3.35, (m, 58 H), δ 1.92 (s, 12 H), δ 1.13–1.11, (m, 168 H)



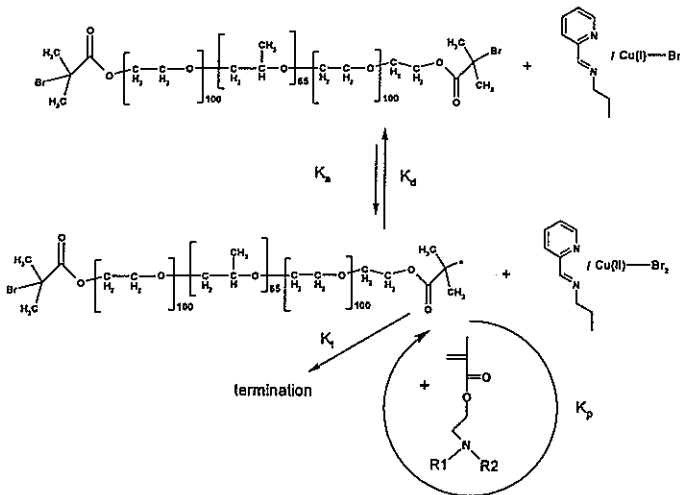
Scheme 3.1. Synthesis of difunctional ATRP macroinitiator based on Pluronic® F127

3.3.3 Synthesis of pentablock copolymer

Successful ATRP, resulting in uniform initiation and growth, requires a dynamic equilibrium between active, propagating radicals and dormant alkyl halides. The dormant species must be favored in the equilibrium to maintain a low concentration of active radicals and suppress normal radical termination reactions. A transition metal catalyst/ligand complex mediates the equilibrium. Copper catalyst was employed in this study due to proven versatility in mediating ATRP of methyl methacrylates [17]. Due to the low solubility of the copper catalyst in most solvents, a complexing ligand is employed to increase the solubility and enhances the activity of the catalyst. The N-propyl-pyridynyl methanimine (N-PPM) ligand was utilized in this investigation. N-PPM has been shown to successfully mediate ATRP of PDEAEM and PDMAEM [15]. The N-PPM ligand was initially developed to overcome the difficulties of polymerizing methacrylate monomers in nonpolar solvents such as toluene [16]. Additionally, N-PPM has been shown to mediate well-controlled ATRP reactions in aqueous media [18]. The effect of varying the relative molar amounts of ligand and catalyst, as well as the solvent on the initiation efficiency, monomer conversion and polydispersity of the product were studied.

A typical synthesis, as depicted in Scheme 3.2, was carried out as follows. Monomers were passed over an inhibitor removal column immediately prior to use. The

macroinitiator was dissolved either in toluene or in a (1:1) water:isopropanol solution, and was added to an argon-flushed round bottom flask with copper(I)bromide (99.99%), ligand and monomer, and degassed via 3 freeze-pump-thaw cycles. A small quantity of copper(0) powder (< 1 mg) was added to the reactions to enhance the stability of the Cu(I)/Cu(II) equilibrium [17]. In some cases, the reaction kinetics were monitored by periodically sampling the reaction with a degassed syringe. The reaction was stopped by precipitation of the copolymer into cold n-hexane. The crude product was dissolved in a 1:1 THF:methylene chloride mixture, passed over a short column of basic alumina and precipitated in n-hexane, yielding a light green or light brown solid. The final product was collected and dried under vacuum overnight.



Scheme 3.2. Synthesis of pentablock copolymers. DEAEM R1=R2= -CH₂-CH₃; DMAEM R1=R2= -CH₃, DiPAEM R1=R2= -CH(CH₃)₂, tBAEM R1=H, R2= -C(CH₃)₃

¹H NMR (CDCl₃) for PDMAEM₅₀-F127-PDMAEM₅₀ copolymer (3.1 g, 92% yield): δ 4.02 (s, 200 H), δ 3.62 (s, 800 H), δ 3.52 (m, 108 H), δ 3.37 (m, 62 H), δ 2.5 (s, 204 H), δ 2.25 (s 604 H), δ 2.03 – 1.794 (m, 165 H), δ 1.12-1.09 (m, 184 H), δ 1.03 (m, 99 H), δ

0.86 (s, 158 H). ^1H NMR (CDCl_3) for PtBAEM₅₀-F127-PtBAEM₅₀ copolymer (2.9 g, 89% yield): δ 4.02 (s, 216 H), δ 3.61 (s, 800 H), δ 3.52 (m, 124 H), δ 3.37 (m, 69 H), δ 2.78 (s, 210 H), δ 1.92-1.79 (m, 228 H), δ 1.09 (m, 1100 H), δ 1.04 (s, 105 H), δ 0.88 (m, 150 H). ^1H NMR (CDCl_3) for PDEAEM₅₀-F127-PDEAEM₅₀ copolymer (3.3 g, 98% yield): δ 3.954 (s, 187 H), δ 3.6 (s, 800 H), δ 3.51 (m, 123 H), δ 3.36 (m, 64 H), δ 2.66 (m, 195 H), δ 2.54 (m, 399 H), δ 1.86 – 1.76 (m, 131 H), δ 1.11-1.08 (m, 186 H), δ 1.04-0.976 (m, 690 H), δ 0.844 (s, 177 H). ^1H NMR (CDCl_3) for PDiPAEM₅₀-F127-PDiPAEM₅₀ copolymer (3.5 g, 91% yield): δ 3.83 (s, 200 H), δ 3.62 (s, 800 H), δ 3.53 (m, 121 H), δ 3.38 (m, 66 H), δ 2.98 (s, 202 H), δ 2.62 (s, 200 H), δ 1.90-1.79 (m, 161 H), δ 1.14-1.11 (m, 187 H), δ 0.99 (s, 1254 H), δ 0.87 (s, 212 H).

3.3.4 Characterization

All ^1H NMR spectra were collected using a Varian VXR400 (400MHz) spectrometer, and chemical shifts are given in ppm. Chloroform-d (98%, Fisher) and D_2O (99%) were used as solvents. The pH of the ^1H NMR in D_2O was adjusted by addition of DCl (30% in D_2O) and NaOD (5 M in D_2O). The copolymer molecular weight and polydispersity index (PDI) were determined using gel permeation chromatography (GPC). The GPC system consisted of a Waters 510 pump, Waters 717 autosampler, a Wyatt Optilab DSP refractometer, and a Wyatt Dawn EOS light scattering detector. Poly(methyl methacrylate) (PMMA) standards from Polymer Laboratories were used for column calibration. The mobile phase was THF with 1% v/v triethylamine at a flow rate of 1 mL/min on four columns (Polymer Laboratories, PLgel 100, 500, 1×10^4 , 1×10^5 Å at 40°C).

A Corning 313 pH/temperature meter was used to conduct potentiometric titrations. All titrations were performed at room temperature under constant stirring with 100 ml of 1.0 wt% pentablock copolymer solution. The polymer was dissolved in dionized water and the pH is adjusted to pH 2.0 with 1.0 M HCl, and subsequently titrated with 25 mM NaOH while pH was monitored. A one-minute lag time was allowed for the reaction to reach equilibrium between additions of base. The meter was periodically calibrated against NIST traceable buffer solutions. Assuming that all dissociated protons effectively protonate amine groups, the degree of protonation was calculated as the ratio of the net molarity of H^+ ions ($C_{H^+}-C_{OH^-}$) and amine groups (C_N) in solution, $\alpha = (C_{H^+}-C_{OH^-})/C_N$ [19].

A Wyatt DAWN EOS Multi Angle Light Scattering (MALS) instrument equipped with a Wyatt QELS detector was used to for static and dynamic light scattering experiments. The absolute values of the scattered intensities were calibrated against filtered toluene and the instrument detectors were normalized with a bovine serum albumin (Sigma Aldrich) for aqueous solutions and polystyrene (30kDa) for THF solutions. The experiments were conducted in micro-batch configuration with the samples being delivered to the flow cell of the DAWN EOS via a syringe pump at 0.5 ml/min. Samples were prepared by removing aliquots of solution from a potentiometric titration of a pentablock copolymer solution as described previously. The samples were diluted to 0.5mg/ml. The QELS measurements were carried out at $27 \pm 0.2^\circ C$ and were clarified with $0.22\mu m$ filters immediately prior to analysis. Data collection and analysis for the light scattering measurements were carried out with ASTRA[®] and QELSBatch[®] software (Wyatt Technology Co.).

Small angle X-ray scattering (SAXS) samples were prepared by dissolving the copolymer samples in the aqueous solutions at the desired ionic and pH conditions. The

solutions were allowed to completely dissolve for several days at 4°C. The samples were then transferred to 1.3mm OD quartz capillary tubes with 0.1mm nominal wall thicknesses and sealed to prevent evaporation. SAXS measurements were carried out on the instrument at the 12-ID beam line at the Advanced Photon Source.[20] A 15 cm x 15 cm CCD detector was used to measure the intensity of scattering and the direct beam intensity was measured using a photodiode. A Peltier heating device controlled the temperature of the sample holder. Five data sets were collected at each temperature with exposure times of 0.5 seconds at incident beam energies of 12 keV ($\lambda = 1.035 \text{ \AA}$). The distance between the detector and the sample was 2 m. The scattering data were appropriately corrected and azimuthally averaged to obtain $I(Q)$; $Q = 4\pi\sin\theta/\lambda$, where 2θ is the scattering angle and λ is the wavelength of x-rays. The one-dimensional data for the five runs were averaged to obtain high precision scattering data for each condition. The scattered intensity was then corrected by subtracting the scattering from a quartz capillary filled with deionized water and normalized to an absolute scale with a polyethylene standard.

Transmission electron microscopy (TEM) allows real-space imaging of objects in the nanometer size regime. Sample solutions at room temperature, were wetted onto the sample grid and blotted prior to rapid cryogenic vitrification. This technique enables direct imaging of micelle nanostructures. A 3 w% solution of pentablock copolymer dissolved in 0.1 M pH 7.4 phosphate buffer solution was imaged at the cryo-TEM housed in the Materials Research Science and Engineering Center (MRSEC) at the University of Minnesota. Sample preparation and instrumentation details are presented elsewhere.[21] Image analysis was done with MetaMorph® 5.0 software from Universal Imaging Corporation.

A Perkin Elmer 7e Dynamic Mechanical Analyzer (DMA) was used to monitor the mechanical properties of pentablock gels as a function of temperature [22]. A cup-and-plate geometry (5 mm diameter) was utilized and the sample was tested in compression at 1 Hz. Gel forming solutions of Pluronic® F127 copolymer were prepared by mixing deionized water with the copolymer and allowing the solution to homogenize at 4°C for several days. Pentablock copolymer solutions were prepared similarly and the pH was adjusted with the 0.1 M HCl. Cooled polymer solutions were poured into the cup assembly and were allowed to equilibrate at 50°C. The sample was then mounted in the analyzer. The applied static and dynamic forces were 9 and 10 mN respectively. The temperature of the sample was decreased at 2°C/min. The temperature control chamber was humidified to keep the sample from drying over the course of the experiment. Temperature calibration of the instrument was conducted with deionized water with the cup and plate sample holder used for this study.

3.4. Results and Discussion

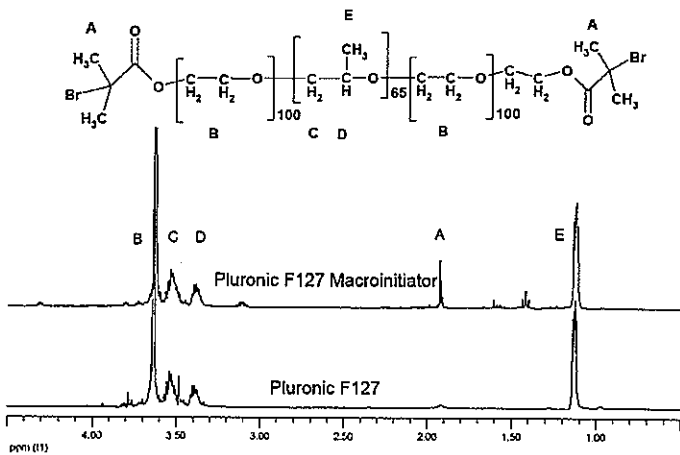
3.4.1 Synthesis and macromolecular characterization

The goal of the work was to develop a relatively easy method of synthesizing a pH and temperature responsive block copolymer. The thermoreversible micellization and gelation of the Pluronic® F127 copolymers and the pH responsive micelle formation of block copolymers incorporating the tertiary amine methacrylate motif served as inspiration to develop the pentablock copolymers described in this report [23].

The preparation of the difunctional macroinitiator based on Pluronic® F127 was accomplished in a single step with quantitative yields via the reaction shown in Scheme 3.1. The ¹H NMR spectra in Figure 3.1 were used to confirm the conversion of hydroxyl end groups to bromides capable of initiating the ATRP reaction. The sharp singlet at 1.9 ppm in

the spectra of the macroinitiator, assigned to the methyl groups in the alpha position relative to the bromide, was integrated relative to the peaks arising from the F127 backbone protons to confirm conversion to difunctional ATRP initiating end groups.

Scheme 3.2 illustrates the ATRP, initiated by the Pluronic® F127 macroinitiator, of the amine methacrylate blocks, resulting in pentablock copolymers with polydispersities ranging from 1.22 to 1.44. The results of these polymerizations are summarized in Table 3.1. Because the pentablock copolymer synthesized via ATRP has a relatively low polydispersity and the reaction typically proceeds to high conversions, the average polymer molecular weight can be controlled by controlling the initial initiator to monomer ratio.



The ^1H NMR in CDCl_3 of four pentablock copolymers (A, B, C and D in Table 3.1) synthesized are shown in Figure 3.2. Monomer conversion was measured with ^1H NMR by utilizing the F127 macroinitiator as an internal reference. Figure 3.3 shows GPC chromatograph traces of the macroinitiator and a $\text{PDEAEM}_{40}\text{-F127-PDEAEM}_{40}$ pentablock copolymer. The molecular weight distribution of the Pluronic® F127 includes a triblock PEO-b-PPO-b-PEO and a lower molecular weight PEO-b-PPO diblock copolymer fraction

that is a result of the commercial synthetic process. As shown in Table 3.1 the PDI of the pentablock copolymers, synthesized in toluene, was typically below 1.3. The molecular weight of the pentablock copolymer obtained by GPC in THF compared very well with the molecular weights calculated from monomer conversion via ^1H NMR, indicating good initiating efficiencies.

ID	Monomer	Target DP	Solvent	Polymer Concentration (g/ml)			Temp (°C)	Conversion (NMR)	$\langle M_n \rangle \times 10^4$ (g/mol) (GPC)	$\langle M_w \rangle \times 10^4$ (g/mol) (GPC)	PDI
				[Cu(I)]	[Ligand]						
A	DMAEM	100	toluene	0.5	1	0.5	70	100%	3.18	4.00	1.26
B	tBAEM	100	toluene	1	2	0.5	70	92%	2.63	3.42	1.30
C	DEAEM	100	toluene	0.5	1	0.5	70	100%	2.89	3.72	1.29
D	DiPAEM	100	toluene	1	2	0.5	70	100%	2.66	3.35	1.26
E	DMAEM	40	toluene	0.5	1	0.5	70	100%	2.43	3.02	1.24
F	DEAEM	50	toluene	0.5	1	0.5	70	96%	2.61	3.53	1.35
G	DiPAEM	50	toluene	1	2	0.5	70	94%	2.56	3.26	1.22
H	DEAEM	100	IPA:water	1	2	0.3	50	93%	2.13	2.95	1.38
I	DEAEM	100	IPA:water	0.5	1	0.3	50	89%	2.09	2.94	1.40
J	DEAEM	100	IPA:water	0.25	0.5	0.3	50	85%	2.38	3.24	1.36
K	DEAEM	100	IPA:water	0.125	0.25	0.3	50	93%	2.37	3.43	1.45

Table 3.1. Summary of the conversion and molecular weight data for the Pluronic® F127-based pentablock copolymers synthesized by ATRP. The concentration of Copper(I) Bromide catalyst [Cu(I)] and Ligand [Ligand] are given relative to molar equivalents of the concentration of initiator.

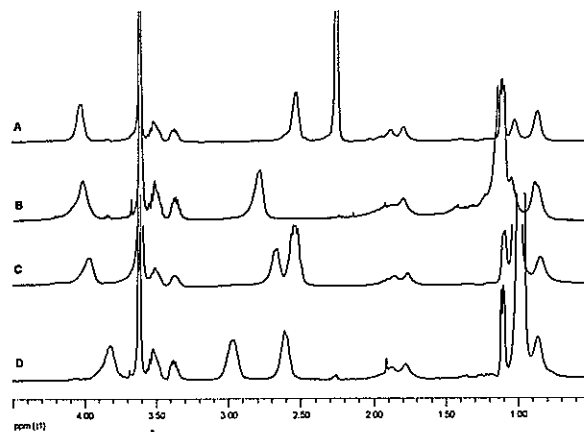


Figure 3.2. ^1H NMR of pentablock copolymers A) PDMAEM₅₀-F127-PDMAEM₅₀ B) PtBAEM₅₀-F127-PtBAEM₅₀, C) PDEAEM₅₀-F127-PDEAEM₅₀, D) PDiPAEM₅₀-F127-PDiPAEM₅₀

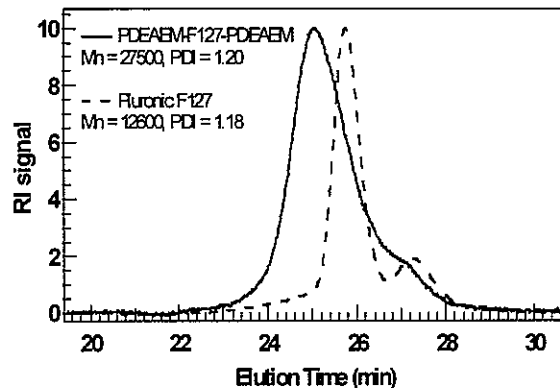


Figure 3.3. GPC chromatograph of Pluronic® F127 macroinitiator (dashed) and a pentablock copolymer (solid)

Synthesis of the pentablock copolymer was carried out in several solvents in an effort to minimize the PDI of the final product. The solubility of the catalyst/ligand complex is a critical factor determining the relative rates of reaction in ATRP. Solvents were selected based on accounts from the literature of ATRP of methylacrylates with the N-PPM ligand.[16, 18] Toluene, isopropyl alcohol (IPA) and water were identified as potential solvents for the reaction, spanning a wide range of polarities. Figure 3.4 contains first order kinetics plots of the ATRP of PDEAEM in toluene, and in 1:1 IPA:water. A linear fit was found to describe the monomer consumption kinetics for the pentablock ATRP in toluene up to very high conversion. The linear fit indicates that the concentration of propagating radical species is constant and that radical termination reactions are not significant on the time scale of the reaction.

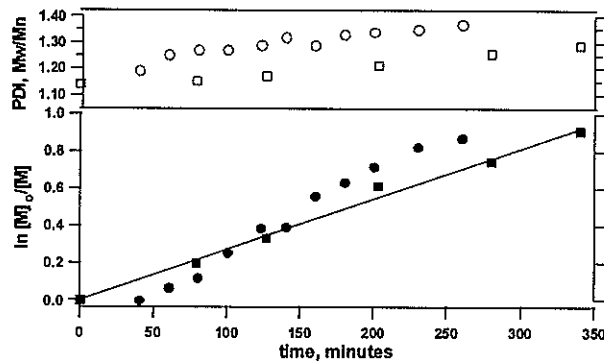


Figure 3.4. Kinetics of the polymerization of PDEAEM in IPA/water at 50°C, [N-PPM]:[CuBr]:[F127]:[DEAEM] = 2:1:1:100, ●, ○ ($\ln[M]_0/[M]$ and PDI); and in toluene at 70°C, [N-PPM]:[CuBr]:[F127]:[DEAEM] = 1:0.5:1:100, ■, □ ($\ln[M]_0/[M]$ and PDI); line represents the best fit through the data. $[M]_0$ = initial monomer concentration, $[M]$ = monomer concentration during the reaction.

ATRP is usually carried out with molar equivalents of catalyst and ligand to initiator. Because of potential biomedical applications for this material, we investigated the possibility of minimizing the catalyst concentration necessary to produce a well-defined pentablock copolymer product. PDEAEM-F127-PDEAEM copolymers were synthesized in toluene

with various concentrations of ATRP ligand and catalyst. As shown in Figure 3.5, the reaction resulted in near complete conversion of monomer at acceptable PDI over a range of catalyst concentrations. Catalyst concentrations of 0.25 to 0.50 molar equivalents, relative to initiator concentrations, consistently resulted in the lowest PDI copolymer product. ATRP carried out with catalyst concentrations below 0.125 molar equivalent resulted in very low conversion and initiation efficiency (data not shown). Increasing the concentration of the catalyst and ligand above [1.0]: [24] molar equivalents did not result in any improvement in the PDI of the pentablock copolymer.

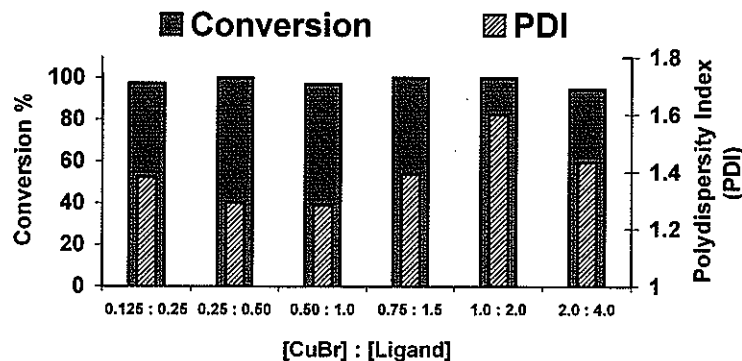


Figure 3.5. Monomer conversion and polydispersity of pentablock copolymer PDEAEM₅₀-F127-PDEAEM₅₀ with varying molar amounts of N-PPM and CuBr in toluene at 70°C.

ATRP in polar solvents, such as water and lower alcohols have been shown to proceed more rapidly than in less polar solvents such as toluene [17]. ATRP of the PDEAEM pentablock copolymers in water resulted in rapid monomer conversion reaching 100% conversion in less than an hour as judged by ¹H NMR. However the product was only fractionally soluble in THF and chloroform, possibly indicating that a crosslinking side reaction had taken place. ATRP of the PDEAEM pentablock copolymers in isopropyl alcohol resulted copolymer with PDIs greater than 1.5 and multimodal molecular weight

distributions due to significant fractions of unreacted macroinitiator. We attributed these results to slow initiation of ATRP from the F127 macroinitiator in this solvent. However ATRP of the pentablock copolymer was successfully achieved in an 1:1 IPA:water solution, resulting in monodisperse molecular weight distributions. **Table 3.1** contains a summary of the ATRP of the PDEAEM-F127-PDEAEM copolymers in IPA:water solutions at various catalyst concentrations. These reactions consistently reached lower conversion and typically had slightly higher PDIs than the analogous reactions in toluene. Figure 3.4 contains a first order kinetics plot of the PDEAEM-F127-PDEAEM pentablock copolymer synthesized in IPA:water. We observed a significant ‘initiation period’ for the ATRP reaction in the IPA:water solution. In contrast to the reaction kinetics in toluene, the kinetics plot for this reaction is linear at low conversions but exhibits curvature at higher conversion, indicating a less controlled ATRP reaction. The more rapid rate of ATRP in the IPA:water solution did not allow for a significant reduction in catalyst concentration necessary to yield pentablock copolymers with PDI below 1.3.

The effective removal of catalyst residues from polymers synthesized via ATRP is especially important for materials in biological applications [5, 25]. Cytotoxicity studies were carried out to investigate the effectiveness of the simply flash chromatography and repeated precipitation technique employed to remove the ATRP catalyst from these pentablock copolymers. Cytotoxicity studies of these pentablock copolymers dissolved in media and exposed to SKOV-3 cells confirmed that the cells were viable in the presence of the polymer and that these polymers can be used for biomedical applications [26].

3.4.2 Characterization of solution behavior

Several techniques were used for characterization of the temperature and pH dependent self-assembly of the pentablock copolymers. The critical micellization concentration (CMC), and the critical micellization temperature (CMT), the concentration and temperature at which micelles start forming, are important parameters in the characterization of self associating block copolymers. In the case of Pluronic® copolymers, the CMC and the CMT values decrease with increasing molecular weight of the hydrophobic PPO block [10]. Additionally, ionic copolymers that exhibit pH-sensitive behavior are commonly characterized with critical pH values that correspond to significant conformational changes in solution [19, 27]. The pendent tertiary amine groups of the methacrylate blocks in the pentablock copolymers are weakly basic. These blocks are electrostatically charged and hydrophilic at low pH and are relatively hydrophobic at high pH. Potentiometric titrations were conducted to determine the critical pH values at which the pendent amines became uncharged. The pH of 10 mg/ml pentablock solutions, as a function of degree of amine protonation (α) are shown in Figure 3.6. The buffering region of the curves indicates the pH range at which the pendent amine groups are partially ionized. $\alpha > 1$ and $\alpha < 0$ correspond to excess acid and excess base in solution respectively. Plotted this way, it is easy to observe the pH range where the amine blocks become uncharged. At low pH, electrostatic interactions between the charged groups along the copolymer chain likely results in extended chain conformations, while uncharged amine methacrylate blocks likely exist in a more compact conformation at higher pH. The hydrophilic character of the charged pendent amine groups decreases in the order tBAEM > DMAEM > DEAEM > DiPAEM.

The PDiPAEM pentablock precipitated above pH 8.3 due to the hydrophobic isopropyl groups. The PDEAEM pentablock copolymer solution precipitated above pH 11

and the PtBAEM and PDMAEM pentablock copolymer solutions did not exhibit pH-induced precipitation. This indicates that the PtBAEM and PDMAEM blocks are remain relatively hydrophilic, even when completely deprotonated.

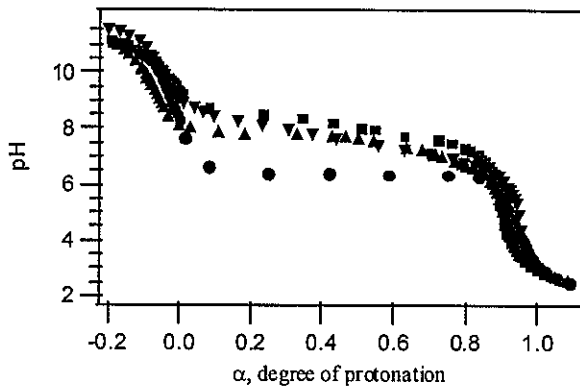


Figure 3.6. Titration curves for four pentablock copolymers. The pH at the inflection point of the curves was taken as the pK_a value of the copolymer: ● $\text{pK}_a(\text{PDiPAEM}_{50}\text{-F127-PDiPAEM}_{50}) = 6.37$; ▲ $\text{pK}_a(\text{PDEAEM}_{50}\text{-F127-PDEAEM}_{50}) = 7.63$; ▼ $\text{pK}_a(\text{PDMAEM}_{50}\text{-F127-PDMAEM}_{50}) = 7.52$; ■ $\text{pK}_a(\text{PtBAEM}_{50}\text{-F127-PtBAEM}_{50}) = 8.06$

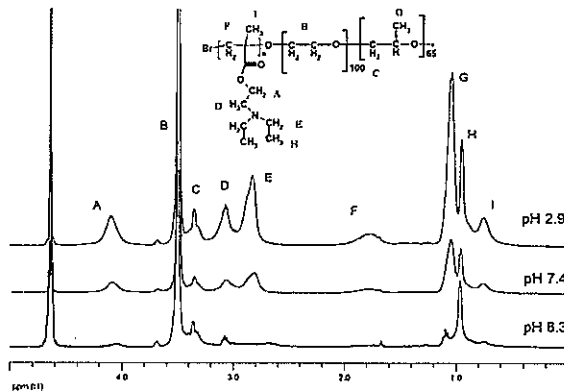


Figure 3.7. ^1H NMR spectra of obtained for PDEAEM₂₅-F127-PDEAEM₂₅ pentablock copolymers at pH values of 2.9, 7.4 and 8.3 in D_2O .

The pH-responsiveness of the pentablock copolymers was investigated with ^1H NMR in D_2O . Figure 3.7 shows the ^1H NMR spectrum obtained for the PDEAEM₂₅-F127-PDEAEM₂₅ copolymer (sample F in Table 3.1) in $\text{D}_2\text{O}/\text{DCl}$ at pH values of 2.9, 7.4 and 8.3. The copolymer solutions were prepared at 2 mg/ml, and measurements were taken at room

temperature. The intensity of the peaks associated with protons adjacent to the amine of the PDEAEM blocks (A, D and E in Figure 3.7) were observed to attenuate with increasing pH relative to the signal associated with the protons in the PEO backbone (B). This reflects the dehydration and reduced mobility of the PDEAEM blocks as they become deprotonated [23]. As the PDEAEM blocks transition from hydrophilic polyelectrolytes to uncharged hydrophobic blocks, upon increasing pH, the copolymers undergo an association process. To further examine the isothermal pH-dependent micellization of the pentablock copolymers, quasielastic light scattering (QELS) and multi angle light scattering (MALS) were utilized to determine the critical micellization onset pH and size of the micellar aggregates formed. Figure 3.8 shows the dependence of the hydrodynamic radius (R_h) of pentablock copolymer micelles as a function of pH. In Figure 3.9, MALS was used to measure the degree of multimerization of the copolymers as they associated into micelles in response to changes in pH.

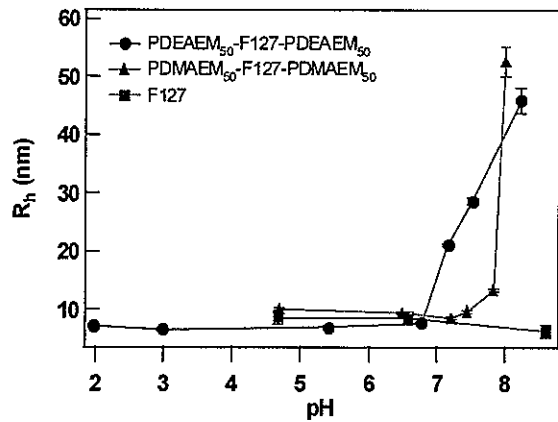


Figure 3.8. Micelle hydrodynamic radius, R_h , as determined by QELS measurements, for 5.0×10^{-4} g/ml pentablock and Pluronic[®] F127 copolymers as a function of pH.

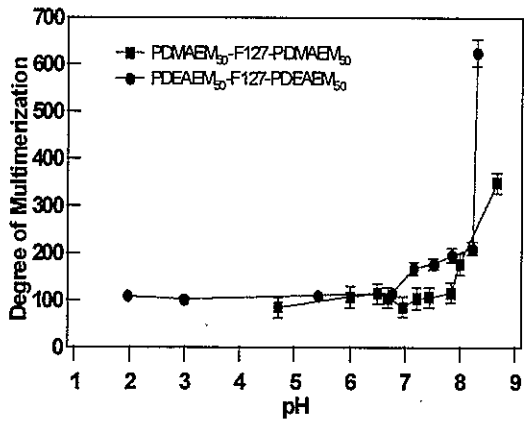


Figure 3.9. Degree of multimerization of pentablock copolymer micelles as a function of solution pH, determined by MALS.

The hydrodynamic radii of Pluronic® F127 micelles showed little dependence on pH as expected. For the pentablock copolymers at low pH, charged unimers or small micelles with $R_h \sim 10$ nm were observed. Within the resolution of these QELS measurements, the low pH pentablock copolymer micelles and the Pluronic® micelles appeared to have the same hydrodynamic radii. The pentablock micelles exhibited an abrupt increase in size above a critical pH value. The amine methacrylate blocks became hydrophobic at high pH, resulting in attractive hydrophobic interactions between micelles. The aggregation of several micelles may explain the large increase in micelle size and aggregation number at high pH. The pH-induced onset of micellar association of the PDEAEM pentablock copolymers occurred when only 20% of the cationic amines had been neutralized. The PDMAEM pentablock micelles did not begin to aggregate until more than half of the pendant groups had become deprotonated. This presumably reflects the greater hydrophobic character of the unprotonated PDEAEM compared to PDMAEM. Lowering the sample pH resulted in a decrease in aggregation number and hydrodynamic radius, demonstrating the reversibility of this aggregation process.

Cryo-TEM was used to directly visualize micelles formed from the pentablock copolymers. Figure 3.10 is a cryo-TEM micrograph of micelles of pentablock copolymers (PDEAEM₂₀-F127-PDEAEM₂₀). The polymer solution, at 27°C and 30 mg/ml in pH 7.4 phosphate buffer, was rapidly vitrified in liquid ethane to preserve the microstructure originally present in the ambient solution. Micelles with dark, electron dense cores surrounded by light coronas were observed. The pentablock copolymer micelles were significantly larger and more polydisperse than Pluronic® F127 micelles visualized with cryo-TEM. Lam and coworkers observed Pluronic® F127 micelles with a mean diameter of

approximately 6 nm in a 5 % solution [28]. There was a considerable size distribution of the pentablock copolymer micelles, and the micelles did not appear to exhibit any long-range order. The micellar dimensions and size distribution were quantified with Metamorph® image analysis software. Figure 3.11 shows the radial size distribution of the micelles and the micelle cores. The average radii of the micelles and micelle cores were 39.4 and 15.2 nm respectively. The dimensions of the micelles visualized with cryo-TEM were in good qualitative agreement with the QELS measurements of the dilute solution of PDEAEM pentablock micelles at pH 7.2

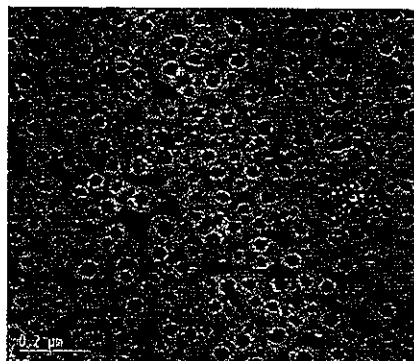


Figure 3.10. Cryo-TEM micrograph of a 3 w% PDEAEM₂₀-F127-PDEAEM₂₀ pentablock copolymer solution in 0.1 M PBS at a pH of 7.4

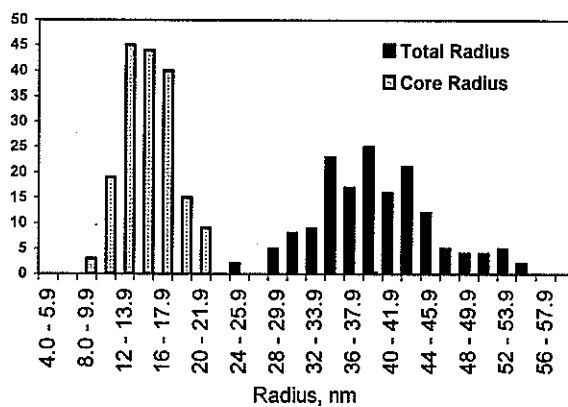


Figure 3.11. Radial size distribution of spherical micelles and the spherical micelle cores obtained by cryo-TEM measurements of 3 w% PDEAEM₂₀-F127-PDEAEM₂₀ pentablock copolymer in pH 7.4 PBS

Small angle X-Ray scattering (SAXS) was used to monitor temperature dependent self-association of the pentablock copolymers in solution. SAXS spectra collected at several temperatures from 50 mg/ml solutions of PDEAEM₅₀-F127-PDEAEM₅₀ at pH 7.4 and 4.4 are shown in Figures 3.12 and 3.13 respectively. The formation of nanometer scale copolymer micelles with increasing temperature was observed as an increase in the scattering intensity in the low Q region. With an increase in temperature, the increase in degree of association of copolymers into micelles further contributed to the intensity of scattering at low Q for both samples.

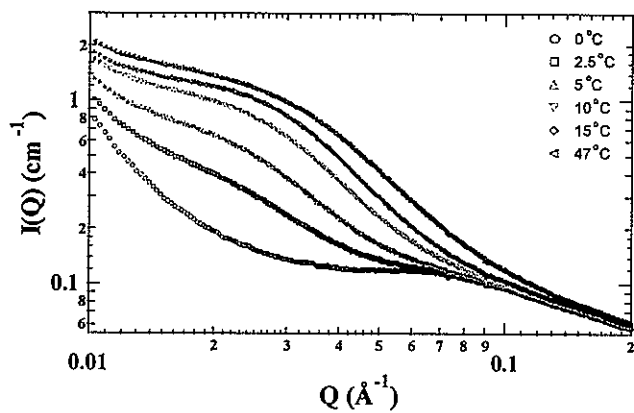


Figure 3.12. Effect of temperature on a pentablock copolymer solution of PDEAEM₅₀-F127-PDEAEM₅₀, 0.05 g/ml, pH 7.4, monitored by SAXS

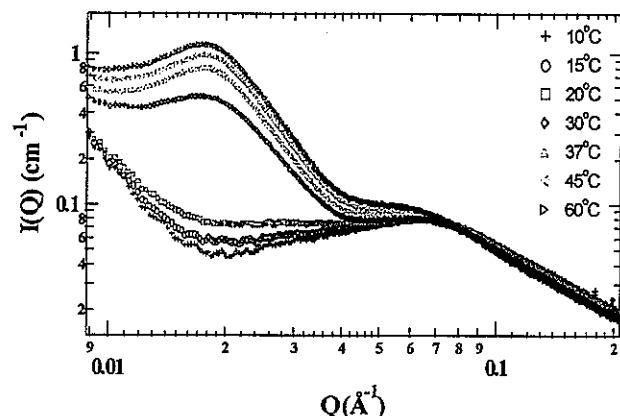


Figure 3.13. Effect of temperature on a pentablock copolymer solution PDEAEM₅₀-F127-PDEAEM₅₀, 0.05 g/ml, pH 4.4, monitored by SAXS.

No correlation peaks were visible in the low Q scattering for the pH 7.4 pentablock solutions but the continuous increase in scattering intensity could be attributed to the formation of a disordered micellar solution phase. Scattering from the pentablock copolymer solutions at pH 4.4 exhibited a more pronounced temperature dependence. Below 20°C, the scattering from the pH 4.4 solution exhibited a broad peak centered on $Q = 0.065$ which may correspond to interactions between charged unimers in solution. Above 20°C, a correlation peak was observed at $Q = 0.0175$ in the scattering pattern from the pH 4.4 pentablock copolymer solution. This suggests the presence of spherical micelles with a correlation length of about 35.7 nm.

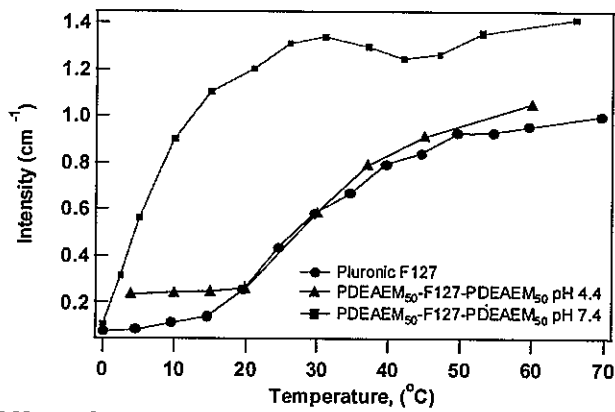


Figure 3.14. Effect of temperature on scattering intensity at $Q = 0.02 \text{ \AA}^{-1}$ in Pluronic® F127 and pentablock copolymer solutions.

The intensity, at $Q = 0.02 \text{ \AA}^{-1}$, for the pentablock copolymers at pH 4.4 and 7.4 and Pluronic® F127 are shown as a function of temperature in Figure 3.14. The CMT of the Pluronic® F127 and the pH 4.4 pentablock solutions both occurred near 20°C. This suggests that micellization of the pentablock in the charged state, at low pH, is due to the LCST of the PPO block. The intensity of scattering at low Q from the pH 7.4 pentablock copolymer solutions increased upon warming and reached a plateau at 25°C. The uncharged pentablock copolymers at pH 7.4 appeared to self-associate in a manner distinct from the micellization

of the pentablock copolymer at pH 4.4. Future small angle neutron scattering studies will examine the detailed structures of the micelles along with pH, and temperature dependent phase behavior of the pentablock copolymers.

The sol-gel transition temperatures and the viscoelastic properties of pentablock copolymer gels were measured with dynamic mechanical analysis (DMA). The sol-gel transition temperature of F127, as determined by this technique, agreed well with literature reports [29, 30]. The elastic modulus of the gel underwent dramatic transitions at the sol-gel temperature. The transition temperature was found to be independent of frequency in the range of 1-50 Hz. The storage moduli of gels (20% by weight) formed by PDEAEM₂₅-F127-PDEAEM₂₅ pentablock copolymer (F in Table 3.1) at several pH's and Pluronic® F127 gels are shown in Figure 3.15. The pentablock copolymers exhibited a thermoreversible sol-gel transition similar to Pluronic® F127. The solutions tested formed transparent, rigid gel phases at elevated temperatures and were free flowing liquids at lower temperatures. In the case of Pluronic® F127 solutions, micelles form in aqueous solutions when the PPO blocks aggregate and dehydrate to form compact cores surrounded by hydrated PEO chains that extend into the solvent forming a corona. Upon warming, PEO blocks become less hydrophilic, leading to the coronal interdigitation and packing into a physical network [31, 32]. The transition from liquid to gel phases is completely reversible. Solutions of PDEAEM₂₅-F127-PDEAEM₂₅ pentablock copolymer (20% by weight) at pH 3.0, 5.5 and 7.7 were found to form thermoreversible gels with transition temperatures around 20°C. At pH 8.3 the pentablock solution remained in the gel phase down to 7°C. This is presumably due to the presence of deprotonated and hydrophobic PDEAEM blocks forming non-temperature sensitive intermicellar network. The pentablock copolymer gels formed a less rigid gel phase

compared to F127 gels. The presence of the PDEAEM blocks in the pentablock copolymer likely disrupts the regular micellar lattice structure, resulting in a softer gel phase.

In keeping with the trends observed in Pluronic® F127 systems, the sol-gel transition temperatures of the pentablock copolymer solutions decreased with increasing concentration (data not shown) [12]. Pentablock copolymers with PDMAEM blocks were found to form thermoreversible gels with similar properties to the PDEAEM containing pentablock copolymer. The copolymers containing PDEAEM blocks were found to form more rigid gels with lower transition temperatures. The more hydrophobic ethyl groups of the PDEAEM blocks likely result in stronger hydrophobic interactions between micelles than the methyl groups of the PDMAEM blocks resulting in a more rigid macroscopic gel phase. The PDiPAEM pentablock copolymer was not easily dissolved at concentrations high enough to form gel phases, presumably due to the increased hydrophobicity of the PDiPAEM blocks. Pentablock copolymers incorporating the PtBAEM blocks did not form gels. We hypothesize that the presence of the bulky pendent *t*-Butyl group inhibits micellar packing and coronal interdigitation.

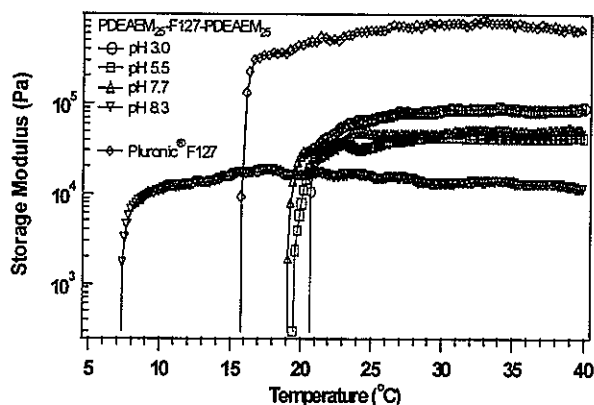


Figure 3.15. The storage modulus, as measured by DMA, of self-assembled gels formed by Pluronic® F127 and the pentablock copolymer.

The pentablock copolymers have potential applications in injectable depot drug delivery formulations. The thermoreversible sol-gel transition and the pH-dependent association properties impart environmentally sensitive solution properties that may be utilized to improve current injectable depot formulation properties [33].

3.5. Conclusions

An ATRP method for the synthesis of a family of novel pentablock copolymers with well-defined molecular weights under mild conditions has been developed. These pentablock copolymers were found to exhibit pH-sensitive micellization and LCST behavior and thermoreversible sol-gel transitions, in dilute and concentrated aqueous solutions respectively. The reversible gelation at around physiological temperatures and pH-dependent micellization make these pentablock copolymers potential candidates for use in injectable drug delivery devices that exhibit pH-regulated release and for injectable gene delivery applications.[26] Further investigations of the nanostructures of the micellar solutions and sol-gel transitions with detailed modeling analysis of small angle neutron scattering data and cryo-TEM will further elucidate the rich phase behavior of these materials.

3.6. Acknowledgements

We are grateful to undergraduate research assistants Amy Karlson and Richard Fulkerson for their help in the laboratory. This work was supported by the U.S. Department of Energy under contract number W-7405-ENG-81. This work benefited from the use of BESSRC-CAT at APS, funded by the U.S. DOE, BES under contract W-31-109-ENG-38 to the University of Chicago

3.7. References

1. Hashidzume, A., Y. Morishima, and K. Szczubialka, *Amphiphilic Polyelectrolytes*, in *Polyelectrolytes and their Applications*, S.K. Tripathy, J. Kumar, and H.S. Nalwa, Editors. 2002, American Scientific Publishers: Stevenson Ranch. p. 2-57.
2. Alexandridis, P. and B. Lindman, *Amphiphilic Block Copolymers: Self-Assembly and Applications*. 2000, New York: Elsevier.
3. Ma, Y., et al., *Synthesis of Biocompatible, Stimuli-Responsive, Physical Gels Based on ABA Triblock Copolymers*. Biomacromolecules, 2003. **4**(4): p. 864-8.
4. Tang, Y., et al., *Solubilization and Controlled Release of a Hydrophobic Drug Using Novel Micelle-Forming ABC Triblock Copolymers*. Biomacromolecules, 2003. **4**(6): p. 1636-1645.
5. Ma, Y., et al., *Well-Defined Biocompatible Block Copolymers via Atom Transfer Radical Polymerization of 2-Methacryloyloxyethyl Phosphorylcholine in Protic Media*. Macromolecules, 2003. **2003**(36): p. 10.
6. McCormick, C.L. and A.B. Lowe, *Aqueous RAFT Polymerization: Recent Developments in Synthesis of Functional Water Soluble (Co)polymers with Controlled Structures*. Accounts of Chemical Research, 2003. **37**(5): p. 312-325.
7. Schierholz, K., et al., *Acrylamide-Based Amphiphilic Block Copolymers via Nitroxide-Mediated Radical Polymerization*. Macromolecules, 2003. **36**(16): p. 5995-5999.
8. Wu, G.C., Benjamin; Schneider, Dieter K., *SANS Study of the Micellar Structure of PEO/PPG/PEO Aqueous Solution*. J. Phys. Chem., 1995. **99**(14): p. 5094-101.
9. Goldmints, I., et al., *Small-Angle Neutron Scattering Study of PEO-PPG-PEO Micelle Structure in the Unimer-to-Micelle Transition Region*. Langmuir, 1997(13): p. 3659-3664.
10. Alexandridis, P., J.F. Holzwarth, and T.A. Hatton, *Micellization of Poly(ethylene oxide)-Poly(propylene oxide)-Poly(ethylene oxide) Triblock Copolymers in Aqueous Solutions: Thermodynamics of Copolymer Association*. Macromolecules, 1994. **27**(9): p. 2414-25.
11. Alexandridis, P. and J.F. Holzwarth, *Differential scanning calorimetry investigation of the effect of salts on aqueous solution properties of an amphiphilic block copolymer (poloxamer)*. Langmuir, 1997. **13**(23): p. 6074-6082.
12. Wanka, G.H., H.; Ulbricht, W., *The aggregation behavior of poly(oxyethylene)-poly(oxypropylene)-poly(oxyethylene) block copolymers in aqueous solution*. Colloid Polym. Sci., 1990. **268**(2): p. 101-17.
13. Chu, B. and Z. Zhou, *Physical chemistry of polyoxyalkylene block copolymer surfactants*, in *Nonionic Surfactants: Polyoxyalkylene Block Copolymers*, V.M. Nace., Editor. 1996, M. Dekker: New York. p. 67-143.
14. Anderson, B.C., et al., *Synthesis and characterization of diblock and gel-forming pentablock copolymers of tertiary amine methacrylates, poly(ethylene glycol), and poly(propylene glycol)*. Macromolecules, 2003. **36**(5): p. 1670-1676.
15. Even, M., D.M. Haddleton, and D. Kukulj, *Synthesis and characterization of amphiphilic triblock polymers by copper mediated living radical polymerization*. European Polymer Journal, 2003(39): p. 633-639.

16. Haddleton, D.M., et al., *Atom Transfer Polymerization of Methyl Methacrylate Mediated by Alkylpyridylmethanimine Type Ligands, Copper(I) Bromide, and Alkyl Halides in Hydrocarbon Solution*. *Macromolecules*, 1999. **32**(7): p. 2110-2119.
17. Matyjaszewski, K. and J. Xia, *Atom Transfer Radical Polymerization*. *Chem. Rev.*, 2001. **101**(9): p. 2921-2990.
18. Wang, X.S., et al., *Unexpected Viability of Pyridyl Methanimine-Based Ligands for Transition-Metal-Mediated Living Radical Polymerization in Aqueous Media at Ambient Temperature*. *Macromolecules*, 2001. **34**(2): p. 162-164.
19. Lee, A.S., et al., *Structure of pH-Dependent Block Copolymer Micelles: Charge and Ionic Strength Dependence*. *Macromolecules*, 2002. **35**(22): p. 8540-8551.
20. Seifert, S., et al., *Design and performance of a ASAXS instrument at the Advanced Photon Source*. *J. Appl. Cryst.*, 2000. **33**: p. 782-784.
21. Zheng, Y., et al., *Directly Resolved Core-Corona Structure of Block Copolymers Micelles by Cryo-Transmission Electron Microscopy*. *The Journal of Physical Chemistry B*, 1999. **103**(47): p. 10331-10334.
22. Menard, K.P., *Dynamic Mechanical Analysis: A Practical Introduction*. 1 ed. 1999, New York: CRC Press LLC. 208.
23. Liu, S., N.C. Billingham, and S.P. Armes, *A Schizophrenic Water-Soluble Diblock Copolymer*. *Angew. Chem. Int. Ed.*, 2001. **40**(12): p. 2328-2331.
24. Barichello, J.M., et al., *Absorption of insulin from Pluronic F-127 gels following subcutaneous administration in rats*. *International Journal of Pharmaceutics*, 1999. **184**(2): p. 189-198.
25. Matyjaszewski, K., T. Pintauer, and S. Gaynor, *Removal of Copper-Based Catalyst in Atom Transfer Radical Polymerization Using Ion Exchange Resins*. *Macromolecules*, 2000. **33**(4): p. 1476-1478.
26. Agarwal, A., R. Unfer, and S.K. Mallapragada, *Novel thermogelling pH-sensitive pentablock copolymers as injectable gene delivery vectors*. *J. Controlled Release* (submitted), 2004.
27. Wang, C., et al., *Self-Assembly Behavior of Poly(methacrylic acid-block-ethyl acrylate) Polymer in Aqueous Medium: Potentiometric Titration and Laser Light Scattering Studies*. *J. Phys. Chem. B*, 2004. **108**(5): p. 1621-1627.
28. Lam, Y.-M.G., Nikolaus; Goldbeck-Wood, Gerhard., *Direct visualization of micelles of Pluronic block copolymers in aqueous solution by cryo-TEM*. *Physical Chemistry Chemical Physics*, 1999. **1**(14): p. 3331-3334.
29. Jeon, S., et al., *Microviscosity in poly(ethylene oxide)-polypropylene oxide-poly(ethylene oxide) block copolymers probed by fluorescence depolarization kinetics*. *Journal of Polymer Science Part B-Polymer Physics*, 2002. **40**(24): p. 2883-2888.
30. Jones, D.S., *Dynamic mechanical analysis of polymeric systems of pharmaceutical and biomedical significance*. *International Journal of Pharmaceutics*, 1999. **179**: p. 167-178.
31. Wanka, G.H., H.; Ulbricht, W, *Phase Diagrams and Aggregation Behavior of Poly(oxyethylene)-Poly(oxypropylene)-Poly(oxyethylene) Triblock Copolymers in Aqueous Solutions*. *Macromolecules*, 1994. **27**(15): p. 414594149.

32. Mortensen, K., W. Brown, and E. Joergensen, *Phase Behavior of Poly(propylene oxide)-Poly(ethylene oxide)-Poly(propylene oxide) Triblock Copolymer Melt and Aqueous Solutions*. *Macromolecules*, 1994. **27**(20): p. 5654-66.
33. Gil, E.S. and S.M. Hudson, *Stimuli-responsive polymers and their bioconjugates*. *Progress in Polymer Science*, 2004: p. 1-50.

**CHAPTER 4. TEMPERATURE AND PH DEPENDENT PHASE
BEHAVIOR OF PENTABLOCK COPOLYMERS BY SMALL ANGLE
NEUTRON SCATTERING**

A paper submitted to the journal Macromolecules

Michael D. Determan¹, Chieh-Tsung Lo², Liang Guo³, Rita Vilensky⁴, Yeshayahu Talmon⁴, P.

Thiyagarajan³, Surya K. Mallapragada^{1†}

4.1. Abstract

The pH- and temperature responsive self association behavior of a pentablock copolymer consisting of poly(N,N-(diethyl amino)ethyl methacrylate)-block-poly(ethylene oxide)-block-poly(propylene oxide)-block-poly(ethyleneoxide)-block-poly(N,N-(diethylamino)ethyl methacrylate) (PDEAEM-PEO-PPO-PEO-PDEAEM) was investigated with SANS and CryoTEM. Aqueous solutions of the pentablock copolymer were observed to form micelles and gels in response to changes in temperature and pH due to the lower critical solution temperature of the PPO block and the polyelectrolyte character of the PDEAEM blocks respectively. Modeling of the SANS data allowed for quantitative assessment of micellar dimensions and shape. The rich phase behavior exhibited by the aqueous pentablock copolymer solutions has potential possible drug delivery applications.

¹ Department of Chemical and Biological Engineering, Iowa State University and Ames Laboratory, 144 Spedding Hall, Ames, IA 50011, USA.

² Experimental Facilities Division, Argonne National Laboratory, 9700 S. Cass Avenue, Argonne, IL 60439, USA.

³ Intense Pulsed Neutron Source, Argonne National Laboratory, 9700 S. Cass Avenue, Argonne, IL 60439, USA.

⁴ Department of Chemical Engineering, Technion-Israel Institute of Technology, 32000, Israel

[†] Corresponding author. Phone: +1 515 294 7407 Fax: +1 515 294 2689 E-mail address: suryakm@iastate.edu

4.2. Introduction

Amphiphilic block copolymers with temperature and pH responsive properties have been recognized as versatile materials for a number of applications from drug delivery to personal care formulations. With the advent of living radical polymerization techniques such as ATRP and RAFT, a number of stimuli responsive block copolymers have been developed using the polymerization of water-soluble, functional monomers.[1, 2] These materials self assemble to form micelles with nanometer dimensions in response to changes in solution conditions. The stimuli responsive self assembly behavior of these materials makes them useful for a number of technological and biomedical applications, such as thermoresponsive viscosity modifiers and targeted drug delivery vectors. Recently synthesized block copolymers that are dual temperature responsive [3] and temperature and pH responsive [4-8] have been reported. In addition, the temperature, concentration and anion dependence of micellization properties of PEO-PPO-PEO triblock copolymers, commercially known as Pluronic or Poloxamers, have been thoroughly investigated in recent years.[9-13] For these studies, small angle scattering techniques turned out to be highly sensitive and thus invaluable in shedding light on the size and structure, as well as the morphological transitions of the self assembled micelles. Nanometer scale micelles with spherical, cylindrical, wormlike[14] and vesicular geometries have been observed in response to changes in pH, temperature and electrolyte concentration.

We have developed a novel amphiphilic block copolymer of poly(N,N-(diethyl amino)ethyl methacrylate)-block-poly(ethylene oxide)-block-poly(propylene oxide)-block-poly(ethyleneoxide)-block-poly(N,N-(diethylamino)ethyl methacrylate) (PDEAEM-PEO-PPO-PEO-PDEAEM) that forms micelles and gels with temperature and pH responsive

properties.[15] The pentablock copolymer exhibits a thermoreversible micellar transition due to the LCST of the central PPO block, resulting in micelles with fairly dehydrated PPO cores surrounded by hydrated PEO-PDEAEM corona. The pendent tertiary amine groups of the PDEAEM blocks are charged and hydrophilic at low pH, but become hydrophobic when they get deprotonated at pH above 7.5, leading to a pH dependent micellar transition of the pentablock copolymer solution. We have designed the pentablock copolymer for use as a biomaterial for drug delivery applications. The pentablock copolymer has been shown to solubilize low molecular weight hydrophobic drugs and form globular complexes with DNA[16, 17]. Cell culture cytotoxicity experiments of the pentablock copolymer gel indicate good overall biocompatibility.

The aim of this work was to examine in detail the pH and temperature responsive phase behavior of the pentablock copolymer in aqueous solutions. Small angle neutron scattering (SANS), cryo-TEM and ^1H NMR were used to probe the dependence of micellar geometry and size with solution conditions. Rheology was used to investigate the properties of aqueous solution of the pentablock copolymer (> 12 wt %) that form a physical hydrogel phase.

4.3. Experimental Section

4.3.1 Materials

The PDEAEM₂₅-PEO₁₀₀-PPO₆₅-PEO₁₀₀-PDEAEM₂₅ pentablock copolymer [$M_n = 21900$ and $M_w/M_n = 1.27$ as revealed by ^1H NMR in chloroform and THF and GPC using poly(methylmethacrylate) calibration standards respectively] was synthesized as previously reported. [15]

4.3.2 NMR

Solutions of pentablock copolymer were prepared by dissolving the pentablock copolymer in D₂O (99.9% deuterium, Aldrich) in 4 wt% solution at pH=3. The pH of the solution was adjusted by addition of DCl (30% in D₂O) and NaOD (5 M in D₂O). Aliquots were periodically removed as the solution was carefully titrated to pH=11. Samples were diluted to 2 wt% with the addition of D₂O. All ¹H NMR spectra were collected using a Varian VXR400 (400MHz) spectrometer, and chemical shifts are given in ppm.

4.3.3 Small Angle Neutron Scattering

SANS experiments were carried out using the time-of-flight small-angle neutron diffractometer (SAND) at the Intense Pulsed Neutron Source (IPNS) in Argonne National Laboratory. This instrument provides data in the Q range of 0.004-1.0 Å⁻¹ in a single measurement by using a 40x40 cm² position-sensitive ³He gas detector and neutrons with wavelengths in the range of 0.5-14 Å ($\Delta\lambda=0.05$ at each λ). Copolymer solutions were sealed in Suprasil cylindrical cells with 2 mm path length for the SANS measurements. A liquid flow thermostat was used to control the temperature to within ± 1 °C. The scattering data were corrected for empty cell and solvent scattering, detector sensitivity, and sample transmission. The differential scattering cross section $I(Q)$ was placed on an absolute scale in the units of cm⁻¹ by using secondary standards whose absolute scattering cross sections are known.

4.3.4 Small Angle Scattering Analysis

SANS experiments were carried out using the time-of-flight small-angle neutron diffractometer (SAND) at the Intense Pulsed Neutron Source (IPNS) in Argonne National Laboratory. This instrument provides data in the Q range of 0.004-1.0 Å⁻¹ in a single

measurement by using a 40x40 cm² position-sensitive ³He gas detector and neutrons with wavelengths in the range of 0.5-14 Å ($\Delta\lambda=0.05$ at each λ). Copolymer solutions were sealed in Suprasil cylindrical cells with 2 mm path length for the SANS measurements. A liquid flow thermostat was used to control the temperature to within ± 1 °C. The scattering data were corrected for empty cell and solvent scattering, detector sensitivity, and sample transmission. The differential scattering cross section $I(Q)$ was placed on an absolute scale in the units of cm⁻¹ by using secondary standards whose absolute scattering cross sections are known.

2.4 Small Angle Scattering Analysis

The scattering intensity for a system of monodisperse particles can be expressed as

$$I(Q) = (\Delta\rho)^2 N_s F(Q) S(Q) + I_{inc} \quad (1)$$

where $(\Delta\rho)^2$ is the contrast factor, N_s is the number density of scattering particles, $F(Q)$ is the single particle form factor, $S(Q)$ is the interparticle structure factor and I_{inc} is the incoherent scattering background. Recent reviews provide analytical expressions of form factors for a number of geometrical shapes and structure factor expressions that can be used to model the scattering data from block copolymer micelles. [18, 19] Although it is readily possible to ascertain the shapes of the micelles from the SANS data alone, complementary information on the shapes from other techniques would enable better characterization of the system. The Pedersen Core-Chain form factor model[20] was selected based on cryo-TEM images that indicated the presence of spherical micelles. This form factor describes a micelle geometry consisting of a condensed spherical core dominated by the PPO segments with attached Gaussian chains of PEO and PDEAEM segments.[20] This form factor was previously

employed to describe the size and shape of the micelles of Pluronic F88 solutions in D₂O. [12, 21] The scattering curves were then fitted using a least squares fitting routine to extract parameters of the miceller system. [22] A structure factor developed to describe the interactions between colloidal macroions was used to model the interaction between the charged pentablock copolymer micelles due to the presence of the ionized end blocks of PDEAEM at low pH. [23, 24] The expression of this structure factor reduces to the Percus-Yevick structure factor for hard spheres when the macroion become neutral at pH > 7.0. The form factor includes four fitting parameters: R_{core} , radius of micelle core, R_g , radius of gyration of the attached Gaussian chain, N , the association number of copolymer chains per micelle, and d , the coronal stretch factor such that d^*R_g is the distance of the center of mass of the attached Gaussian coil from the micelle core surface. The structure factor also includes three parameters: R_{hs} , hard sphere radius, ϕ , the micelle volume fraction and, Z , the effective micelle surface charge. The charge, Z , is expressed in effective surface charge per micelle. [25] Known parameters in the model include the ionic strength, temperature, valance of counter ions [Na⁺, Cl⁻], scattering length contrast in D₂O of the core (PPO), $b_s = -0.0371$ Å, and corona (PEO and PDEAEM) segments $b_c = -0.0903$ Å.

4.2.5 Cryo-TEM

Cryo-TEM images were acquired with a Philips CM 120 Transmission Electron Microscope equipped with a Gatan cooled-CCD 1024x1024 pixel MultiScan 791 camera. Samples solutions were wetted onto hydrophilicly modified holey carbon grids and were vitrified with a Gatan Controlled Environment Vitrification System. An Oxford CT3500 cryo-holder and transfer-station were used to manipulate the vitrified sample prior to imaging.

4.2.6 Rheometry

A Haake Rheostress RS80 controlled stress rheometer equipped with the water-cooled peltier temperature controller was employed for the rheological measurements (Thermo Haake, Karlsruhe, Germany). A stainless steel C40/4 cone-and-plate (diameter 40mm and angle 4°) sensor with a shear rate and frequency controlled at 1 Pa and 1 Hz was used to obtain the viscosity data of the copolymer solution. The temperature sweeps were conducted at 5°C/min between 10 and 75°C. A thin layer of Dow Corning Fluid was used to prevent evaporation of water from the copolymer solution over the course of the measurement. A stress sweep was performed prior to the temperature studies to ensure the test conducted in the linear viscoelastic regime.

4.4. Results and Discussion

4.4.1 ^1H NMR of Pentablock copolymer

The pK_a of the PDEAEM blocks were determined by potentiometric titration of a 2 wt % pentablock copolymer solution at 25°C as shown in Figure 4.1. The inflection at pH 7.5 is taken as the pK_a . The titration data is plotted as the degree of amine protonation, or the fraction of DEAEM amine groups that are ionized, based on the acid-base stoichiometry of the copolymer solution. The uncharged PDEAEM is hydrophobic and is expected to form collapsed coils that phase separate from the aqueous solution. The ^1H NMR of the pentablock copolymer solutions as a function of pH were performed to examine the extent of hydration of the PDEAEM blocks. A ^1H NMR of the pentablock copolymer in D_2O at pH=3.0 is shown in Figure 4.2. The spectra were recorded at 25°C of the 2 wt % pentablock copolymer aliquots taken during the course of the titration. The ^1H NMR peaks associated with the pendent amine groups of the PDEAEM, labeled as A, D, E and H in Figure 4.2, are

progressively attenuated with increasing pH due to the decrease in hydration and mobility of these groups as the tertiary amine is deprotonated. The extent of hydration is inferred using the integral of the signal at pH $\delta = 4.1$. At pH=3 the PDEAEM blocks are completely protonated and fully hydrophilic. As the pH of the solution is adjusted during the course of the titration the degree of hydration decreases sharply around pH=7.5 as shown in Figure 4.1. Previously dynamic laser light scattering experiments indicated the formation of large aggregates of copolymer in solution around pH 7.5.[15]

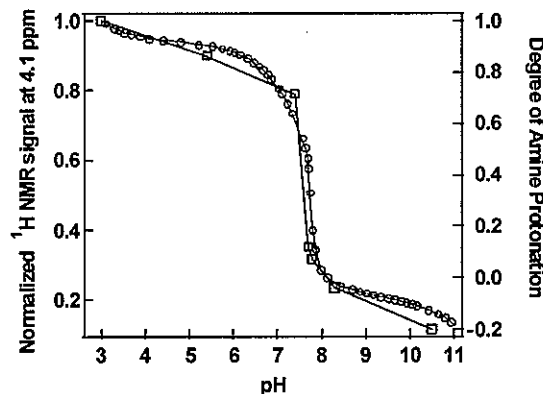


Figure 4.1. The normalized in ^1H NMR signal at 4.1 ppm, corresponds to the degree of PDEAEM block hydration (□, left axis), and the degree of amine protonation (solid line, right axis) determined by potentiometric titration.

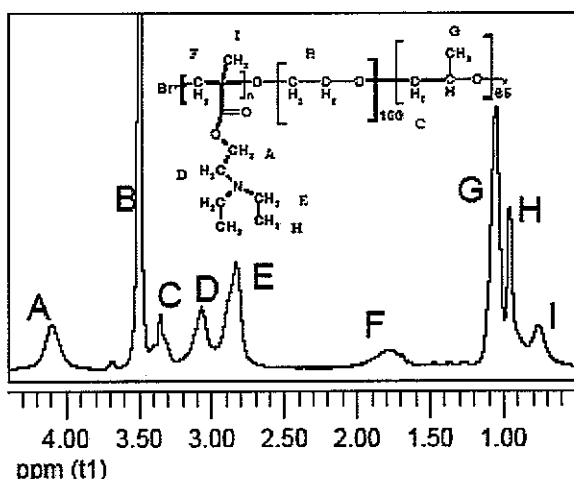


Figure 4.2. ^1H NMR in D_2O of pentablock copolymer, pH=3.0 and 25°C

4.4.2 SANS and Cryo-TEM of pentablock copolymer micelles

SANS was used to investigate the micelle size and morphology of pentablock copolymer solutions at various conditions. Solutions were prepared at 2 wt % and at several pH values in the range of 3 to 10.5. These solutions were examined at several temperatures to investigate the temperature-responsive self assembly of the copolymers in solution. Based on ^1H NMR and previous light scattering studies, a significant transition of micellar morphology was anticipated to occur around the pK_a of the PDEAEM blocks. Solutions of Pluronic F127 micelles were also examined with SANS as the control case. These solutions were similarly prepared with D_2O and an equivalent weight percent of PPO that correspond to 1.2 wt % of Pluronic triblock copolymer. The neat F127 solutions at pH 3, 7 and 10 exhibited identical scattering curves within the sampling error of the instrument (data not shown). On the other hand, the pentablock copolymer solutions exhibited strong pH dependence in the scattering data. The SANS data from the pentablock solutions were fitted using the Pedersen Core-Corona form factor and both Percus-Yevick hard sphere structure factor at higher pH and the Hayter-Penfold macroion structure factor at low pH. For 2 wt % pentablock copolymer solutions at pH 3, 7.4, 7.7 and 7.8, the Hayter-Penfold macroion structure factor, with a non-zero surface charge parameter, yielded the best description of the scattering data, particularly in the low Q region. At pH=8.3 the SANS data was best fit by setting the surface charge parameter to zero, effectively reducing the structure factor contribution to hard sphere interactions. The SANS data and model fits of 2 wt % pentablock copolymer solutions at different temperature and pHs are shown in Figure 4.3. The best-fit parameters for both Pluronic F127 and pentablock copolymer micelle solutions are shown in Table 1. The fitting

parameters were checked by the calculation of the copolymer concentration from the aggregation number, derived from the form factor expression, and the hard sphere interaction radius, derived from the structure factor expression, as shown below

$$\text{concentration} = \frac{3\phi NM}{4\pi R_{hs}^3 N_A} \quad (2)$$

where M is the molar mass of the copolymer and N_A is the Avogadro's number.

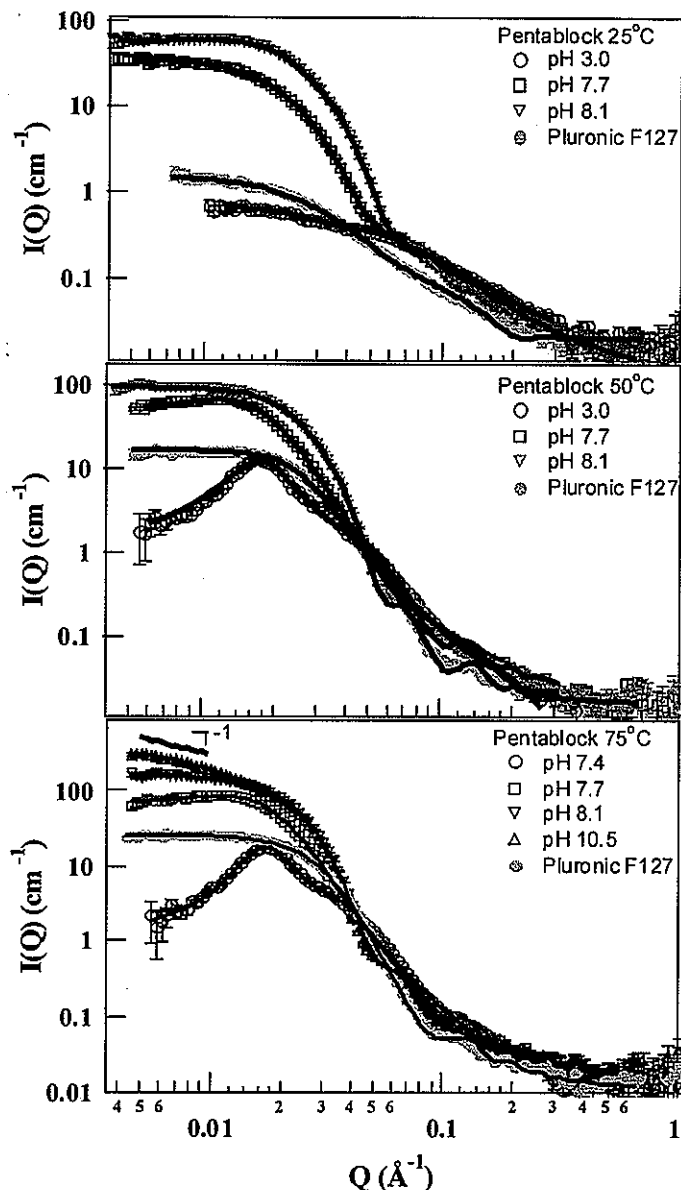


Figure 4.3. SANS data of 2 wt % pentablock copolymer at different pH and temperatures. SANS data of 1.2% Pluronic F127 at different temperatures is also included.

The concentration of Pluronic F127 calculated from the fit parameters was 1.1 wt % above 25°C compared to the experimental concentration of 1.2 wt %. Similar results were obtained for the copolymer concentration of the pentablock copolymer samples, where the calculated concentrations ranged from 0.4 wt % to 1.7 wt % compared to the experimental concentration of 2.0 wt %. In all cases, the calculated concentration of the pentablock copolymer was less than the sample concentration. This is consistent with the fact that the micelle volume contains a non-negligible amount of D₂O while the equation attributes the entire volume of the micelle to copolymer molecules.[10, 12] This provides a good check of the consistency of the model assumptions with the micelle morphology in the copolymer solutions.

The scattering from the Pluronic F127 solutions was modeled with the Pedersen core-shell model with the Percus-Yevick hard sphere potential. The radius and volume fraction of the Pluronic® F127 copolymer micelles increased from 8.6 nm and 0.6 % at 25°C to 11.5 nm and 7.6 % at 37°C. A 2 wt % Pluronic F127 copolymer solution at 25°C is close to the critical micellization temperature. The increase in size, aggregation number and volume fraction of micelles at 37°C is due to the progressive dehydration of the PPO blocks of the copolymer with increasing temperature. In the transition region between 25 and 37°C, the equilibrium of the copolymer shifts from predominantly dissolved unimers in solution to micelles. At 50 and 75°C, the size and volume fraction of the micelles remained essentially the same as at 37°C. The small increase in the size of the core and decrease in the size of the corona have been attributed to the incorporation of PEO units into the dehydrated PPO core of the micelle at elevated temperatures.[12] The size of the Pluronic F127 micelles was in good agreement with the previous SANS studies of F127 micelles.[26]

Sample	R_o (Å)	R_g (Å)	N_{agg}	ϕ	R_{hs} (Å)	Z
25°C						
F127 pH 7.0	20	33	21	0.006	86	Na
PB pH 3.0	15	23	3	0.003	28	33
PB pH 7.4	15	25	2	0.006	28	26
PB pH 7.7	42	37	21	0.020	75	3
PB pH 7.8	42	36	31	0.057	122	8
PB pH 8.1	48	32	51	0.046	150	0
37°C						
F127 pH 7.0	43	36	41	0.076	112	Na
PB pH 3.0	17	34	11	0.036	102	31
PB pH 7.4	21	40	11	0.036	99	34
PB pH 7.7	42	42	36	0.046	98	12
PB pH 7.8	45	51	52	0.055	122	8
PB pH 8.1	50	32	69	0.037	158	0
50°C						
F127 pH 7.0	45	33	46	0.065	110	Na
PB pH 3.0	21	42	13	0.057	115	41
PB pH 7.4	20	41	14	0.050	113	40
PB pH 7.7	42	48	46	0.110	153	9
PB pH 7.8	43	48	70	0.110	188	7
PB pH 8.1	50	30	89	0.022	150	0
PB pH 10.3	43	26	87	0.003	85	0
75°C						
F127 pH 7.0	47	31	48	0.060	108	Na
PB pH 3.0	26	39	17	0.062	127	46
PB pH 7.4	26	39	18	0.055	126	46
PB pH 7.7	46	53	59	0.120	159	10
PB pH 8.1	54	35	104	0.022	140	0

Table 4.1. Micellar parameter from modeling of SANS data of 2 wt% Pluronic F127 and pentablock (PB) copolymer solutions in D_2O at different pH and temperature. R_o is the core radius, R_g is the radius of gyration of the chains attached to the core, N_{agg} is the aggregation number of the micelle, ϕ is the micelle volume fraction, R_{hs} is the hard sphere interaction radius, and Z is the effective surface charge.

The size of the pentablock copolymer micelles was found to depend strongly on the temperature and pH of the solution. SANS data from pentablock copolymer solutions at pH 3.0 and 7.4 were nearly identical and yielded similar fitted micellar parameters. With increasing temperature, the volume fraction of the micellar aggregates increased dramatically, which is similar to the behavior of the Pluronic F127 solutions. However, the

scattering data exhibited a strong correlation peak at $Q = 0.016 \text{ \AA}^{-1}$ that was absent in the SANS data from the Pluronic F127 solutions. The large peak indicates the presence of high concentration of micelles separated by the repulsive electrostatic interactions between micelles due to the presence of polyelectrolyte PDEAEM blocks in the micelle corona. Pedersen core-chain form factor and the Hayter-Penfold macroion potential structure factor that accounts for the electrostatic interactions between charged colloidal particles, when used together yielded a better fit to the SANS data. With increasing temperature, the micellar radius, aggregation number and micelle volume fraction of the pentablock copolymer solutions at pH 3.0 and 7.4 of the copolymer increased. This increase was most substantial between 25 and 37°C. The increase in aggregation number with temperature corresponded to a significant increase in the effective surface charge per micelle. The effective surface charge of the pentablock micelles decreased with increasing pH, which corresponds to the decrease in amine protonation of the PDEAEM blocks. At pH > 8.1, the PDEAEM in pentablock copolymer are essentially deprotonated and the SANS data was better described by setting the effective surface charge to zero. This deprotonation of the outer PDEAEM blocks was accompanied by a progressive increase in scattering in the low-Q, suggesting that micelles are growing in size. This change in the scattering pattern was reflected in the calculated micellar parameters as increasing size and aggregation number of the micelles at a given temperature. Increasing the pH from 3.0 to 7.8 resulted in a 4.7 fold increase in the aggregation number and slightly less than a doubling of the average micellar volume. This indicates that micelles formed above pH=7.5 were larger and contained a lower fraction of D₂O.

At each temperature, the calculated volume fraction at pH=8.1 deviated from the trend of increasing micelle volume fraction with increasing solution pH. Whereas the model was able to fit the SANS data satisfactorily, the departure from the trend is an indication that geometric assumptions of the model are less valid. Indeed, upon further increasing the pH to 10.3 at 75°C, the SANS intensity exhibited a negative slope with a Q^{-1} dependence, which indicates the presence of rod like or cylindrical micelles. Modified Guinier analysis was used to extract the apparent cross sectional radius of gyration, R_c , of the rod-like micelles. The presence of a linear region with a negative slope is a good indication of the presence of cylindrical micelles. The Guinier equation was fit to the linear region of the $\ln(Q^*I(Q))$ vs Q^2 plot of the SANS data from the pH=10.3 solution at 75°C. The linear fit to the data in the region where maximum Q used in the fit is less than $1/R_c$, yielded an apparent radius of 44.5 ± 0.4 Å that corresponds to a radius of 62.9 ± 0.6 Å. Particular solution conditions have been shown to induce a spherical to cylindrical micelles transitions in other block copolymer systems. At 73°C in the presence of concentrated divalent salt, K_2CO_3 , triblock copolymer Pluronic F88 micelles transition from spherical to cylindrical, rod like micelles.[12] The transition was attributed to the aggregation of spherical micelles at these conditions. Similar transition from “sphere-to-worm-like” micelles was observed in aqueous micellar solutions of diblock copolymer poly(oxyethylene)-block-poly(oxybutylene) in water.[27] These authors suggest that as the micelle core increases in size due to increases in aggregation number caused by particular solution conditions, the surface-to-volume ratio of the core is necessarily reduced. In order to maintain a uniform density throughout the core under these conditions, the micelle morphology transitions from spherical to cylindrical structure. These arguments are easily adopted to give a phenomenological and geometrical explanation of the

spherical to cylindrical micelle transition of the pentablock copolymer system. At pH values above the pK_a of the PDEAEM blocks the pentablock copolymer micelles increased in size and aggregation number due to the self association of the hydrophobic PDEAEM blocks within the corona and between the coronas of neighboring micelles. At elevated temperatures, where the scattering clearly indicates the predominance of cylindrical micelles, the decreased solubility of the PEO blocks also results in the growth of the core phase of the micelles. These stimuli responsive changes in the relative solubility of the blocks result in the formation of cylindrical or rod like micelles.

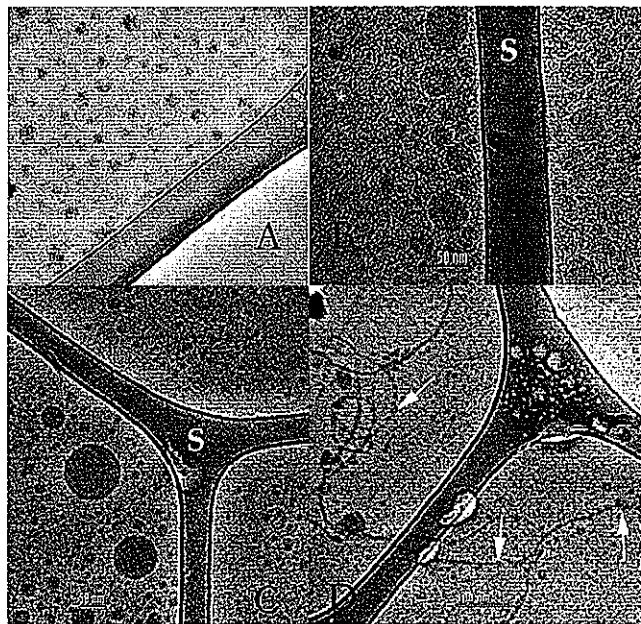


Figure 4.4. Cryo-TEM images of pentablock copolymer micelles with 1 wt % of 22.1 kDa pentablock copolymer at (A) pH 3.0, (B) pH 7.4 (C) pH 7.7, (D) pH 8.1. Asterisk indicates background texture.

Because no analytical expression is currently available, to our knowledge, to quantitatively evaluate the SANS data of interacting cylindrical micelles, a direct visualization technique was utilized to examine the nature of the cylindrical pentablock copolymer micelles. Figure

4.4 shows the CryoTEM micrographs of pentablock copolymer micelles at pH 3.0, 7.4, 7.7 and 8.1. The spherical pentablock copolymer micelles visualized at pH=3 appear to have relatively uniform diameters of 20 nm. This is in excellent agreement with the size of micelles extracted from the SANS data. At pH 7.4 and 7.7 (Figures 4.4(B) and (C)) larger micelles are observed that have a considerable size distribution between 20 and 50 nm in diameter. In the TEM micrograph the larger micelles appear to have a more disc like structure than the smaller micelles. With the pentablock copolymer solution at pH=8.3 as shown in Figure 4.4(D), the white arrows point to long worm like micelles that appear to coexist with a population of spherical micelles. It is difficult to measure the length of the worm like micelles visualized. However the diameter is similar in value derived from the modified Guinier analysis of the SANS data at 75°C and pH=10.5. The cryo TEM samples were prepared at room temperature prior to vitrification. This suggests that the structural transition of the pentablock copolymer micelles, from spherical to worm-like, is a continuous process, presumably due to the polydispersity of the copolymers.

4.4.4 Pentablock copolymer hydrogel

Aqueous solutions of the pentablock copolymer exhibit a reversible thermoresponsive sol-gel transition at concentrations greater than 12 wt %. Shear rheometry and SANS were used to investigate the viscoelastic properties and the structure of the hydrogel of 14 wt % pentablock copolymer solutions. The strong intermicellar interactions at 14 wt % precluded the quantitative modeling analysis of the SANS data.

The viscosity of the pentablock copolymer solution was monitored with constant stress, oscillatory shear rheometry at several temperatures between 10 and 75°C. In Figure 4.5 the measured viscosity of solutions at pH 3.0, 7.7 and 8.3 are shown. The viscosity of the

pentablock copolymer solution at pH=3 increases more than 3 orders of magnitude at the sol-gel transition temperature, which is around 20°C. This is qualitatively consistent with the SANS data shown in Figure 4.6 for the same solution (not undergoing shear) at 10 and 50°C. At pH =3.0 and 10°C the copolymer solution exhibited very low levels of coherent scattering, which is indicative of the presence of disorganized copolymers in solution. At pH = 3.0 and 50°C, peaks in the SANS data indicate hexagonal packing of micelles that are presumably due to the macroassembly of rod-like micelles. It is well known that such worm-like micelles will exhibit high viscosity as shown in Figure 4.5 for the 14 wt% sample at higher temperatures.

At pH=7.7, which is near the pK_a of the copolymer, the solution formed a lower viscosity gel phase compared to that of the pH=3.0 solution. The broad peak at low Q in the SANS data of the pH=7.7 solution suggests the presence of large, poorly ordered micelles at 10°C. At pH=7.7 the micelles become uncharged and the increasingly hydrophobic PDEAEM blocks are microphase separated from solution as observed in the ¹H NMR results. This could be accomplished by the aggregation of several micelles into clusters, resulting in high scattering intensity at low Q and the broad correlation peak. At 50°C, where a gel phase forms, a more distinct peak was observed and the maximum intensity shifts from 0.0179 to 0.02291 Å⁻¹. The strong scattering at low Q also suggests the presence of large aggregates of micelles. The presence of large aggregations of micelles with different sizes may decrease the ordering of the micellar gel, resulting in a softer gel phase.

At pH=8.3 the PDEAEM blocks of the pentablock copolymer becomes completely uncharged. At 10°C the solution was notably more viscous than pH 3.0 and 7.7 solutions. SANS data indicated the presence of interacting cylindrical micelles, inferred by the I(Q) ~

Q^{-1} region at low Q and the strong correlation peak at 0.0253 \AA^{-1} . The pH=8.3 solution exhibited a modest increase in viscosity between 20 and 35°C, which corresponds to an increase in the intensity of the SANS. The overall shape of the SANS data remained relatively constant between 10 and 50°C with a small increase in the intensity at low Q . This indicates that the increase in viscosity is due to an increase in the size or number density of the cylindrical micelles due to the progressive dehydration of the PPO segments.

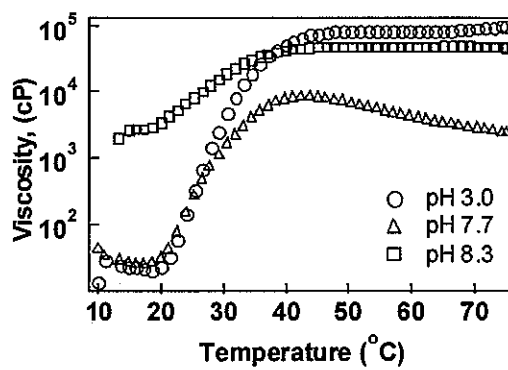


Figure 4.5. Shear rheometry temperature sweep data of 14 wt % pentablock copolymer solutions at different pH.

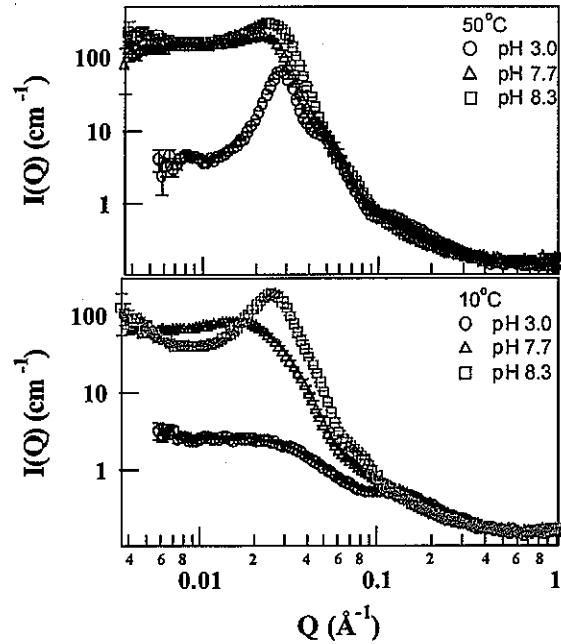


Figure 4.6. SANS data of 14 wt % pentablock copolymer at different pH and temperatures.

4.5. Conclusions

In summary SANS, cryo-TEM, and NMR data confirmed that the pentablock copolymers form multi responsive micelles assemble due to both the LCST of PPO blocks and the deprotonation of the PDEAEM blocks. Rheology was used to examine the resulting solution gelation due to micellar packing and interdigitation as a result of changes in temperature and solution pH. The Pedersen core-chain form factor and the Haytor-Penfold macroion structure factor successfully describe the data and yield information on micellar dimensions. Micelles formed below the pK_a of the PDEAEM blocks interact as charged colloid particles and exhibit sharp correlation peaks due to the repulsive columbic interactions. The deprotonation of the PDEAEM blocks at pH higher than 7.5 resulted in increasing aggregation number, as well as size and size distribution of the micelles as observed by SANS and cryo-TEM. The progressive dehydration of the PDEAEM blocks results in the formation of cylindrical thread-like micelles, observed at pH=8.1 with Cryo TEM. Because of the polydispersity of the aggregates the scattering results do not unambiguously identify the presence of thread like micelles until the solution conditions were pH=10.5 and 50°C.

4.6. Acknowledgment

This work was supported by the U.S. Department of Energy under contract number W-7405-ENG-81 to Iowa State University. In addition, this work benefited from the use of IPNS funded by the US DOE, BES under contract W-31-109-ENG-38 to the University of Chicago.

4.7. References

1. McCormick, C.L. and A.B. Lowe, *Aqueous RAFT Polymerization: Recent Developments in Synthesis of Functional Water Soluble (Co)polymers with Controlled Structures*. Accounts of Chemical Research, 2003. 37(5): p. 312-325.

2. Lecolley, F., et al., *Synthesis of functional polymers by living radical polymerisation*. *J. Mater. Chem.*, 2003. **13**: p. 2689-2695.
3. Arotcüare'na, M., et al., *Switching the Inside and the Outside of Aggregates of Water-Soluble Block Copolymers with Double Thermoresponsivity*. *Journal of American Chemical Society*, 2002. **124**(14): p. 3787-3793.
4. Schilli, C.M., et al., *A New Double-Responsive Block Copolymer Synthesized via RAFT Polymerization: Poly(N-isopropylacrylamide)-block-poly(acrylic acid)*. *Macromolecules*, 2004. **37**(21): p. 7861-7866.
5. Lee, A.S., et al., *Structure of pH-Dependent Block Copolymer Micelles: Charge and Ionic Strength Dependence*. *Macromolecules*, 2002. **35**(22): p. 8540-8551.
6. Lee, A.S., et al., *Characterizing the Structure of pH Dependent Polyelectrolyte Block Copolymers Micelles*. *Macromolecules*, 1999. **32**: p. 4302-4310.
7. Liu, S., N.C. Billingham, and S.P. Armes, *A Schizophrenic Water-Soluble Diblock Copolymer*. *Angew. Chem. Int. Ed.*, 2001. **40**(12): p. 2328-2331.
8. Mertoglu, M., et al., *Stimuli responsive amphiphilic block copolymers for aqueous media synthesised via reversible addition fragmentation chain transfer polymerisation (RAFT)*. *Polymer*, 2005. **46**(2005): p. 7726-7740.
9. Chu, B., G. Wu, and D.K. Schneider, *A scattering study on intermicellar interactions and structures of polymeric micelles*. *J. Polym. Sci., Part B: Polym. Phys.*, 1994. **32**(16): p. 2605-14.
10. Goldmints, I., et al., *Small-Angle Neutron Scattering Study of PEO-PP0-PEO Micelle Structure in the Unimer-to-Micelle Transition Region*. *Langmuir*, 1997(13): p. 3659-3664.
11. Mortensen, K., *Phase behavior of poly(ethylene oxide)-poly(propylene oxide)-poly(ethylene oxide) triblock-copolymer dissolved in water*. *Europhys. Lett.*, 1992. **19**(7): p. 599-604.
12. Mao, G., et al., *PEO-PPO-PEO Block Copolymer Micelles in Aqueous Electrolyte Solutions: Effect of Carbonate Anions and Temperature on the Micellar Structure and Interaction*. *Macromolecules*, 2001. **34**(3): p. 552-558.
13. Guo, L., et al., *Micellar structure changes in aqueous mixtures of nonionic surfactants*. *Journal of Rheology*, 2001. **45**(5): p. 1223.
14. Flood, C., C.A.D. Croce, and T. Cosgrove, *Wormlike Micelles Mediated by Polyelectrolyte*. *Langmuir*, 2005. **21**(17): p. 7646-7652.
15. Determan, M.D., et al., *Synthesis and characterization of the temperature and pH-responsive pentablock copolymers*. *Polymer*, 2005. **46**: p. 6933-6946.
16. Agarwal, A., R. Unfer, and S.K. Mallapragada, *Novel thermogelling pH-sensitive pentablock copolymers as injectable gene delivery vectors*. *J. Controlled Release*, 2004. **103**(1): p. 245-258.
17. Anderson, B.C., et al., *Synthesis and characterization of diblock and gel-forming pentablock copolymers of tertiary amine methacrylates, poly(ethylene glycol), and poly(propylene glycol)*. *Macromolecules*, 2003. **36**(5): p. 1670-1676.
18. Pedersen, J.S. and C. Svaneborg, *Scattering from block copolymer micelles*. *Current Opinion in Colloid & Interface Science*, 2002. **7**: p. 158-166.
19. Castelletto, V. and I.W. Hamley, *Small-Angle Scattering Functions of Micelles*. *Fibre Diffraction Review*, 2003. **11**: p. 36-43.

20. Pedersen, J.S. and M.C. Gerstenberg, *Scattering Form Factor of Block Copolymer Micelles*. *Macromolecules*, 1996. **29**(4): p. 1363.
21. Mao, G., et al., *PEO-PPO-PEO Block Copolymer Micelles in Aqueous Electrolyte Solutions: Effect of Carbonate Anions and Temperature on the Micellar Structure and Interaction* Volume 34, Number 3, January 30, 2001, pp 552-558. *Macromolecules*, 2001. **34**(13): p. 4666.
22. Pedersen, J.S., *Analysis of small-angle scattering data from colloids and polymer solutions: modeling and least-squares fitting*. *Advances in Colloid and Interface Science*, 1997. **70**: p. 171-210.
23. Hayter, J.B. and J. Penfold, *An analytic structure factor for macroion solutions*. *Molecular Physics*, 1981. **42**(1): p. 109-118.
24. Hansen, J.-P. and J.B. Hayter, *A rescaled MSA structure factor for dilute charged colloidal dispersions*. *Molecular Physics*, 1982. **46**(3): p. 651-656.
25. Gorski, N., M. Gradzielski, and H. Hoffmann, *Mixtures of Nonionic and Ionic Surfactants. The Effect of Counterion Binding in Mixtures of Tetradecyldimethylamine Oxide and Tetradecyltrimethylammonium Bromide*. *Langmuir*, 1994. **10**(8): p. 2594-2603.
26. Prud'homme, R.K., G. Wu, and D.K. Schneider, *Structure and Rheology Studies of Poly(oxyethylene-oxypropylene-oxyethylene) Aqueous Solution*. *Langmuir*, 1997. **12**(20): p. 4651-4659.
27. Hamley, I.W., et al., *A Small-Angle Neutron Scattering Study of Spherical and Wormlike Micelles Formed by Poly(oxyethylene)-Based Copolymers*. *Langmuir*, 2001. **17**(20): p. 6386-6388.

CHAPTER 5. SUPRAMOLECULAR SELF-ASSEMBLY OF MULTIBLOCK COPOLYMERS IN SOLUTION

A paper submitted to the journal Langmuir

Michael D. Determan¹, Liang Guo², P. Thiagarajan², Surya K. Mallapragada^{1,†}

5.1 Abstract

A unique pH-dependent phase behavior from a copolymer micellar solution to a collapsed hydrogel with micelles ordered in a hexagonal phase was observed. Small angle neutron scattering (SANS) was used to follow the pH-dependent structural evolution of micelles formed in a solution of a pentablock copolymer consisting of poly((diethylaminoethylmethacrylate)-b-(ethylene oxide)-b-(propylene oxide)-b-(ethylene oxide)-b-(diethylaminoethylmethacrylate)) ($\text{PDEAEM}_{25}\text{-b-PEO}_{106}\text{-b-PPO}_{69}\text{-b-PEO}_{106}\text{-b-PDEAEM}_{25}$). Between pH 3.0 and pH 7.4, we observed the presence of charged spherical micelles. Increasing the pH of the micelle solution above pH 7.4 resulted in increasing in size of the micelles due to the increasing hydrophobicity of the PDEAEM blocks above their pK_a of 7.6. The increase in size of the spherical micelles resulted in a transition to a cylindrical micelle morphology in the pH range of 8.1 to 10.5, and at pH > 11, the copolymer solution undergoes macroscopic phase separation. Indeed, the phase separated copolymer

¹ Department of Chemical and Biological Engineering, Iowa State University and Ames Laboratory, 144 Spedding Hall, Ames, IA 50011, USA.

² Intense Pulsed Neutron Source, Argonne National Laboratory, 9700 S. Cass Avenue, Argonne, IL 60439, USA.

[†] Corresponding author. USA Phone: +1 515 294 7407 Fax: +1 515 294 2689 E-mail address: suryakm@iastate.edu

sediments and coalesces into a hydrogel structure that consists of 25-35 wt % water. Small angle X-ray scattering (SAXS) clearly indicated that the hydrogel has a hexagonal ordered phase. Interestingly, the process is reversible, as lowering of the pH below 7.0 leads to rapid dissolution of the solid into homogeneous solution. We believe that the hexagonal structure in the hydrogel is a result of the organization of the cylindrical micelles due to the increased hydrophobic interactions between the micelles at 70°C and pH 11. Thus we have developed a pH/temperature dependent, reversible hierarchically self-assembling block copolymer system with structures spanning nano- to micro- scale dimensions.

5.2. Introduction

Nature exhibits a variety of self-assembled structures that researchers have tried to mimic to facilitate a bottom-up approach to materials design and fabrication.[1] In particular, the self-assembly of organic molecules and synthetic polymers have been extensively investigated in recent years.[2, 3] These studies reported nanoscale to microscale morphologies such as spherical or cylindrical micelles, vesicles, ribbons, fibers, bowls and toroids.[4-9]

Of particular interest are stimuli responsive materials that allow for the directed or modulated self-assembly on the nanoscale in aqueous solution. Materials with stimuli responsive physical properties have potential uses in food, cosmetic and drug delivery applications. In some instances, the presence of nanoscale morphologies formed through self-assembly translates into macroscopic phenomena such as the formation of a hydrogel phase.. Hydrogel forming, block and star copolymers have been synthesized that exhibit either temperature or pH-responsive behavior by incorporation of blocks that exhibit either lower

critical solution temperature (LCST)[10] and polyelectrolyte properties.[11, 12] The ability to control the block composition and copolymer architecture of these wholly synthetic materials allows for tuning of these materials stimuli-responsive properties. Peptide based materials have also been shown to form hydrogel networks in response to physical or chemical stimuli.[13-17] These materials utilize the primary modes of self-association in peptides, the hydrophobic aggregation of β -strands and coiling of helices, to form long-range networks that lead to hydrogel formation. In this work, we have developed new synthetic block copolymers that respond to *both* pH and temperature, providing the ability to tune the nanoscale and macroscale structures formed using two independent environmental stimuli, giving rise to unique phase behavior and formation of dehydrated elastic solids by self-assembly that has not been seen in other systems.

The synthesis of amphiphilic pentablock copolymers consisting of poly((diethylaminoethylmethacrylate)-b-(ethylene oxide)-b-(propylene oxide)-b-(ethylene oxide)-b-(diethylaminoethylmethacrylate)) ($\text{PDEAEM}_{25}\text{-b-PEO}_{106}\text{-b-PPO}_{69}\text{-b-PEO}_{106}\text{-b-PDEAEM}_{25}$), that exhibits temperature and pH induced micelle self association and gelation was recently reported.[18] The pentablock copolymer was designed to undergo thermoresponsive micellization due to the presence of the PPO block, which exhibits a LCST around 8°C, and pH responsive micellization due to the polycationic PDEAEM blocks. At physiological temperatures and pH conditions, aqueous solutions of the pentablock copolymers formed physical hydrogels due to micellar packing and interdigitation. This unique combination of properties make the pentablock copolymer an attractive material for stimuli-responsive drug delivery applications. The hydrogel phase formed at physiological conditions maintains a constant weight fraction of water during the gelation process. Here,

we describe the reversible temperature and pH-responsive self-assembly of this pentablock copolymer in aqueous solutions to form organized elastic solids with substantially lower water content than the original copolymer solution. At pH 11 and 70°C, the network of pentablock micelles precipitates and contracts as it expels water to reach the new equilibrium resulting in a shrunken hydrogel that maintains the cross-sectional shape of the vial it is contained in. This phase transition was attributed to increasing hydrophobicity of the copolymer at conditions above the pK_a of the PDEAEM blocks and the LCST of the PEO blocks. Herein we report a detailed investigation of origins and structure of this hydrogel phase.

5.3. Experimental Section

5.3.1. Sample preparation

A pentablock copolymer poly((diethylaminoethylmethacrylate)-b-(ethylene oxide)-b-(propylene oxide)-b-(ethylene oxide)-b-(diethylaminoethylmethacrylate)) (PDEAEM₂₅-b-PEO₁₀₆-b-PPO₆₉-b-PEO₁₀₆-b-PDEAEM₂₅) ($M_n = 22000$ g/mol and PDI = 1.34), shown in Figure 5.1, was synthesized by atom transfer radical polymerization (ATRP). Details of the synthesis and characterization of these block copolymers are described previously.[18]

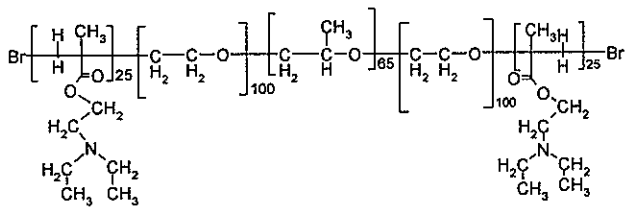


Figure 5.1. Chemical formula of the pentablock copolymer

The self-assembled macroscale solids were prepared by first dissolving the copolymer at 5 wt.% in water at pH 3. The solution was cooled overnight at 4°C to ensure complete dissolution. The solution was titrated at room temperature to pH 11 with 2 mol/L NaOH,

where a cloud point indicating the precipitation of the copolymer, was observed. The cloudy suspension was heated in a convection oven at 75°C, above the LCST of the PEO blocks, for 24 hours to form an organized solid. The solid was removed from solution for characterization by SAXS and Dynamic Mechanical Analysis (DMA).

5.3.2. Small Angle Neutron Scattering

The self-assembly of the pentablock copolymers into micellar structures in aqueous solutions was investigated by SANS. The copolymer was dissolved in D₂O, and the pH was adjusted by the addition of DCl and NaOD. Additional D₂O was added to adjust the concentration to 2 wt.% for all samples. SANS experiments were carried out by using the time-of-flight small-angle neutron diffractometer (SAND) at the Intense Pulsed Neutron Source (IPNS), at the Argonne National Laboratory. This instrument provides data in the Q [$(4\pi \sin \theta/\lambda)$, where 2θ is the scattering angle and λ is the wavelength of the neutrons] range of 0.004-0.8 Å⁻¹ in a single measurement by using a 40x40 cm² position-sensitive ³He gas detector and neutrons with wavelengths in the range of 0.8-14 Å. Copolymer solutions were sealed in Suprasil cylindrical cells with 2 mm path length for the SANS measurements. A liquid flow thermostat was used to control the temperature to within ±1°C. The scattering data were corrected for empty cell and solvent scattering, detector sensitivity, and sample transmission. The differential scattering cross section $I(Q)$ was placed on an absolute scale in the units of cm⁻¹ by using a secondary NIST standard of 50% deuterated polystyrene, whose absolute scattering cross sections is known.

5.3.3. Small angle X-ray Scattering

SAXS measurements were carried out on the instrument at the 12-ID beam line at the Advanced Photon Source.[19] A 15 cm x 15 cm CCD detector was used to measure the

intensity of scattering and the transmitted beam intensity was measured using a photodiode. Samples were held in quartz capillaries with 1.5 mm outer diameter and 0.01 mm wall thickness (Hampton Research). Data was collected at 0.5 second exposure times at incident beam energies of 12 keV ($\lambda = 1.035 \text{ \AA}$). The distance between the detector and the sample was 2 m. The scattering data were appropriately corrected and azimuthally averaged to obtain $I(Q)$. The scattering intensity data were normalized to an absolute scale with a polyethylene standard. The one-dimensional data for five exposures were averaged for each sample. Scattering intensity from an empty quartz capillary and fitted power-law scattering in the low Q region was subtracted from the sample data.

5.3.4. Dynamic Mechanical Analysis

A Perkin Elmer 7e Dynamic Mechanical Analyzer (DMA) was used to measure the thermal/mechanical properties of pentablock copolymer and self assembled solids. A cup-and-plate geometry (5 mm diameter) was utilized and the sample was tested in compression, in controlled stress mode, at 1 Hz. The static and dynamic forces applied were 25 and 20 mN respectively. Samples were heated from 10 to 90°C at 3°C/min.

5.4. Results and Discussion

Temperature and pH responsive amphiphilic copolymers are a new class of materials with interesting properties.[20, 21] The combination of polyelectrolyte and hydrophilic blocks that exhibit a lower critical solution temperature (LCST) results in multi-responsive copolymers. The pentablock copolymer combines the LCST properties of the Pluronic® F127 triblock copolymer with PEO and PPO blocks and the pH responsive properties of a cationic polyelectrolyte block of PDEAEM. Aqueous solutions of PEO₁₀₀-PPO₆₅-PEO₁₀₀ triblock copolymers (MW = 12,600) form micelles and liquid crystal mesophases resulting in rigid

gels as a function of temperature and concentration due to the LCST of the PPO block around 8°C.[22, 23] PDEAEM is a cationic polymer that exhibits a sharp pH-sensitive solubility behavior.[24, 25] The degree of ionization of the pendant amines of the PDEAEM chains is highly dependent on the solution pH. The amines are cationic below the pK_a of the polyelectrolyte and become deprotonated when the solution pH is greater than the pK_a . Deprotonation of the tertiary amine pendent group of the DEAEM unit \sim pH 7.6 causes the PDEAEM chain to transition from a highly hydrated expanded chain to a collapsed hydrophobic state.[26] In aqueous solutions, the pentablock copolymer exhibits a thermoreversible sol-gel phase transition as well as pH responsive micellization behavior.[18]

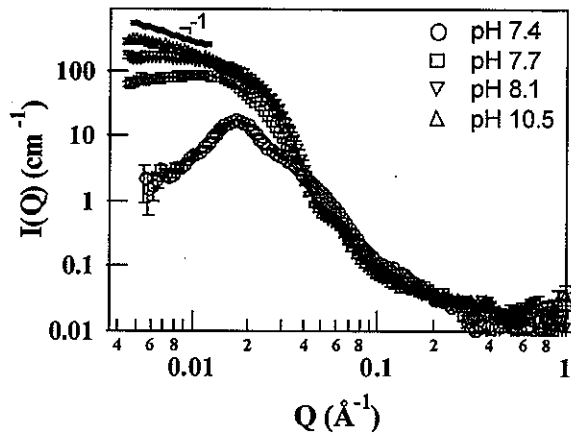


Figure 5.2. SANS data of 2 w% PDEAEM₂₅-PEO₁₀₀-PP0₆₅-PEO₁₀₀-PDEAEM₂₅ at 75°C in aqueous solution at different pH.

SANS experiments were conducted to investigate the pH dependent evolution of micellar structure in the pentablock copolymer solutions. Figure 5.2 shows the scattering data from 2 wt.% copolymer solutions at pH 7.4, 7.7, 8.1 and 10.5 and at 75°C. The scattering data collected at pH 3 (not shown) was identical, within instrumental error, of the data collected at pH 7.4. This indicates that in a wide pH range below the pK_a of the PDEAEM blocks the

micellar structure of the pentablock copolymer micelles remains unchanged. At pH 7.4 the scattering pattern is indicative of presence of spherical micelles. At 75°C, the PPO blocks formed nearly completely dehydrated spherical micelle cores surround by a corona of substantially more hydrated PEO and the ionized PDEAEM blocks. Upon increasing solution pH to 7.7, slightly above pK_a of the PDEAEM blocks, the scattering intensity at low Q increased by nearly two orders of magnitude, indicating the formation of much larger micelle structures. The critical micellization temperature (CMT) of the pentablock copolymer at 2 wt % is 25°C.[18] Therefore at 75°C, there was a negligible amount of copolymer unincorporated into the micelles, so growth in size of the micelles was likely due to aggregation of multiple micelles. At pH 7.7, the partially unionized PDEAEM blocks became increasingly hydrophobic, resulting in attractive hydrophobic forces between micelles. The position of the scattering intensity maxima at pH 7.4 and 7.7 was 0.01709 to 0.01157 \AA^{-1} respectively. This corresponds to an increase in the intermicellar spacing from 36.7 to 54.3 nm. At pH 8.1 the intensity of scattering at low Q continued to increase indicating further aggregation of micelles. The scattering intensity at low Q exhibited a negative slope, and the intensity peak observed at pH 7.4 and 7.7 was no longer distinguishable. This is an indication of the further aggregation of micelles and agrees with previous light scattering studies that indicated the aggregation number of micelles increases dramatically above the pK_a of the PDEAEM blocks.[18] At pH 10.5, the scattering intensity in the low Q region exhibited a Q^{-1} power law relationship that implies the presence of cylindrical micelles in solution. Figure 5.3 shows the modified Guinier plot for the rod-like particles of the SANS data for the solution at pH 10.5 and at 75°C. The presence of a linear region with a negative slope is a good indication of the presence of cylindrical micelles. The

measured cross sectional radius of gyration of the rod-like micelles, R_c , was $44.5 \pm 0.4 \text{ \AA}$ that corresponds to a radius of $62.9 \pm 0.6 \text{ \AA}$. The bend over in the low Q^2 region indicates that the length of the cylindrical micelles is finite. The pentablock copolymer solution remained transparent at pH 10.5 and 75°C. Thus the micellar morphology of the pentablock copolymer transitioned from spherical to cylindrical micelles through a mechanism of micellar aggregation due to the increasing hydrophobicity of the PDEAEM blocks with increasing pH.

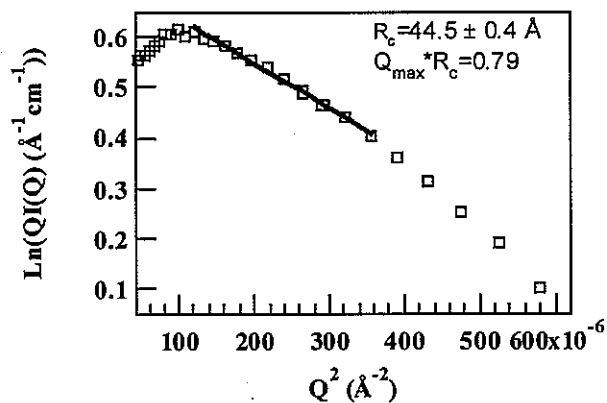


Figure 5.3. Modified Guinier plot for the rod-like particles of SANS data for PDEAEM₂₅-PEO₁₀₀-PP0₆₅-PEO₁₀₀-PDEAEM₂₅ pentablock copolymer, 2 wt %, at 75°C and pH 10.5.

At pH 11, the solution became turbid due to precipitation of the copolymer micelles. This precipitation occurred regardless of the temperature of the solution. At temperatures below 70°C the precipitant formed an easily disturbed layer and remained indefinitely. Upon heating the suspension of precipitated copolymer above 70°C the precipitate was observed to coalesce and assemble into an elastic solid hydrogel. The self-assembled solid was found to be a relatively dehydrated with only 25-35 wt % water. Figure 4 illustrates the stages of the self-assembly of the macroscopic solid. Interestingly the shape of the macroscopic solids retained the cross-sectional shape of the vial in which they were formed, but their dimensions were smaller as revealed by the short cylindrical shaped hydrogel in Figure 5.4. The process

illustrated in Figure 5.4 occurred over the course of 24 hours. We attribute the coalescence and self-packing of the precipitated copolymer micelles occurring above 70°C due to the much reduced solvating power of water for the PEO blocks under these conditions.[27] That is, upon increasing the temperature of the copolymer suspension above 70°C the PEO blocks become more hydrophobic, leading to further self association of the precipitated micelles into an organized solid. The hydrogel exhibited very little temperature sensitivity after formation, exhibiting a small amount of swelling upon cooling to room temperature. The hydrogel was easily removed from solution and was mechanically stable at room temperature out of solution. However, the self-assembly behavior was found to be completely reversible with pH. When the pH was lowered to 7.0, the hydrogel dissolved again, but could be reformed by increasing pH and temperature. ^1H NMR and gel permeation chromatography were used to confirm the absence of polymer chain decomposition during this process.

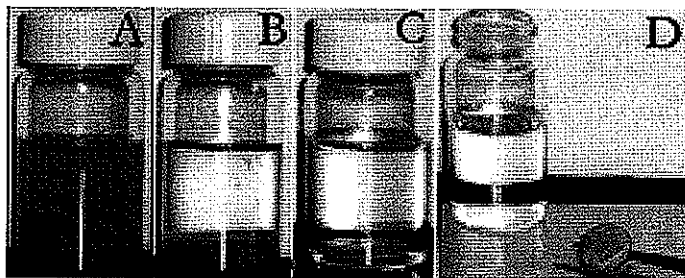


Figure 5.4. A) A 5 wt.% solution of pentablock copolymer, PDEAEM₂₅-PEO₁₀₀-PP0₆₅-PEO₁₀₀-PDEAEM₂₅ at room temperature is adjusted from pH 3 to 10, resulting in an immediate increase in turbidity. B) Upon heating to 70°C the copolymer precipitant begins to sediment. C) After 24 hours the copolymer has assembled into a hydrogel D) The hydrogel (25-35 wt % water) is mechanically stable at room temperature in solution and can be removed from solution without losing its shape.

SAXS was used to investigate the ordered phases in the macroscopic self-assembled solid. SAXS data from the self-assembled solid, shown in Figure 5.5, exhibited distinct diffraction peaks indicative of a hexagonally packed crystal structure $\{1:3^{1/2}:4^{1/2}:7^{1/2}:9^{1/2}\}$ and the first

order peak corresponds to a d-spacing of 151 Å. We interpret this to be due to the cylindrical micelles organized into an ordered hexagonal phase. This is in distinct contrast to the morphology of the precipitated copolymer in the bulk state, annealed for 24 hours at 70°C, that exhibited three broad peaks at $Q = 0.020 \text{ \AA}^{-1}$, 0.036 \AA^{-1} and 0.072 \AA^{-1} (Figure 5.5). We could not unambiguously attribute this scattering pattern to any specific ordered structure and further scattering experiments will be necessary to characterize the morphology of the pentablock copolymer bulk phase. However, the ratio of 2 for the Q values of the 2nd and 3rd peaks may indicate the presence of a lamellar structure with a d spacing of 175 Å. Thus the organization of the bulk copolymer is quite different from that in the self assembled hydrogel.

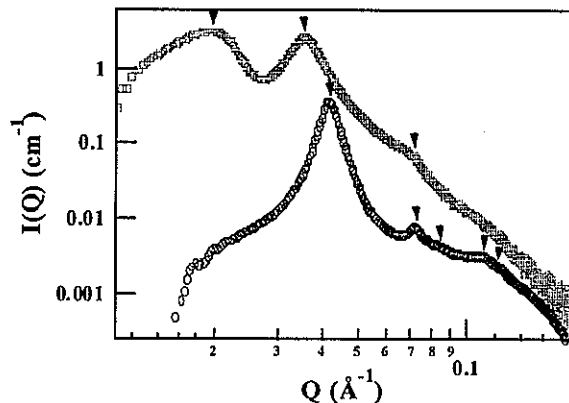


Figure 5.5. SAXS of self assembled solid, \circ , and pentablock copolymer melt, \square , annealed at 70°C for 24 hours. The scattering intensity data from the melt was multiplied 20x for clarity. Power-law scattering in the low Q region was subtracted in order to enhance the scattering peaks.

Dynamic mechanical analysis was used to investigate the mechanical properties of the self-assembled solid. The elastic storage modulus of the self-assembled solid and the bulk pentablock copolymer are shown in Figure 5.6. The bulk copolymer sample melts at 35°C as noted by the loss of elastic properties, where the self-assembled solid maintained mechanical stability up to 90°C. This represents a remarkable shift in thermomechanical properties

through an entirely self-directed self-assembly process. The increase in melting temperature is attributed to the presence of hexagonally packed cylindrical micelles forming a fibril-like crystalline phase. In an attempt to understand the role that elevated temperature plays in the self-assembly process, the precipitated copolymer was centrifuged at room temperature. The resulting granular pellet did not exhibit the elastic properties of the solid hydrogel phase formed at 70°C.

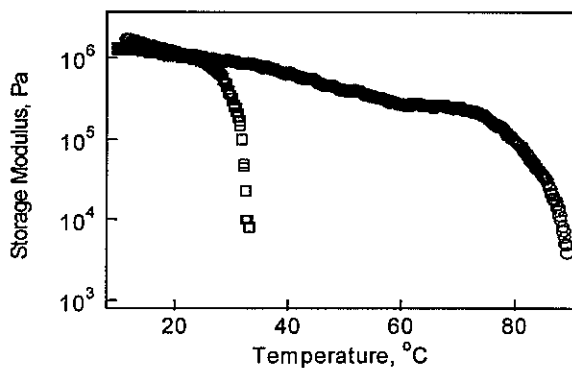


Figure 5.6. The elastic storage modulus of the bulk pentablock copolymer, □, and the self-assembled hydrogel, ○. Storage modulus was monitored by dynamic mechanical analysis.

These studies help elucidate the mechanism of self-assembly of the polymer at multiple length scales. The pentablock copolymer, in the charged state, forms micelles above a critical micellization temperature (CMT) due to the LCST of the PPO block. Above the LCST of the PPO block, spherical micelles consisting of a compact hydrophobic PPO core enclosed in a two layer corona of PEO and charged PDEAEM form. The CMT of the ionized pentablock is attributed to the same hydrophobic driving force resulting in micellization of Pluronic copolymers.[28] Micellization of the pentablock copolymer could also be induced by increasing the pH of the solution above the pK_a of the PDEAEM block.[18] Further increasing the pH of the pentablock copolymer solutions resulted in increasing the size of the micelle aggregates, followed by the transition to cylindrical micelle morphology as observed

with SANS. As the size of the spherical micelles increased with increasing pH, the energetic penalty of stretching chains in the core of the micelle resulted in a transition to cylindrical micelles. This is consistent with molecular dynamics simulations studies of these systems showing that changes in hydrophobicity of the individual blocks relative to each other, can lead to a shift from spherical to cylindrical micelles.[29] Further growth and aggregation of the cylindrical micelles resulted in precipitation of the micelle clusters. At 70°C, where the assembly of the solid hydrogel was observed, the increasing hydrophobicity of the PEO blocks at this temperature caused the aggregation of the cylindrical micelles into a hexagonal packed morphology. The ability to tailor such self-assembly behavior by two different parameters, temperature as well as pH, provides a powerful method to tune the self-assembly behavior. This unique long-range reversible self-assembly behavior in solution, where the macroscopic solid exhibits very ordered nanostructure is important in bottom-up approaches for materials design.

5.5. Conclusions

In this report we have demonstrated a unique transition between a homogeneous micellar solution to a phase-separated, self-assembled elastic solid phase. Aqueous solutions of the pentablock copolymer at pH<7.5 formed charged spherical micelles as determined by SANS. Increasing the pH above 7.6 caused the cationic PDEAEM blocks to deprotonate and become hydrophobic. This alteration of the hydrophobic/hydrophilic balance of the block copolymer resulted in increased micelle size and a transition from spherical-to-cylindrical micelles. At pH 11 the copolymer micelles precipitated from solution. Further self-assembly of the cylindrical micelles into ordered hexagonal phase occurred at even higher temperatures due to the decreased solubility of the PEO blocks in water above 70°C. The ability to trigger this

unique reversible self-assembly at multiple length scales ranging from nanoscale to macroscale by changing pH and temperature conditions offers exciting possibilities in bottom-up approaches to materials design and fabrication.

5.6. Acknowledgement

This work was supported by the U.S. Department of Energy under contract number W-7405-ENG-81 to Iowa State University. This work benefited from the use of BESSRC-CAT at APS, and the IPNS, funded by the U.S. DOE, BES under contract W-31-109-ENG-38 to the University of Chicago. The authors are indebted to D. G. Wozniak for his assistance in the SANS measurements. Special thanks to undergraduate students Suzan Cox and James Cox who helped with different aspects of this work.

5.7. References

1. Whitesides, G.M. and B. Grzybowski, *Self-assembly at all scales*. Science, 2002. **295**(5564): p. 2418.
2. Stupp, S.I., et al., *Supramolecular Materials: Self-Organized Nanostructures*. Science, 1997. **176**: p. 384-389.
3. Bucknall, D.G. and H.L. Anderson, *Polymers get organized*. Science, 2003. **302**(5652): p. 1904-1905.
4. Jenekhe, S.A. and X.L. Chen, *Self-Assembly of Ordered Microporous Materials from Rod-Coil Block Copolymers*. Science, 1999(283): p. 372.
5. Muller, F., et al., *Ordering of urchin-like charged copolymer micelles: electrostatic, packing and polyelectrolyte correlations*. European Physical Journal E: Soft Matter, 2000. **3**(1): p. 45-53.
6. Discher, D.E. and A. Eisenberg, *Polymer Vesicles*. Science, 2002. **297**: p. 967.
7. Hartgerink, J.D., E. Beniash, and S.I. Stupp, *Peptide-amphiphile nanofibers: A versatile scaffold for the preparation of self assembling materials*. PNAS, 2002. **99**(8): p. 5133-5138.
8. Liu, X., et al., *Bowl-Shaped Aggregates from the Self-Assembly of an Amphiphilic RandomCopolymer of Poly(styrene-co-methacrylic acid)*. Macromolecules, 2005. **38**(16): p. 6749 - 6751.
9. Chen, Z., et al., *Unique Toroidal Morphology from Composition and Sequence Control of Triblock Copolymers*. J. Am. Chem. Soc., 2005. **127**(24): p. 8592.

10. Li, C., et al., *Synthesis and Characterization of Biocompatible Thermo-Responsive Gelators Based on ABA Triblock Copolymers*. *Biomacromolecules*, 2005. **6**(2): p. 994-999.
11. Ma, Y., et al., *Synthesis of Biocompatible, Stimuli-Responsive, Physical Gels Based on ABA Triblock Copolymers*. *Biomacromolecules*, 2003. **4**(4): p. 864-8.
12. Li, Y., et al., *Biomimetic Stimuli-Responsive Star Diblock Gelators*. *Langmuir*, 2005. **21**(22): p. 9946-9954.
13. Tang, A., et al., *The coiled coils in the design of protein-based constructs: hybrid hydrogels and epitope displays*. *J. Controlled Release*, 2001. **72**: p. 57-70.
14. Claussen, R.C., B.M. Rabatic, and S.I. Stupp, *Aqueous Self-Assembly of Unsymmetric Peptide Bolaamphiphiles into Nanofibers with Hydrophilic Cores and Surfaces*. *J. Am. Chem. Soc.*, 2003. **125**(42): p. 12680-12681.
15. Collier, J.H., et al., *Thermally and Photochemically Triggered Self-Assembly of Peptide Hydrogels*. *J. Am. Chem. Soc.*, 2001. **123**(38): p. 9463-9464.
16. Mawer, P.J., et al., *Small-Angle Neutron Scattering from Peptide Nematic Fluids and Hydrogels under Shear*. *Langmuir*, 2003. **19**(12): p. 4940-4949.
17. Deming, T.J., *Polypeptide hydrogels via a unique assembly mechanism*. *Soft Matter*, 2005. **1**: p. 28-35.
18. Determan, M.D., et al., *Synthesis and characterization of the temperature and pH-responsive pentablock copolymers*. *Polymer*, 2005. **46**: p. 6933-6946.
19. Seifert, S., et al., *Design and performance of a ASAXS instrument at the Advanced Photon Source*. *J. Appl. Cryst.*, 2000. **33**: p. 782-784.
20. Liu, S., N.C. Billingham, and S.P. Armes, *A Schizophrenic Water-Soluble Diblock Copolymer*. *Angew. Chem. Int. Ed.*, 2001. **40**(12): p. 2328-2331.
21. Mertoglu, M., et al., *Stimuli responsive amphiphilic block copolymers for aqueous media synthesised via reversible addition fragmentation chain transfer polymerisation (RAFT)*. *Polymer*, 2005. **46**(2005): p. 7726-7740.
22. Wanka, G.H., H.; Ulbricht, W., *The aggregation behavior of poly(oxyethylene)-poly(oxypropylene)-poly(oxyethylene) block copolymers in aqueous solution*. *Colloid Polym. Sci.*, 1990. **268**(2): p. 101-17.
23. Chu, B. and Z. Zhou, *Physical chemistry of polyoxyalkylene block copolymer surfactants*, in *Nonionic Surfactants: Polyoxyalkylene Block Copolymers*, V.M. Nace., Editor. 1996, M. Dekker: New York. p. 67-143.
24. Weaver, J.V.M., S.P. Armes, and S. Liu, *A "Holy Trinity" of Micellar Aggregates in Aqueous Solution at Ambient Temperature: Unprecedented Self-Assembly Behavior from a Binary Mixture of a Neutral-Cationic Diblock Copolymer and an Anionic Polyelectrolyte*. *Macromolecules*, 2003. **36**: p. 9994-9998.
25. Lee, A.S., et al., *Characterizing the Structure of pH Dependent Polyelectrolyte Block Copolymers Micelles*. *Macromolecules*, 1999. **32**: p. 4302-4310.
26. Tonge, S.R. and B.J. Tighe, *Responsive hydrophobically associating polymers: a review of structure and properties*. *Adv Drug Deliv Rev*, 2001. **53**: p. 109-122.
27. Hey, M.J., S.M. Ilett, and G. Davidson, *Effect of Temperature on Poly(ethylene oxide) Chains in Aqueous Solution*. *J. Chem. Soc. Faraday Trans.*, 1995. **91**(21): p. 3897-3900.

28. Wanka, G.H., H.; Ulbricht, W, *Phase Diagrams and Aggregation Behavior of Poly(oxyethylene)-Poly(oxypropylene)-Poly(oxyethylene) Triblock Copolymers in Aqueous Solutions*. *Macromolecules*, 1994. **27**(15): p. 414594149.
29. Chushak, Y. and A. Travesset, *Coarse-Grained Molecular Dynamics Simulations of the Self-Assembly of Pentablock Copolymers into Micelles*. *J. Chem. Phys.*, 2005. **123**(21).

CHAPTER 6. DRUG RELEASE FROM PH-RESPONSIVE THERMOGELLING PENTABLOCK COPOLYMERS

A paper submitted to the Journal of Biomedical Materials

Michael D. Determan¹, James P. Cox¹, Surya K. Mallapragada^{1†}

6.1 Abstract

A novel pH-dependent injectable sustained delivery system was developed by utilizing a cationic pentablock copolymer that exhibits a thermoreversible sol-gel transition. Aqueous solutions of the pentablock copolymer, consisting of poly(2-diethylaminoethyl-methyl methacrylate)- poly(ethylene oxide)-poly(propylene oxide)-poly(ethylene oxide)-poly(2-diethylaminoethyl-methyl methacrylate) (PDEAEM₂₅-PEO₁₀₀-PPO₆₅-PEO₁₀₀-PDEAEM₂₅) exhibit temperature and pH dependent micellization due to the lower critical solution temperature of the PPO blocks and the polyelectrolyte character of the PDEAEM blocks, respectively. Aqueous solutions of the copolymers above 12 wt % are free flowing liquids at room temperature and form elastic physical hydrogels reversibly above 37°C. Hydrophobic probe absorbance studies indicate that pentablock copolymer micelles increase the solubility of sparingly soluble drugs. Solutions of the pentablock copolymer that form gels at body temperature exhibit sustained zero-order release in *in vitro* experiments. The release rates of model drugs and proteins were significantly influenced by the pH of the release media, thereby making these polymers ideal candidates for modulated drug delivery.

¹ Department of Chemical and Biological Engineering, Iowa State University and Ames Laboratory, 144 Spedding Hall, Ames, IA 50011, USA.

† Corresponding Author. USA Phone: +1 515 294 7407 Fax: +1 515 294 2689 E-mail address: suryakm@iastate.edu

6.2 Introduction

Proper dosing and targeting of therapeutics is a non-trivial step in the development of effective drug therapies. The controlled delivery of therapeutic drugs with polymeric materials is currently the focus of intense academic and industrial research [1]. In particular, the development of a material capable of controlled drug release in response to environmental stimuli is an essential step towards the development of a closed-loop drug delivery formulation [2, 3]. Injectable formulations of micro- or nano- sized particles, composed of absorbable or amphiphilic block copolymers, have been shown to be effective for controlled drug delivery applications [4, 5]. Implantable crosslinked hydrogels with thermo-, pH-, and glucose-responsive drug release kinetics have been developed to respond to specific physiological conditions [6, 7]. However, the invasive nature of subcutaneous implantation and removal of chemically crosslinked hydrogels is an issue.

Injectable formulations consisting of copolymer micelles or hydrogel nanoparticles that exhibit pH-responsive drug delivery have been utilized to extend the circulation time and bioavailability of therapeutic proteins [8-13]. Therapeutic drugs or proteins can be incorporated into these colloidal sized particles, and release of the drug is triggered by a specific pH condition. The ability to modulate drug release as a function of pH allows for the possibility to enhance and tailor the targeting of drug therapies.

Thermoresponsive hydrogels that are not chemically crosslinked, but are formed by entanglement of polymer micelles, are a unique class of materials with enormous potential for controlled drug delivery applications [14]. They do not suffer from disadvantages of the chemically crosslinked hydrogels. These materials are low viscosity liquids at low temperatures and form a physically crosslinked gel phase around physiological temperatures, allowing for subcutaneous injection of a drug loaded formulation followed by *in situ*

hydrogel formation. Under *in vivo* conditions, the ingress of water into the hydrogel results in dissolution or degradation of the hydrogel matrix, resulting in sustained release of drug. Typically the hydrogel will dissolve or degrade into components that can be excreted through the renal system, precluding invasive removal procedures of the polymeric material. Numerous thermoresponsive hydrogels have been investigated for controlled drug delivery applications [15-21]. In particular, the thermoreversible gel forming Pluronic® F127 triblock copolymer has been studied extensively due to its proven clinical effectiveness in injectable and topical drug delivery formulations [22-24]. However, the Pluronic® copolymer gels are fast-dissolving, and are also not sensitive to pH and therefore cannot be used in applications such as glucose-sensitive release of insulin from pH-sensitive gels by incorporation of glucose oxidase [7, 25].

An amphiphilic, polycationic pentablock copolymer, poly(2-diethylaminoethyl-methyl methacrylate)- poly(ethylene oxide)-poly(propylene oxide)-poly(ethylene oxide)-poly(2-diethylaminoethyl-methyl methacrylate) (PDEAEM₂₅-PEO₁₀₀-PPO₆₅-PEO₁₀₀-PDEAEM₂₅) has been synthesized by atom transfer radical polymerization [26]. The pentablock copolymer is composed of commercially available tri-block Pluronic® F127 polymer and two blocks of poly(2-diethylaminoethyl-methyl methacrylate) (PDEAEM). This copolymer was specifically designed to exhibit thermoreversible gelation, slower dissolution compared to Pluronic® gels, as well as exhibit pH dependent solubility around physiological pH.

The thermoreversible properties of the pentablock copolymers were designed to arise from the lower critical solution temperature (LCST) of the central poly(propylene oxide) (PPO) block. The tertiary amines of the PDEAEM groups are protonated and hydrophilic below the pK_a (7.5) of the monomer. Above the pK_a, the PDEAEM blocks are sparingly soluble in water. Micellar solutions of the pentablock copolymer, above a critical gel

concentration (CGC), would form a lyotropic liquid crystalline phase that results in a transparent hydrogel. The amphiphilic nature of the copolymer should allow for incorporation of hydrophobic drugs or therapeutic proteins into the copolymer micelles [27-29]. Release of drug from the pentablock copolymer hydrogel would occur as water penetrates the gel, lowering the copolymer concentration below the CGC, resulting in erosion of the gel. The drug release rate from a pentablock copolymer hydrogel can respond to changes in pH because the hydrophilic/hydrophobic balance of the copolymer varies with pH. This material has great potential as an injectable biomaterial for modulated drug delivery, as well as a non-viral gene therapy vector [12]. The goal of this work is to evaluate the pH modulated drug release from the thermoreversible gel formed by aqueous solutions of the pentablock copolymers. A low molecular weight model drug, nile blue chloride (NBC), and a model protein drug, lysozyme were used for the *in vitro* release experiments.

6.3. Materials and methods

6.3.1 Materials

Pluronic® F127 was donated by BASF and used without further modification. Lysozyme (lysozyme chicken egg white lyophilized powder, ~50,000 units/mg protein) and nile blue chloride (NBC) were purchased from Sigma. The PDEAEM₂₅-PEO₁₀₀-PPO₆₅-PEO₁₀₀-PDEAEM₂₅ pentablock copolymer [$M_n = 21900$ and $M_w/M_n = 1.27$] as judged by ¹H NMR (in deuterated chloroform) and GPC (THF mobile phase, poly(methylmethacrylate) calibration standards) respectively was synthesized as previously reported.[26]

6.3.2 Probe absorbance measurements

The probe absorbance technique was used to investigate the critical micellization temperature (CMT) of the pentablock copolymer. 1,6-diphenyl-1,3,5-hexatriene (DPH) was

purchased from Sigma. Copolymer solutions at 0.7 wt% were prepared by dissolving the pentablock copolymer in 50 mM PBS (150mM NaCl) at pH 3.0, 4.5 and 7.4. Measured amounts of 0.4 mM DPH in acetone were added to several volumetric flasks, the acetone was evaporated and pentablock copolymer solutions were added to obtain a final DPH concentration of 4×10^{-6} M. The solutions were placed in a dark to equilibrate for 24 hours. A Quantum Northwest TLC Temperature controller provided stirring and controlled the temperature of the sample solutions. The CMT of the pentablock copolymer micelles was determined by monitoring the absorbance of DPH at 391 nm with a Shimadzu 1602 UV-VIS.

6.3.3 Thermal analysis

The CMT at different concentrations of pentablock copolymers in aqueous solutions was determined by monitoring the heat of micellization with a Perkin Elmer Pyris 1 Differential Scanning Calorimeter (DSC). Pentablock copolymer solutions at pH 7.0 were prepared at several concentrations and sealed in aluminum pans to prevent loss of moisture during DSC analysis. The DSC samples were held at -5°C for 5 minutes before beginning a temperature scan from -5°C to 40°C at a rate of $5^{\circ}\text{C}/\text{min}$ under helium purge. The critical micellization temperature was determined by the onset of the endothermic micellization transition peak from the baseline.

The onset of thermoreversible gelation of pentablock copolymer solutions was monitored by the tube inversion technique. Five ml of the sample solution were placed in a 20 ml scintillation vial and sealed. The vials were initially incubated at 50°C and cooled in steps of 2°C . The vials were inverted after 5 minutes at each temperature: if no flow was observed over the course of 10 seconds the gel was considered a rigid gel.

A Perkin Elmer 7e Dynamic Mechanical Analyzer (DMA) was used to monitor the mechanical properties of pentablock gels as a function of temperature. A cup-and-plate geometry (5 mm diameter) was utilized and the sample was tested in compression at 1 Hz. The elastic modulus and the solution-gelation transition of a pentablock copolymer solution (22.5 wt %) and a copolymer (22.5 wt %) with lysozyme (20 mg/ml) were measured. Solutions, at 4°C, were poured into the cup and allowed to warm to 50°C. The probe was lowered to contact the gel: the applied static and dynamic forces were 9 and 10 mN respectively. The temperature of the sample decreased at 2°C/min and the sample chamber was humidified to keep the sample from drying over the course of the experiment.

6.3.4 Protein stability

Circular dichroism (CD) was used to investigate the structural integrity of lysozyme protein in solution with the pentablock copolymer. Lysozyme (0.125 mg/ml) was incubated in the presence of the pentablock copolymer (0.125 mg/ml) at 37°C to simulate the *in vitro* receptor media conditions. CD spectra were collected on a JASCO J-710 CD spectrometer using filtered protein solutions in 10 mM PBS pH 7.4 in a 0.1 cm cell. CD spectra were collected after 1 day, 1 week and 4 weeks. Each CD spectrum was the accumulation of eight scans at 50 nm·min⁻¹ with a 1 nm slit width and a time constant of 0.5 s for a nominal resolution of 0.2 nm. Data was collected from 185 to 260 nm. CD spectra were background corrected and scaled to mean residual ellipticity based on the absorbance at 205 nm. K2D web based calculator was utilized to estimate the percentages of protein secondary structure from the CD spectra.

6.3.5 Release studies

The *in vitro* release of NBC and lysozyme from the pentablock copolymer gels were carried out in with a Hanson Research SRII 6 flask dissolution test station, configured as USP Apparatus 1 with modification of 500 ml flasks. Phosphate buffer saline (PBS) solution (50 mM with 150 NaCl) was used as receptor media. The buffer pH was adjusted to the target pH by addition of 1M HCl or NaOH. Sample solutions were prepared by dissolving the lysozyme (20 mg/ml) or NBC (1mg/ml) in pH 7.4 PBS solution. The pentablock copolymer was added at 22.5 wt % to the solution and was allowed to dissolve at 4°C. The pentablock copolymer solution was poured into glass dishes, 14 mm diameter and 10 mm height, that were covered and warmed to 37°C where the solution formed a gel phase. The samples were submerged in the 400 ml of PBS maintained at 37°C. Rotating paddles were used to stir the dissolution wells at 60 rpm. Samples were periodically removed from the dissolution wells and tested for NBC or lysozyme concentration. The concentration of NBC was determined by the intensity of the absorption at 636 nm using a Shimadzu 1602 UV-VIS spectrophotometer. NBC calibration curves were prepared for each pH used in the release study. Samples with lysozyme were analyzed by high-performance liquid chromatography (HPLC). HPLC was performed with a Shimadzu HPLC system operating with 50 mM PBS (150mM NaCl) at pH 7.4 mobile phase at 1 ml/min equipped with two pL aquagel-OH Analytical columns (PL aquagel-OH 30 8 μ l and 50 8 μ l). A Shimadzu UV-Vis detector was used to monitor lysozyme concentration at 280 nm. Lysozyme concentrations were determined from a calibration curve of standards ranging from 5 to 100 μ g/ml. Three replications were run for each release experiment.

Dye release experiments during which step changes were made to the receptor media pH were carried out with a slightly modified protocol. The sample was similarly prepared and submerged in the dissolution media. A peristaltic pump was used to continuously circulate the receptor media through a flow cell mounted in the sample chamber of the Shimadzu 1602 UV-VIS. The pH of the release media was adjusted between 7.8 and 7.0 small additions of 2 M HCl or NaOH. This protocol, which allows for more continuous monitoring of the release media, was adopted to observe the rapid changes in release rate of the dye upon changing the pH of the release media.

6.4. Results and Discussion

6.4.1 Solution behavior of the pentablock copolymers

The thermoreversible gelation and pH dependent phase behavior of the aqueous pentablock copolymer solutions were investigated to demonstrate the potential utility of the material for drug delivery formulations. The pentablock copolymer exhibits thermoreversible micellization due to the LCST of the PPO block. The heat of micellization, arising from the dehydration of the PPO block at the LCST, was observed calorimetrically [30, 31]. The critical micellization temperature (CMT) of pentablock copolymer solutions at pH 7.0 and several concentrations between 1 to 30 wt %, decreased with increasing concentration. DSC thermographs obtained from several samples at different concentrations of pentablock copolymer are shown in Figure 6.1.

Copolymer solutions with greater than 12 wt % pentablock copolymer in pH 7 PBS solution exhibited macroscopic gelation at 35°C, as determined by the tube inversion technique. The transition temperatures, between dissolved unimers and micelles, and micellar solution to hydrogel phase, are plotted in Figure 6.2.

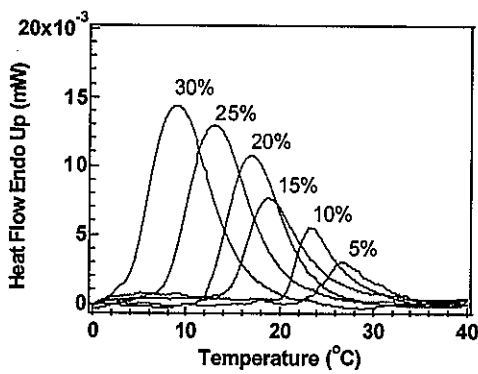


Figure 6.1. DSC thermographs of pentablock copolymer solutions at pH 7 and different concentrations (wt%).

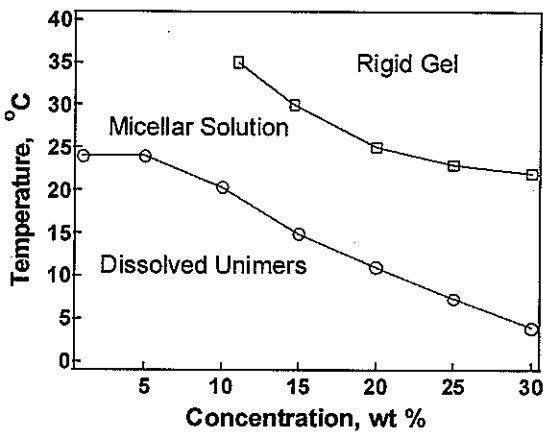


Figure 6.2. Phase behavior of the PDEAEM₂₅-PEO₁₀₀-PPO₆₅-PEO₁₀₀-PDEAEM₂₅ pentablock copolymer dissolved in 50 mM PBS at pH 7.0. The CMT is indicated by the circle markers, the onset of a self supporting gel phase in indicated by the square markers. Lines are drawn as a guide for the eye.

The solution to hydrogel transition is a result of the increase in volume fraction of pentablock copolymer micelles, resulting in ordered packing of the micelles into a crystalline lattice. The onset of gelation occurs at lower temperatures with increasing copolymer concentration due to the lower CMT and higher micelle volume fraction at higher copolymer concentration. The thermoreversible sol-gel transition exhibited by the pentablock copolymer solution at physiological temperature and at concentrations as low as 12 wt. % makes it an ideal material for an injectable thermoreversibly gelling drug depot system.

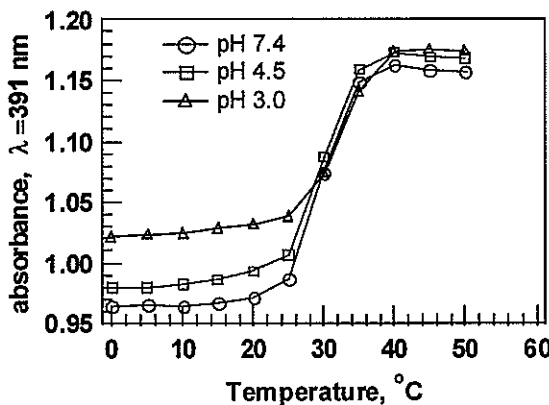


Figure 6.3. Plot of DPH absorbance, at 391 nm, in a 0.7 wt % solution of pentablock copolymer at pH 3.0, 4.5 and 7.4 at various temperatures.

A molecular probe technique was used to investigate the ability of pentablock copolymer micelles to incorporate hydrophobic molecules into the micelle core. The solubilization of DPH, a hydrophobic probe molecule, has previously been utilized to investigate the CMT of Pluronic® block copolymer solutions [32]. The absorbance of the DPH molecule in aqueous media is extremely low but exhibits strong absorbance when dissolved in apolar media, such as the dehydrated core of a copolymer micelle. The effect of solution pH on the CMT of the pentablock copolymers was also investigated. DPH (4×10^{-6} M) was dissolved in PBS solution with the pentablock copolymer (0.7 wt %) at three pHs, 3.0, 4.5 and 7.4. In Figure 6.3 the absorbance, at 391 nm, of the DPH/copolymer solution is shown at several temperatures. The CMT of the pentablock copolymer was observed at 25°C for each pH, as indicated by the increase in absorbance. This result agrees with the observed CMT from the DSC measurements. It is inferred from these results that the CMT of the pentablock copolymer is independent of solution pH below the pK_a of the PDEAEM blocks. This suggests that the phase diagram in Figure 6.2 is representative for pentablock copolymer solutions up to the pK_a , pH 7.5, of the PDEAEM blocks. The ability to incorporate

hydrophobic probe molecules indicates that the pentablock copolymer can increase the solubility of sparingly soluble drugs through incorporation of the drug molecules into the micelle core.

6.4.2 Dye release from pentablock copolymer hydrogel

The release of NBC from pentablock copolymer gels was investigated to establish the sensitivity of release rate on pH of the receptor media. The release data of NBC from pentablock copolymer gel into receptor media at several pHs is shown in Figure 6.4. Release rate of NBC from pentablock copolymer gels showed significant dependence on the pH of the release media. The rate of NBC release decreased with increasing pH of the receptor media. For comparison the NBC release from a Pluronic® F127 gel at pH 7.4 is also shown in Figure 6.4. As expected, the release rate of NBC from the Pluronic® F127 gel showed no dependence on pH. Nearly all of the dye was released from the F127 gel and the pentablock copolymer gel at pH 5.4 after 4.5 hours. Quantitative release of the NBC was accompanied by complete dissolution of the gel in both cases. The mechanism for drug release from self assembled hydrogels involves the diffusion of water into the gel matrix, solvating a boundary layer of gel and decreasing the concentration below the critical gelation temperature and allowing for entrapped drug to be released from the gel [15, 33].

The release rate of NBC from the pentablock copolymer gel responded to step changes in pH of the receptor media. During the course of the NBC release experiment, the initial pH of 7.8 was changed to 7.0 at 75 minutes and back to pH 7.8 at 95 minutes as noted on in Figure 6.5. The release rate was observed to increase almost 20 times upon lowering the pH of the receptor media. The release rate decreased upon switching the receptor media back to pH 7.8. The ability to modulate the release rate of NBC by step changes in the release media

pH is due to the reversible, pH dependent hydrophilicity of the PDEAEM blocks. At pH 7.8 the PDEAEM blocks are unprotonated and relatively hydrophobic. Lowering the pH of the release media below the pK_a of the PDEAEM blocks results in protonation of the tertiary amine pendent groups and increases the overall hydrophilic character of the copolymer. Previously 1H NMR and laser light scattering have been used to investigate the pH dependent micellization of the PDEAEM blocks in the pentablock copolymer [26]. These studies show that above pH 7.5 the PDEAEM blocks are relatively dehydrated. The decrease in hydration of the PDEAEM blocks, results in the formation of dehydrated microdomains containing the unprotonated PDEAEM blocks. A pentablock copolymer hydrogel, exposed to aqueous media with pH greater than the pK_a of the PDEAEM, forms a poorly soluble surface layer, due to the presence of the hydrophobic PDEAEM microdomains. This hydrophobic surface layer restricts the diffusion of water into the bulk hydrogel phase, resulting in a decrease in gel dissolution rate and drug release. Below pH 7.5, the tertiary amines of the PDEAEM are protonated and exist as charged polyelectrolyte chains. The charged coronas of the pentablock copolymer micelles interact repulsively, decreasing the resistance for diffusion of water into the hydrogel and increasing the dissolution rate. Previous examples of pH-responsive crosslinked hydrogels that incorporated the DEAEM monomer were shown to exhibit pH modulated release of an anti-inflammatory drug as a result of reversible swelling of the crosslinked network due to the protonation of the tertiary amine of the DEAEM monomer [34, 35].

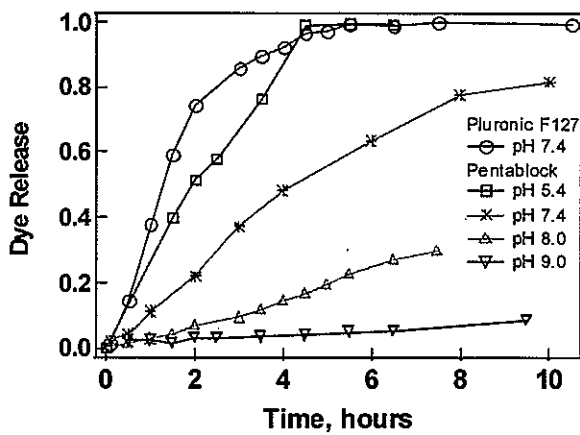


Figure 6.4. In vitro dye release kinetics from Pluronic F127 and pentablock copolymer gel formulations incubated in dissolution media at different pH.

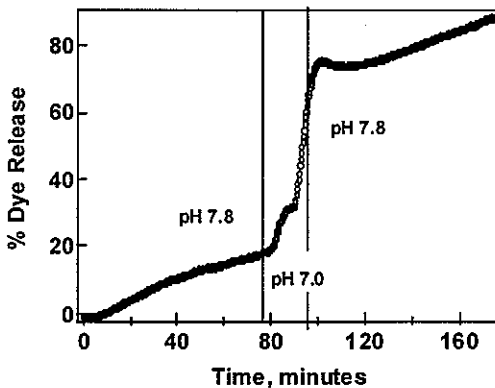


Figure 6.5. In vitro dye release kinetics from pentablock copolymer gel formulation. The pH of the release media is changed from 7.8 to 7.0 at 75 minutes, and back to pH 7.8 at 95 minutes.

6.4.3 Thermal analysis of protein loaded hydrogels

The thermoresponsive properties of the pentablock copolymer gels containing 20 mg/ml lysozyme were investigated to understand the effect of the lysozyme on gel elasticity and gelation temperature. The dynamic mechanical analysis measurements were used to monitor the elastic modulus of the gel as a function of temperature. The elastic modulus of the pentablock copolymer gel (22.5 wt % copolymer), with and without lysozyme, is shown in Figure 6.6. The pentablock copolymer gel without protein exhibits solution-gel transition at 22 ± 2 °C, in agreement with the results from tube inversion experiments.

The addition of 20mg/ml of lysozyme results in a more rigid gel phase and decreased the sol-gel transition temperature to 12 ± 2 °C. Both solutions were free flowing liquids below the sol-gel transition temperature. The rigidity of micellar gel phase, as measured by the storage modulus, increased from 89 ± 4 kPa to 315 ± 16 kPa upon the addition of 20 mg/ml lysozyme. The effects of electrolytes[36, 37], pharmaceutically acceptable organic solvents[23] and polysaccharides[12, 38] proteins[29], and mammalian cell-culture media[39], on reducing the sol-gel transition temperature of aqueous Pluronic® copolymer solutions have been reported previously. Because the mechanism for the thermoreversible gelation of the pentablock copolymer solution is essentially the same as that of Pluronic® F127 solutions, it was anticipated that the sol-gel transition temperature would be effected by the high concentration of the lysozyme. The presence of the lysozyme, which contains several amino acids with non-polar functional groups, increases the attraction between PPO blocks, resulting in a decrease of the CMT. The reduction in CMT results in an increase in volume fraction of micelles at lower temperatures and a lowering of the sol-gel transition temperature.

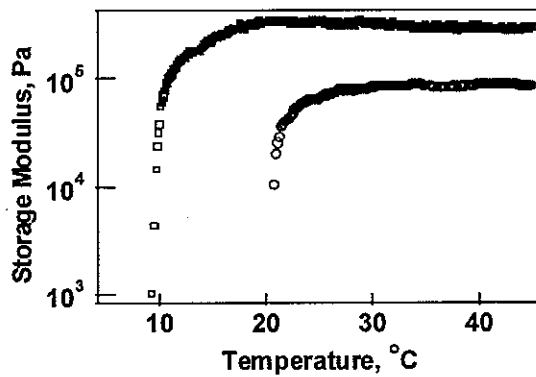


Figure 6.6. The storage modulus of a 22.5 wt % pentablock copolymer gel formulation: □, with 20 mg/ml lysozyme, and ○, without lysozyme.

6.4.4 Protein Release

The delivery of therapeutic biomacromolecular drugs is of particular interest due to the large number of new protein or plasmid drugs currently under development [40]. Many protein drugs, with their hierarchy of structural features, are susceptible to rapid enzymatic denaturation *in vivo*. A successful delivery formulation would provide a sustained release of active protein and encourage prolonged circulation of released protein. The effectiveness of the pentablock copolymer gel as a vehicle for sustained protein delivery was investigated with *in vitro* dissolution testing. A model protein drug, chicken egg lysozyme, was selected for the study. Lysozyme was incorporated in the pentablock copolymer solution by mixing at low temperature, resulting in a transparent solution. Release experiments were conducted to determine the protein release kinetics from the copolymer formulation. The results, in Figure 6.7, indicate that the pentablock gel formulation maintained a zero order release of lysozyme over an 80-hour period. The decrease in release rates between pentablock copolymer gel loaded with NBC and lysozyme can be explained by the difference in rigidity of the gel; water diffusion into the more rigid, lysozyme loaded gel, is more hindered, thereby reducing the dissolution rate of the gel. A similar decrease in release rate was observed when the copolymer concentration of the Pluronic® F127 gel was increased [33]. The pH of the release media influenced the release rate of lysozyme from the pentablock copolymer gel. The release experiments were conducted at pH 7.0, 7.4 and 8.0. The release rate of lysozyme from the gel at pH 7.0 increased 49% compared to the release rate at pH 8.0.

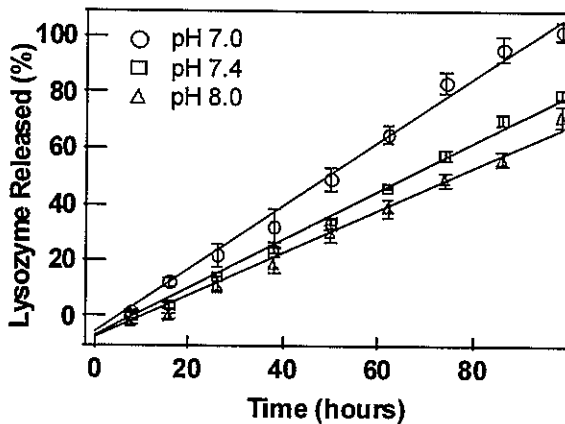


Figure 7. The release behavior of lysozyme from 22.5 wt % pentablock copolymer gels at pH 7.0, 7.4 and 8.0 at 37°C.

Polymeric materials included in a sustained drug delivery formulation must exhibit good biocompatibility. Previously reported cell cytotoxicity experiments indicate that the pentablock copolymer exhibits good biocompatibility [12]. Additionally, the stability of the lysozyme structure in the presence of the pentablock copolymer was confirmed with CD measurements. The secondary structure of the protein was unaltered after 4 weeks of incubation at 37°C in receptor media with 0.125 mg/ml of pentablock copolymer. This suggests that the presence of the pentablock copolymer did not accelerate or induce the degradation of lysozyme structure in solution.

6.5. Conclusions

This study has demonstrated the influence of pH on the drug release rate of a model low molecular weight drug, NBC, and a model therapeutic protein, lysozyme, from an injectable thermoreversible pentablock copolymer gel formulation. In vitro drug release experiments have demonstrated reversible triggered release of NBC in response to changes in pH of the receptor media in the proximity of physiological pH values. The thermoreversible pentablock gels exhibited zero-order sustained release of lysozyme *in vitro* over the course of

80-100 hours. The presence of the pentablock copolymer has been shown to have low cytotoxicity response and negligible effect on the secondary structure of lysozyme. These features make the pentablock copolymer a biomaterial with great potential for modulated drug delivery applications.

6.6. Acknowledgments

Thanks to undergraduate students Suzan Cox and Chris Wong for their assistance with different aspects of this work. This work was supported by the U.S. Department of Energy under contract number W-7405-ENG-81 to Iowa State University.

6.7. References

1. Shalaby, S.W. and K.J.L. Burg, *Absorbable and Biodegradable Polymers*. 2003, Boca Raton: CRC Press.
2. Kost, J. and R. Langer, *Responsive Polymeric delivery systems*. Adv Drug Deliv Rev, 2001. **46**: p. 125-148.
3. Steil, G.M., A.E. Panteleon, and K. Rebrin, *Closed-loop insulin delivery-the path to physiological glucose control*. Adv Drug Deliv Rev, 2004. **56**(2): p. 125-44.
4. Kipper, M.J., et al., *Design of an injectable system based on bioerodible poly(anhidride) microspheres for sustained drug delivery*. Biomaterials, 2002. **23**(22): p. 4405-12.
5. Rosler, A., G.W. Vandermeulen, and H.A. Klok, *Advanced drug delivery devices via self-assembly of amphiphilic block copolymers*. Adv Drug Deliv Rev, 2001. **53**(1): p. 95-108.
6. Matsumoto, A., R. Yoshida, and K. Kataoka, *Glucose-Responsive Polymer Gel Bearing Phenylborate Derivative as a Glucose-Sensing Moiety Operating at the Physiological pH*. Biomacromolecules, 2004. **5**: p. 1038-1045.
7. Podual, K., F.J. Doyle, and N.A. Peppas, *Preparation and dynamic response of cationic copolymer hydrogels containing glucose oxidase*. Polymer, 2000. **41**: p. 3975-3983.
8. Simoes, S., et al., *On the formulation of pH-sensitive liposomes with long circulation times*. Adv Drug Deliv Rev, 2004. **56**(7): p. 947-65.
9. Sant, V.P., D. Smith, and J.C. Leroux, *Novel pH-sensitive supramolecular assemblies for oral delivery of poorly water soluble drugs: preparation and characterization*. J Control Release, 2004. **97**(2): p. 301-12.
10. Barreiro-Iglesias, R., et al., *Pluronic-g-poly(acrylic acid) copolymers as novel excipients for site specific, sustained release tablets*. Eur J Pharm Sci, 2005.

11. Wei, J.S., et al., *Temperature- and pH-sensitive core-shell nanoparticles self-assembled from poly(n-isopropylacrylamide-co-acrylic acid-co-cholesteryl acrylate) for intracellular delivery of anticancer drugs*. *Front Biosci*, 2005. **10**: p. 3058-67.
12. Agarwal, A., R. Unfer, and S.K. Mallapragada, *Novel thermogelling pH-sensitive pentablock copolymers as injectable gene delivery vectors*. *J. Controlled Release*, 2004. **103**(1): p. 245-258.
13. Lee, E.S., K. Na, and Y.H. Bae, *Super pH-sensitive multifunctional polymeric micelle*. *Nano Lett*, 2005. **5**(2): p. 325-9.
14. Shalaby, S.W., *Thermoreversible Gels*. *ACS Symp. Ser.*, 1991. **467**: p. 502-506.
15. Chung, Y.-M., et al., *Sol-Gel Transitiong Temperature of PLGA-g-PEG Aqueous Solutions*. *Biomacromolecules*, 2002(3): p. 511-516.
16. Choi, H.S., et al., *Rapid induction of thermoreversible hydrogel formation based on poly(propylene glycol)-grafted dextran inclusion complexes*. *Macromol. Biosci.*, 2002. **2**(6): p. 298-303.
17. Cappello, J., et al., *In-situ self-assembling protein polymer gel systems for administration, delivery, and release of drugs*. *J. Controlled Release*, 1998. **53**(1-3): p. 105-117.
18. Byeongmoob Jeong, S.W.K., You Han Bae, *Drug release from biodegradable injectable thermosensitive hydrogel of PEG-PLGA-PEG triblock copolymers*. *J. Controlled Release*, 1999(63): p. 155-163.
19. Bromberg, L., *Synthesis and Self-Assembly of Poly(ethylene oxide)-b-poly(propylene oxide)-b-poly(ethylene oxide)-g-poly(acrylic acid) Gels*. *Ind. Eng. Chem. Res.*, 2001. **40**(11): p. 2437-2444.
20. Chetoni, P., et al., *Pharmacokinetics and anti-inflammatory activity in rabbits of a novel indomethacin ophthalmic solution*. *J. Ocul. Pharmacol. Th.*, 2000. **16**(4): p. 363-372.
21. Cohn, D., A. Sosnik, and A. Levy, *Improved reverse thermo-responsive polymeric systems*. *Biomaterials*, 2003. **24**(21): p. 3707-3714.
22. Guzman, M., et al., *Polyoxyethylene-Polyoxypropylene Block Copolymer Gels as Sustained-Release Vehicles for Subcutaneous Drug Administration*. *Int. J. Pharm.*, 1992. **80**(2-3): p. 119-127.
23. Ivanova, R., B. Lindman, and P. Alexandridis, *Effect of pharmaceutically acceptable glycols on the stability of the liquid crystalline gels formed by poloxamer 407 in water*. *J Colloid Interf Sci*, 2002. **252**(1): p. 226-235.
24. Johnston, T.P., M.A. Punjabi, and C.J. Froelich, *Sustained Delivery of Interleukin-2 from a Poloxamer-407 Gel Matrix Following Intraperitoneal Injection in Mice*. *Pharmaceut. Res.*, 1992. **9**(3): p. 425-434.
25. Ishihara, K., et al., *Glucose-induced permeation control of insulin through a complex membrane consisting of immobilized glucose oxidase and a polyamine*. *Polym. J. (Tokyo)*, 1984. **16**(8): p. 625-31.
26. Determan, M.D., et al., *Synthesis and characterization of the temperature and pH-responsive pentablock copolymers*. *Polymer*, 2005. **46**: p. 6933-6946.
27. Wang, P.L. and T.P. Johnston, *Sustained-Release Interleukin-2 Following Intramuscular Injection in Rats*. *Int. J. Pharm.*, 1995. **113**(1): p. 73-81.

28. Katakam, M., W.R. Ravis, and A.K. Banga, *Controlled release of human growth hormone in rats following parenteral administration of poloxamer gels*. J. Controlled Release, 1997. **49**(1): p. 21-26.
29. Stratton, L.P., et al., *Drug Delivery Matrix Containing Native Protein Precipitates Suspended in a Poloxamer Gel*. J. Pharm. Sci., 1997. **86**(9): p. 1006-1010.
30. Wanka, G.H., H.; Ulbricht, W, *Phase Diagrams and Aggregation Behavior of Poly(oxyethylene)-Poly(oxypropylene)-Poly(oxyethylene) Triblock Copolymers in Aqueous Solutions*. Macromolecules, 1994. **27**(15): p. 414594149.
31. Anderson, B.C., et al., *Synthesis and characterization of diblock and gel-forming pentablock copolymers of tertiary amine methacrylates, poly(ethylene glycol), and poly(propylene glycol)*. Macromolecules, 2003. **36**(5): p. 1670-1676.
32. Kabanov, A.V., et al., *Micelle Formation and Solubilization of Fluorescent Probes in Poly(oxyethylene-b-oxypropylene-b-oxyethylene) Solutions*. Macromolecules, 1995. **28**(7): p. 2303-14.
33. Anderson, B.C., N.K. Pandit, and S.K. Mallapragada, *Understanding drug release from poly(ethylene oxide)-b-poly(propylene oxide)-b-poly(ethylene oxide) gels*. J Controlled Release, 2001. **70**(1-2): p. 157-167.
34. Hariharan, D. and N.A. Peppas, *Characterization, dynamic swelling behavior and solute transport in cationic networks with applications to the development of swelling-controlled release systems*. Polymer, 1996. **37**(1): p. 149-61.
35. Schwarte, L.M.P., Kairali; Peppas, Nicholas A, *Cationic hydrogels for controlled release of proteins and other macromolecules*. ACS Symp. Ser., 1998. **709**: p. 56-66.
36. Mao, G., et al., *PEO-PPO-PEO Block Copolymer Micelles in Aqueous Electrolyte Solutions: Effect of Carbonate Anions and Temperature on the Micellar Structure and Interaction*. Macromolecules, 2001. **34**(3): p. 552-558.
37. Jain, N.J., et al., *Salt induced micellization and micelle structures of PEO/PPO/PEO block copolymers in aqueous solution*. Colloids Surf., A, 2000. **173**(1-3): p. 85-94.
38. Coeshott, C.M., et al., *Pluronic® F127-based systemic vaccine delivery systems*. Vaccine, 2004. **22**: p. 2396-2405.
39. Sharma, P.K., J.E. Matthew, and S.R. Bhatia, *Structure and assembly of PEO-PPO-PEO co-polymers in mammalian cell-culture media*. J. Biomater. Sci. Polymer Edn., 2005. **16**(9): p. 1139-1151.
40. Frokjaer, S. and D.E. Otzen, *Protein drug stability: a formulation challenge*. Nat Rev Drug Discov, 2005. **4**(4): p. 298-306.

CHAPTER 7. GENERAL CONCLUSIONS

This work has contributed to the fields of materials research with the synthesis and characterization of an amphiphilic block copolymer that forms hydrogels and exhibits stimuli responsive properties. In addition this work has demonstrated the potential uses in controlled drug delivery and gene therapy formulations for the pentablock copolymer. The characterization of the stimuli responsive self assembled nanostructures formed by the pentablock copolymer has inspired additional research in the fields of biomineralization and bioinspired nanoparticles. Future work involving the pentablock copolymer system will focus on enhancing and tuning the cell specific targeting of DNA/pentablock copolymer polyplexes. Furthermore, the results of experimental investigations on the pentablock copolymer system have motivated new theoretical investigations into the physics of complex multiblock copolymer systems [1].

Chapter three of this thesis details the copolymer synthesis and macromolecular characterization of these new materials. The temperature and pH-responsive nature of the copolymer micelles and hydrogels was established in this investigation. This introductory study on the pentablock copolymer established the rich phase behavior and potential uses for the copolymer system. The pentablock copolymer containing PDEAEM blocks, with a pK_a around 7.5-7.6 was identified as the most biomedically relevant and was the primary focus of the rest of the research in this thesis.

A more thorough investigation of the pH and temperature responsive behavior of the pentablock copolymer was detailed in chapters four and five. The SANS technique allowed for detailed measurement of intra- and inter-particle dimensions with nanometer resolution. CryoTEM results, gained through collaborations with Dr. Talmons group at Technion in Israel, provided invaluable corroborating evidence for the characterization of the pentablock

copolymer micelles. These techniques provided insight into the cascade of nanoscale morphological changes that occurs during the assembly of copolymer micelles and hydrogels. The analysis techniques utilized to quantitatively evaluate the micelle dimensions was the first reported use of the Pedersen core-chain form factor in combination with the Haytor-Penfold structure factor for charged colloidal properties. The algorithm developed for the implementation of this model has been added to the library of SANS analysis tools available to DOE and visiting scientist at the Intense Pulsed Neutron Source at Argonne National Laboratory.

In chapter six, the potential biomedical applications of the pentablock copolymer were investigated with *in vitro* drug release studies. The thermoresponsive gelation of the aqueous pentablock copolymer formulations make it a superb candidate for an *in situ* forming hydrogel drug depot system. The controlled release of nile blue chloride dye was used to illustrate the pH-responsive modulated release of a low molecular weight drug from the pentablock copolymer hydrogel. In an *in vivo* setting where changes in pH are associated with deviations from homeostasis, the pH responsiveness of the pentablock hydrogel formulation may be utilized to self regulate controlled release of drug. In addition, the controlled release of a model therapeutic protein was demonstrated in chapter six. The ability to facilitate the sustained release of protein drugs, which contain a hierarchy of delicate macromolecular features necessary for efficacy, is an emerging challenge in the field of drug delivery.

These results contribute to the knowledge necessary for further tailoring of these, and other functional block copolymer materials for biomedical applications. Future directions of this work include using the pentablock copolymer micelles as templates for mineralization of bone-like calcium apatite. Also, the conjugation of the pentablock copolymer with specific

aptamers and proteins to direct the self-assembly of magnetic nano-particles is currently being explored.

Additional ongoing work will seek to use the pentablock copolymer architecture to generate a hydrogel forming copolymer that exhibits direct glucose responsive properties through the incorporation of a poly(4-(1,6-dioxo-2,5-diaza-7-oxamyl) phenyl-boronic acid) PDDOPBA segments. Such a material would have potential uses for treatment of diabetes, which requires frequent monitoring of glucose levels. The pendent boronic acid moiety of this monomer is commonly utilized in affinity chromatography columns due to its strong affinity for sugar molecules. Incorporation of this monomer into crosslinked hydrogels of P(NIPAAm) resulted in a glucose dependent swelling behavior [2]. The RAFT polymerization technique will be used to add blocks of PDDOPBA to the ends of Pluronic F127 chains, resulting in a pentablock copolymer as shown in Figure 7.1.

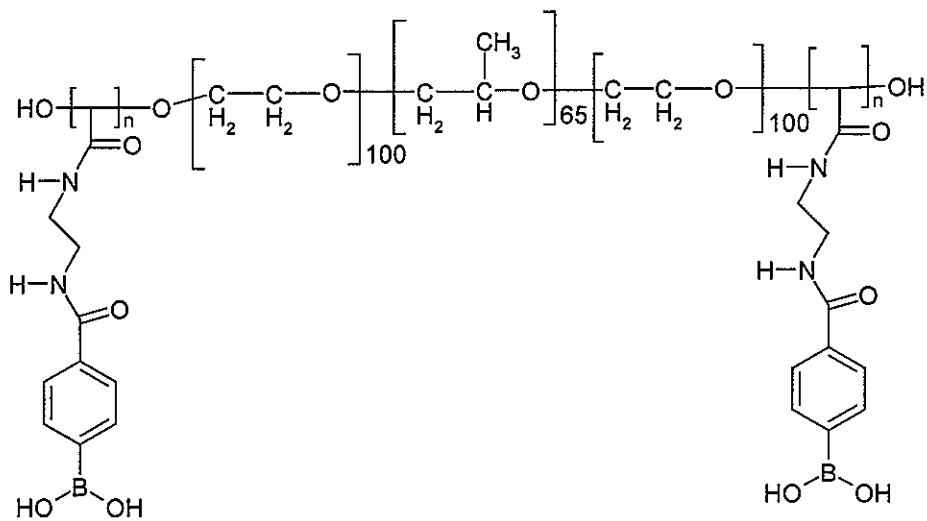


Figure 7.1. Pentablock copolymer based on Pluronic F127 with P(DDOPBA) segments

By incorporating this functionality into a pentablock copolymer we hope to realize direct glucose responsive phase behavior. That is, due to the presence of PDDOPBA chains

segments in the pentablock copolymer, the hydrophobic/hydrophilic balance of the copolymer will exhibit glucose dependence. The presence of glucose in solution will cause ionization of the boronic acid groups and lead to an increase in hydrophilic character, the absence of glucose will result in a pentablock copolymer with hydrophobic end blocks. This stimuli responsive property in a copolymer capable of forming a physical hydrogel phase could be utilized in the development of a glucose responsive drug delivery formulation.

These outgrowths from the research presented in chapters Chapters 3 through 6 are evidence of the impact and contribution of this work.

7.2 References

1. Chushak, Y. and A. Travesset, *Coarse-Grained Molecular Dynamics Simulations of the Self-Assembly of Pentablock Copolymers into Micelles*. J. Phys. Chem., 2005. submitted.
2. Matsumoto, A., et al., *Glucose-Responsive Polymer Bearing a Novel Phenylborate Derivative as a Glucose-Sensing Moiety Operating at Physiological pH Conditions*. Biomacromolecules, 2003. 4(5): p. 1410-1416.

7.3 Acknowledgments.

Thanks to my best friend and wife, Amy, for her love and support. Thanks to my parents, their love, guidance and encouragement has been ever present.

I am greatly indebted to Dr. Mallapragada for her invaluable mentorship over the past four years. Thanks to my Program of Study committee for their diligence and gracious assistance throughout the development of this thesis. Thanks to the numerous undergraduates that aided in the experimental aspects of this work: James Cox, Suzan Cox, Chris Wong, Richerd Fulkerson, and Amy Karlson. Thanks to the fellow graduate students whose helpful discussions aided this work in so many ways: Ankit Agarwal, Sim-Siong Wong, Erik Hagberg, Dejan Andjelkovic, and Sergiy Peleshanko. Thanks to Dr. Narasimhan and Matt Kipper at Iowa State University, as well as Dr. Thiagarajan, Sonke Seifert, Liang Guo, Kevin Lo, and Denis Wozniak at Argonne National Laboratory for their assistance with the small angle scattering experiments. Likewise Dr. Ishi Talmon and Rita Vilensky at Technion-Israel and Dr. Matt Kramer at Iowa State University made the Cryo TEM experiments possible. Thanks to Alex Travasset for his many helpful discussions. Thanks to the faculty and staff of the Chemical and Biological Engineering department, for their dedication to fostering the culture of outstanding academic merit and leadership at Iowa State University.

This document has been authored by the Iowa State University of Science and Technology under Contract No. W7405-ENG-82 with the U.S. Department of Energy. The U.S. Government retains a non-exclusive, paid-up, irrevocable, world-wide license to publish or reproduce the published form of this document, or allow others to do so, for U.S. Government purposes.